SOURCE TERM REDUCTION FOR ADVANCED AND SMALL MODULAR BOILING WATER REACTORS

PHASE 1 FEASIBILITY STUDY TO ESTABLISH THE POTENTIAL FOR REDUCED SOURCE TERM ESTIMATES WITH ADVACNED AND SMR SPECIFIC BWR FISSION PRODUCT DEPOSITION MODELS

TECHNICAL REPORT

PT-PR-19-021

REPORT FOR THE US DEPARTMENT OF ENERGY

DE-NE0008835

U.S. Department of Energy Program Manager: Rebecca Onuschak

Office of Nuclear Energy

U.S. Department of Energy

Pittsburgh Technical Project Manager: Sola Talabi

Project Period: May 2019 – July 2020

ACKNOWLEDGMENTS

The following organizations were involved in the conduct of this study and preparation of this report:

Pittsburgh Technical LLC. – Sola Talabi Ph.D., Principal Investigator

Redus and Associates LLC. – Kenneth Redus, Principal

Electric Power Research Institute – Cristian Marciulescu, Principal Technical Leader, Advanced Nuclear Technology

Acknowledgment:

This material is based upon work supported by the U.S. Department of Energy.

Notice of Federal Support and Applicable Government License:

This work was generated with financial support from the U.S. Government through Contract/Award No. DE-NE0008835 and as such the U.S. Government retains a paid-up, nonexclusive, irrevocable, world-wide license to reproduce, prepare derivative works, distribute copies to the public, and display publicly, by or on behalf of the Government, this work in whole or in part, or otherwise use the work for Federal purposes.

VERSION HISTORY

Version #	Implemented By	Revision Date	Comments
0	Rohan Biwalkar Kenneth Redus Teffik Gemci Ph.D.	7/15/2020	Original Version

Revision Approvals

Name	Role	Signature	Date
Sola Talabi Ph.D.	Project Manager, Pittsburgh Technical	Sola Talabi	7/15/2020

Executive Summary

The United States Department of Energy (US DOE) is currently supporting the development of various advanced and small modular reactor (SMR) designs. Several of these designs have commenced license application with the US Nuclear Regulatory Commission (US NRC). These reactors have improved safety features that may significantly reduce radiological source terms in the event of design and beyond-design basis accidents. Specifically, some reactors feature a smaller containment volume relative to the available fission product depositional surface area, which supports increased fission product retention in the containment vessel. Pressurized water reactors (PWR) and boiling water reactors (BWR) with this feature include the integral pressurized water reactor (iPWR) and the BWRX-300 design by General Electric. A prior research program supported by the US DOE quantified the source term reduction associated with light water iPWRs and developed iPWR-specific theoretical models for fission product deposition rates. This program included a sequence of research projects that started with a feasibility study, development of theoretical models that predict higher deposition rates, and finally, development of empirical data for verification and validation of the theoretical models. The current project, which is a feasibility study, is the first step in a similar program to quantify the source term reduction associated with small and advanced light water BWRs.

To support timely utilization of research outcomes for the nuclear industry, this project leveraged lessons-learned and prior research outcomes from the iPWR source term reduction program by developing an identical roadmap. This was possible because both projects were performed by the same research entity (Pittsburgh Technical / EPRI), and both evaluated designs are light water reactors that have similar geometric and thermal hydraulic parameters that are critical to fission product deposition. The US NRC is a critical stakeholder that is engaged at each phase of the projects. Specifically, for the iPWR project, the NRC reviewed and commented on the research outcomes, visited the Pittsburgh Technical Small Modular and Advanced Reactor Testing (SMART) lab, and provided feedback on preferred approaches to utilization of the research outcomes. The feedback on utilization included a recommendation for the research outcomes to support the NRC's objective to improve existing coarse models for applicability to advanced reactors. Hence, a major outcome of both projects is the development of a set of theoretical models that can be applied to existing coarse models and software. The basic theoretical models developed from the iPWR project are described within this report, which also describes the activities required to refine these models with BWR-specific data in future phases of this project.

This study is designed to provide broad applicability to advanced boiling water reactors, and hence, available information from both small and large advanced boiling water reactors are used, which includes the GE BWRX-300, ABWR and ESBWR. Considering the BWRX-300 design is currently in development as of the date of this report, relevant ABWR and ESBWR critical parameters are evaluated to provide bounding assumptions in certain cases.

Background

Small Modular Reactors (SMRs) such as the iPWR and BWRX-300 have containment volumes that are relatively smaller than those of current generation III reactors. Consequently, these reactors have a larger fission product depositional surface-area-to-volume ratio, as compared to generation III containments. In addition to the in-containment features, there are other fission product retention features such as underground placement of the reactors that support source term reduction through natural occurring processes and phenomena. The applicability of this study is expected to extend to advanced boiling water reactors that have critical parameters that are within the regimes of similitude for which the evaluated and developed theoretical models of fission product transport and deposition apply. Hence, although the primary focus of this project is SMR-type BWRs, an extensive review of other advanced BWRs was conducted and findings applicable to those reactors are described.

Fission product retention through naturally occurring phenomena has a greater significance for advanced reactors because some reactors have simplified designs that eliminate certain mechanical and active fission product retention systems, such as sprays. Concomitantly, naturally occurring phenomena are more effective for these reactors because of the relatively lower fission product inventory and more favorable thermal hydraulic conditions, such as higher thermal and steam concentration gradients that support the occurrence of the phenomena.

The project will be conducted in a manner that will have work scopes that are similar to the related iPWR project. The first step is a feasibility study that identifies the appropriate fission product deposition models, the second step will develop BWR-specific validation data through experiments and simulation, while the last phase will include the refinement and validation of the deposition models with the data.

Objectives

The objectives of this project include:

1. Improve the characterization of mechanistic source terms associated with post-accident fission product release for advanced BWRs with critical parameters that support higher fission product deposition rates.
2. Develop a roadmap that leverages prior research and lessons learned from the iPWR source term reduction project to achieve synergy and research efficiency.
3. Describe the subsequent activities and work scopes required to develop advanced BWR-specific fission product deposition models in future phases.
4. Provide stakeholders information required to advance and inform regulatory positions related to advanced BWR source terms.

Approach

1. Identify critical and bounding BWR fission product transport parameters by reviewing relevant information on advanced BWR designs including the ABWR, ESBWR and BWRX-300.

2. Elicit stakeholder confirmation regarding relevant design-related source term attenuation parameters, which include geometry, thermal-hydraulics, aerosol characteristics, and specific systemic features, such as suppression pools/chambers.

3. Establish appropriate classification of advanced BWR designs by regimes of similitude where aerosol depletion characteristics are similar. Classifications may include size (small and large), thermal power, thermal hydraulic regimes, and systemic features. Specifically, classification will refine the two methods and modeling approaches for decontamination factor estimation, and establish the limits of applicability of existing methods and models:

    a. **Similitude Approach for Codes like MAAP (Modular Accident Analysis Program):** This will support a scaling approach based on characteristic parameters.

    b. **Discrete Approach for Codes like MELCOR (Methods for Estimation of Leakages and Consequences of Releases), GOTHIC (Generation of Thermal-Hydraulic Information for Containments) and Codes with Computational Fluid Dynamics (CFD) approaches:** This will support refinement of equations for deposition velocities based on the discretization of the zones of influence (superheated, saturated and condensation), flow regimes (continuum, slip-flow, intermediate and free-molecule). Applicable parameters may include the Knudsen number, Cunningham slip correction etc.

4. Perform a gap analysis for available experimental data and computer codes for aerosol retention in aerosol depletion pathways including through specific systems such as suppression chambers/pools.

5. Gain stakeholder consensus on the project objectives, and agreement on the technical approach. This includes measurement techniques used to collect experimental data, and computer codes used for simulation and modeling.

6. Use the USNRC's Best Estimate Plus Uncertainty (BEPU) approach, which requires an uncertainty analysis and phenomena prioritization using a Phenomena Identification and Ranking Table (PIRT).

7. Use expert elicitation in-lieu of available data: Develop a PIRT for the A-BWR passive safety mechanisms in terms of their order of importance and knowledge.

8. Based on the PIRT and supplemental stakeholder inputs, assess the following:

    a. Identify data requirements to improve current modeling approaches

b. Identify experimentation requirements to develop the required data: This includes identifying specific equipment to emulate thermal-hydraulic environments and collect data.

c. Develop optimal research strategies by leveraging knowledge and resources across similar source-term investigation research projects, which include Phase 3 of the iPWR aerosol project.

d. Develop specific recommendations to improve modeling and simulation capabilities for both similitude and discrete approaches to support continued use of existing codes such as MAAP, SUPRA (Suppression Pool Retention Analysis), SPARC (Suppression Pool Aerosol Removal Code), ASTEC (Accident Source Term Evaluation Code), BUSCA (Bubble Scrubbing Algorithm), MELCOR, GOTHIC and codes using CFD.

9. Estimate decontamination factors associated with advanced BWRs, which will be used to determine the expected range of empirical values.

10. Perform an uncertainty analysis to inform the experimental phase of the project by determining parameters to which the figures of merit are most sensitive.

Results

This study has established a roadmap to improve the characterization of source terms for advanced and SMR-type BWRs. The characterization includes the development of theoretical models that describe higher rates of fission product transport and deposition. The study also verified the potential for significant reduction in the estimated advanced BWR source term, if the proposed activities to validate the models by developing BWR-specific data are further executed and completed. The study identified critical geometric, thermal hydraulic, aerosol characteristics and systemic parameters that influence fission product behavior and deposition. The most critical of these parameters were identified by stakeholder input through a PIRT exercise, modeling, and uncertainty analysis. Additional experimental data needs and analytical correlation requirements to properly model unique design features and transient containment post-accident thermal-hydraulic behavior were identified. This study also identified the need to separately assess small and large A-BWRs due to the different geometric and thermal hydraulic regimes in which their depositional phenomena occur. The importance of this separation is to identify the limits of applicability of existing fission product models, which are based on large LWR data (US NRC NUREG-6189 and NUREG-6153).

Applications, Value, and Utilization

This project is expected to directly benefit SMR-type BWRs and may also benefit advanced large BWRs by developing refined predictive models for fission product transport and deposition, along with development of more recent experimental data that can be used to improve analytical correlations for natural aerosol deposition mechanisms. These potential model revisions are expected to result in a more realistic calculation of containment aerosol natural deposition and concomitant reduction of source terms for both design basis (intact containment) and beyond design basis (delayed containment failure) accident sequences. These expected improvements are intended to be complementary to existing methods and codes and are not expected to replace the existing analytical tools and frameworks.

Keywords

1. BWRX-300
2. ESBWR
3. ABWR
4. SMR
5. Fission product
6. Aerosol transport
7. Diffusiophoresis
8. Gravitational settling/Sedimentation

Contents

List of Acronyms

Acronym	Full Form
A-BWR	Advanced Boiling Water Reactor (Generic)
ABWR	Advanced Boiling Water Reactor (GE-Hitachi Design)
ARCC	Advanced Reactor Computational fluid dynamics Code
ASTEC	Accident Source Term Evaluation Code
BMIX++	Berkeley mechanistic MIXing code in C++
BUSCA	Bubble Scrubbing Algorithm
BWR	Boiling Water Reactor
CFD	Computational Fluid Dynamics
CMU	Carnegie Mellon University
CV	Containment Vessel
DCC	Direct Contact Condensation
EPRI	Electric Power Research Institute
ESBWR	Economic Simplified Boiling Water Reactor
FOM	Figure of Merit
FORTRAN	FORmula TRANslation
GE	General Electric
GOF	Goodness of Fit
GOTHIC	Generation of Thermal-Hydraulic Information for Containments
ICS	Isolation Condenser System
IRWST	In-Containment Refueling Water Storage Tank
iPWR	Integral Pressurized Water Reactor
KNGR	Korea Next Generation Reactor
LLWR	Large Light Water Reactor
LUT	Lappeenranta University of Technology
LOCA	Loss of Coolant Accident
MELCOR	Methods for Estimation of Leakages and Consequences of Releases
NEA	Nuclear Energy Agency
NUREG	NUclear regulatory commission REGulation
PASSAM	Passive and Active Systems on Severe Accident source term Mitigation
PCCS	Passive Containment Cooling System
PCMM	Predictive Capability Maturity Model
PDF	Probability Density Function
PIRT	Phenomena Identification and Ranking Table
PNNL	Pacific Northwest National Laboratory
POOLEX	POOL EXperiments (condensation pool texting facility)
POSEIDON	(suppression pool research facility)
PPOOLEX	(containment test facility)
PSI	Paul Scherrer Institute
PWR	Pressurized Water Reactor
RCIC	Reactor Core Isolation Cooling
RV	Reactor Vessel
SGTR	Steam Generator Tube Rupture
SIET	Societa Informazioni Esperienze Temoidrauliche
SMART	Small Modular and Advanced Reactor Testing
SMR	Small Modular Reactor
SNL	Sandia National Laboratory

SPARC	Suppression Pool Aerosol Removal Code
SUPRA	Suppression Pool Retention Analysis
TRACG	Transient Reactor Analysis Code
TRISTAN	Tube rupture in Steam generator: multi-phase-flow investigations
US DOE	United States Department of Energy
US NRC	United States Nuclear Regulatory Commission

List of Figures

List of Tables

Conversion Factors

Conversion factors for relevant mathematical quantities are given as follows.

Parameter	Conversion
Area	1 in^2 = 6.45 cm^2 1 ft^2 = 929 cm^2
Density	1 lb/ft^3 = 16 kg/m^3 1 g/cm^3 = 0.036 lb/in^3
Distance	1 µm = 10^{-6} m = 0.00004 in. 1 mm = 0.0394 in. 1 ft = 0.305 m 1 in. = 2.54 cm
Energy	1 J = 0.738 lbf-ft
Flow	1 L/min = 0.264 gpm
Gas constant	1 ft-lbf/slug°R = 0.1672 N-m/kgK
Gravity	32.2 ft/sec^2 = 9.81 m/sec^2
Mass	1 g = 0.0353 oz 1 lb = 0.4536 kg
Pressure	1 psi = 6.89 kPa
Temperature	°C = (°F – 32) × 5/9 °C = K – 273.15 °C = (°R – 491.67) × 5/9 °F = (°C × 9/5) + 32 °F = K × 9/5 – 459.67 °F = °R – 459.67
Torque	1 N-m = 0.738 lbf-ft
Velocity	1 ft/sec = 0.3048 m/sec
Viscosity	1 lb/ft-sec = 1488.164 cP

Nomenclature

Symbols used in this document are listed in this section, along with the relevant units. The symbol and subscript are listed separately for clarity. As an example, for an equation that contains the symbol 'd_p', referring to this list will indicate that 'd_p' means particle diameter, since the symbol 'd' refers to diameter and the subscript 'p' refers to particle.

Latin Alphabets: Uppercase

A: Area [m^2]
DF: Decontamination factor [-]
H: Height [m]
M: Molecular Weight [kg/mol]
N: Dimensionless particle concentration/mass [-]
P: Reactor Thermal Power [MWth], Pressure (in velocity equations) [Pa]
T: Temperature [K]
$\tilde{T}$: Average Fluid Temperature [K]
U: Flow Velocity [m/s]
V: Volume [m^3]
X: Mass fraction [-]

Latin Alphabets: Lowercase

d: Diameter [m]
g: Acceleration due to gravity [m/s^2]
k: Thermal conductivity [W/m-K]
m: Particle Mass [kg]
$\dot{m}''$: Steam Condensation Flux [kg/m^2-s]
n: Cell Thickness to calculate gradient [m]
r: Radius [m]
t: Time [s]
v: Particle Velocity [m/s]
x: Distance [m]

Greek Symbols

α: Decontamination coefficient [s-1]
ε: Efficiency [-]
λ: Aerosol removal rate [hr-1, min-1 or s-1]
μ: Gas Phase Viscosity [kg/m-s]
ρ: Density [kg/m3]
$\bar{\rho}$ Average Density [kg/m3]
φ: Bend Angle [rad]

Subscripts

0: Initial
a: Air
cond: Condensation
c: Turbulent Convection
d: Diffusiophoresis, deposition
f: Fluid
g: Gravitational settling (for velocity), Gas (for fluid properties)
p: Particle
s: Steam
t: Thermophoresis

Correction Factors

$C_s = 1.17$
$C_m = 1.14$
$C_t = 2.18$

Dimensionless numbers

C_c: Cunningham Correction Factor
Kn: Knudsen Number
Stk: Stokes Number
Re: Reynolds Number

1 Introduction

1.1 Project Objectives

The objective of this project is to improve the characterization of mechanistic source terms associated with post-accident radionuclide release for advanced boiling water reactors (BWRs) that have critical features that support higher rates of fission product deposition. Specifically, this will include Small Modular Reactor (SMR) -type BWRs and may also benefit other large advanced boiling water reactors (A-BWRs) that are within the applicable range of similitude for critical fission product deposition parameters. Improved characterization has the potential to reduce the estimated source terms associated with postulated accidents associated with these reactors. It should be noted that although this project is primarily focused on the BWR SMR, an extensive review of other advanced BWRs was conducted and findings applicable to those reactors are described. The expected outcomes and utilization of this study are based on the realized outcomes from a similar DOE-funded project, conducted by Pittsburgh Technical and the Electric Power Research Institute (EPRI), which included the investigation of the radionuclide particle decontamination potential of Integral Pressurized Water Reactors (iPWR) (EPRI, 2018a). Significantly higher decontamination factors were estimated for iPWRs based on thermal-hydraulic and geometric parameters that are expected to be in the range of parameters for SMR-type BWRs. These parameters include a relatively high depositional-surface-area-to-volume ratio and certain thermal-hydraulic characteristics (EPRI, 2018b). Similar to the iPWR program, the objective of this project is to establish decontamination factors appropriate for A-BWRs by establishing the theoretical constructs for the depositional phenomena of interest and describing a roadmap for empirical data gathering in future phases.

Specifically, this study will provide refined data used by safety analysts for Level II Probabilistic Risk Analysis (PRA) and dose estimates. Level II PRA provides an estimate of a nuclear plant's response to a severe accident, and based on this response, a measure of the potential radioactivity release. The PRA includes an assessment of the radioactivity retention capacity of the defense-in-depth systems, which are systems and structures that serve as barriers to radioactivity release. For existing light water reactors, the major barriers include the fuel matrix and cladding, the primary circuit boundary (reactor) and containment (Figure 1-1). Containment refers to the physical barrier to aerosolized radionuclide particles, which has traditionally been achieved with a containment vessel structure. For a comprehensive mechanistic source term analysis, radionuclide particle confinement should also include an assessment of potential containment by-pass and additional features and structures on the aerosol pathway beyond the containment vessel.

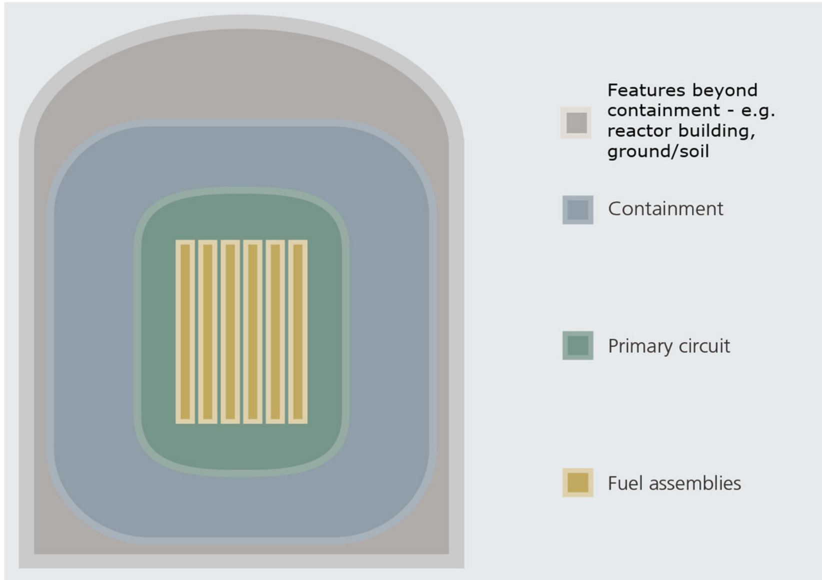

Figure 1-1: Barriers to radioactivity release

For advanced reactors and small modular reactors that are intended to be placed underground, these features may include the radioactivity retention through the ground, which may be assessed through exfiltration analysis. The technical approach of this study as illustrated in Figure 1-2, includes characterizing the aerosol transport pathway and discretely assessing the decontamination factor associated with each step in the pathway. Considering the current BWRs are above ground, prior decontamination assessments have been limited to the containment vessel, however it is expected that future designs such as the GE BWRX-300 will be below ground. Hence, this study identifies the full aerosol transport pathway, to include systems and features beyond the containment vessel. As described in the technical approach section, the study leverages prior knowledge from studies that were limited to the containment vessel, and hence, the referenced phenomena of interest are limited to the containment vessel. However, the results of this study will inform future research to characterize the aerosol transport pathway and additional barriers beyond the containment vessel.

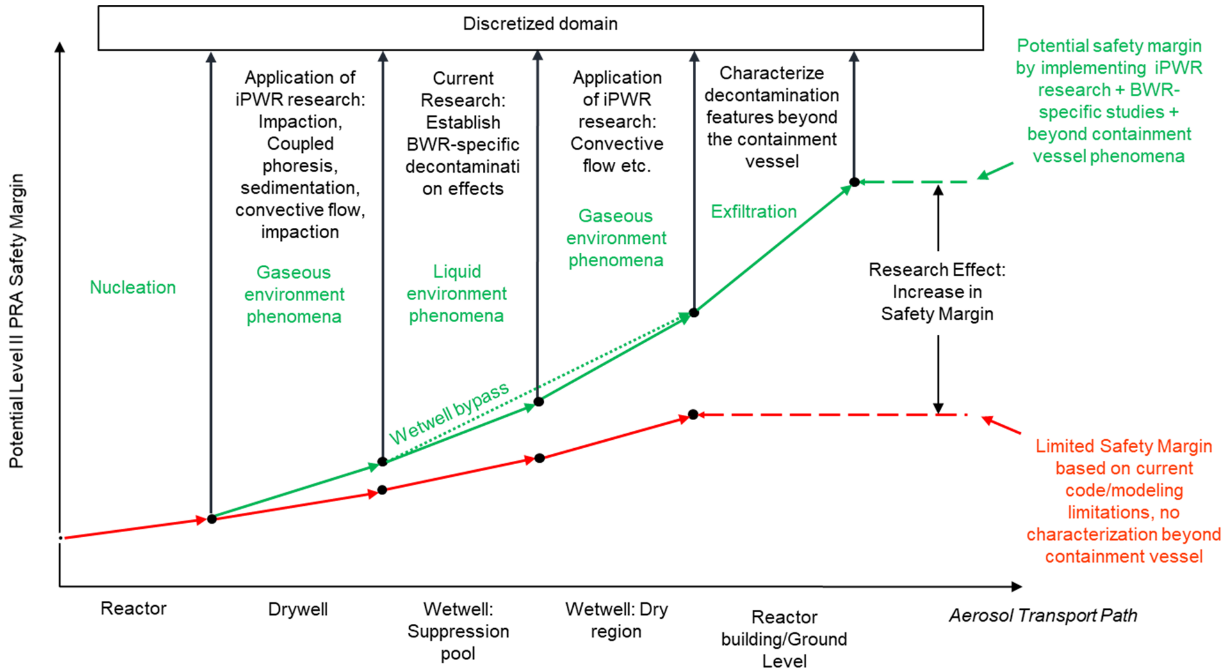

Figure 1-2: Discretized aerosol transport pathway

The outcomes of this study will provide stakeholders with the information required to advance and inform regulatory positions related to A-BWR source terms. The final outcomes of the research activities may be used by safety analysts to calculate mechanistic source-terms and address NRC SECY 10-0034 licensing requirements. In addition, understanding the mechanistic source-terms and passive mechanisms such as higher-pressure condensation within containment or in-containment behavior of fission products, aids in understanding the timing of release of radionuclides into the environment relative to the initiation of core melt and vessel damage. Broadly, the final outcomes of this project are a set of recommendations to improve the characterization of post-accident A-BWR radionuclide particle source-terms, which can provide the technical basis to support possible regulatory amendments to source terms.

In summary, the objectives of the project include:

1. Improve the characterization of mechanistic source terms associated with post-accident fission product release for SMR BWRs.
2. Develop a roadmap that leverages prior research and lessons learned from the iPWR aerosol project to achieve synergy and research efficiency.
3. Describe the subsequent activities and work scopes required to develop BWR SMR-specific fission product deposition models in future phases.
4. Provide stakeholders information required to advance and inform regulatory positions related to A-BWR source terms

1.2 Summary of Results and Major Findings

1. For SMR-Type Advanced BWRs:
    - The current assumptions for large BWR in-containment fission product removal may not be appropriate for SMR type BWRs. Specifically, the critical parameters for fission product retention analysis, which include aerosol characteristics, thermal hydraulic environment, geometry, and systemic features are significantly different for the BWRX-300 design. An example of this is the material density, which in the ex-vessel phase is estimated to be between 3.50 to 6.15 g/cm^3 due in part to the "vigorous interaction between core debris and concrete" (NRC, 1996). Considering there is no concrete in the BWRX-300 containment under consideration, the aerosol material density is expected to be higher than this range. It is recommended that the subsequent phase of this study includes a characterization of the constitution of the aerosolized radionuclides for BWRX-300.
    - The critical parameters that determine the limits of applicability of the existing iPWR data and models have been described and provided for comparison with the BWRX-300 characteristics. Per NUREG 6189, the naturally occurring deposition phenomena for the BWR drywell and the PWR containment vessel are similar (NRC, 1996). Therefore, the following improvements made to the theoretical constructs of these phenomena the iPWR Phase 2 project should apply to the BWR drywell phenomena, and also to the BWRX-300, as it is assumed that the large BWR parameters bound the BWRX-300:
        1. Consideration of the Cunningham Slip Correction factor for diffusiophoresis.
        2. Use of local gradients to calculate thermophoresis and diffusiophoresis velocities.
        3. Characterization of fluid flow inside the containment.
        4. Discretized thermal hydraulic zones of influence (superheated, saturation and condensation) for thermophoretic, diffusiophoretic and impaction phenomena respectively.

2. For Larger Advanced BWRs:
    - To reflect the effects of particle-laden bubbles on aerosol deposition, it is proposed that future studies characterize a drag modification factor, which quantifies the drag influence of particles on the bubble velocity through a force analysis.

3. Modeling and Simulation Opportunities:
    - The current fission product deposition models, which use large LWR data, may not be applicable to SMRs based on the stated limits of applicability in the US NRC reference that provides correlations for fission product deposition estimates related to reactor power (NRC, 1996).
    - Examination of A-BWR models and codes has identified opportunities to modify existing codes for more specific and refined analyses of fission product deposition.

An example is characterization of convective flow as an applicable fission product transport and deposition mechanism. Considering convective flow has not been included as an applicable fission product removal mechanism in containment vessels, this study provides the basis for attribution of this mechanism. The results could be factored into codes that use the similitude approach by inclusion of correlations for turbulence and impaction.

- Support the enhancement of existing codes by developing analytical inputs that improve the existing frameworks, model fidelity and confidence associated with outputs. An example of this is the development of drag modification factors that can be included in existing codes.

4. Applicability of existing regulatory-recognized analytical frameworks and correlations to advanced boiling water reactors:
    - As described in Section 4.1, the existing correlations for aerosol decontamination estimates may not be directly applicable to advanced reactors. The existing correlations as described in references such as NUREG 6189 relate power to decontamination estimates, and the power ranges for the advanced reactors are outside of the range of applicability described in NUREG 6189. However, there are thermal hydraulic parameters that are similar. Hence, on a phenomenological basis, similar methods and models may be used to perform deposition estimates between the reactor types. For application of the simplified models provided in NUREG 6153 and 6189, there is a need to establish specific correlations for the advanced reactors based on their power range.

2 A-BWR Descriptions

The advanced BWR designs that were examined for the current project include the following:

- **Advanced Boiling Water Reactor (ABWR), General Electric-Hitachi**: The ABWR has a relatively simpler design with enhanced safety features than Gen I and II reactors. It includes a compact reactor building and reactor internal pumps for enhanced water circulation, more sophisticated control systems that increase the overall plant safety through monitoring, control and diagnostics, and a compact structure with an improved seismic response. The ABWR containment building houses a suppression pool for protection against over-pressurization and has a power output of 1371 MWe (GE-Hitachi, 2007).
- **Economic Simplified Boiling Water Reactor (ESBWR), General Electric-Hitachi**: The ESBWR builds on the ABWR design and employs passive safety design features such as the Passive Containment Cooling System (PCCS), which protects the containment from over-pressurization. It eliminates about 25% of the pumps, valves and motors for an overall simplified safety system. It also houses a suppression pool like the ABWR and has a power output of 1600 MWe (GE-Hitachi, 2011). A progression of the development of BWR designs is shown in Figure 2-1.

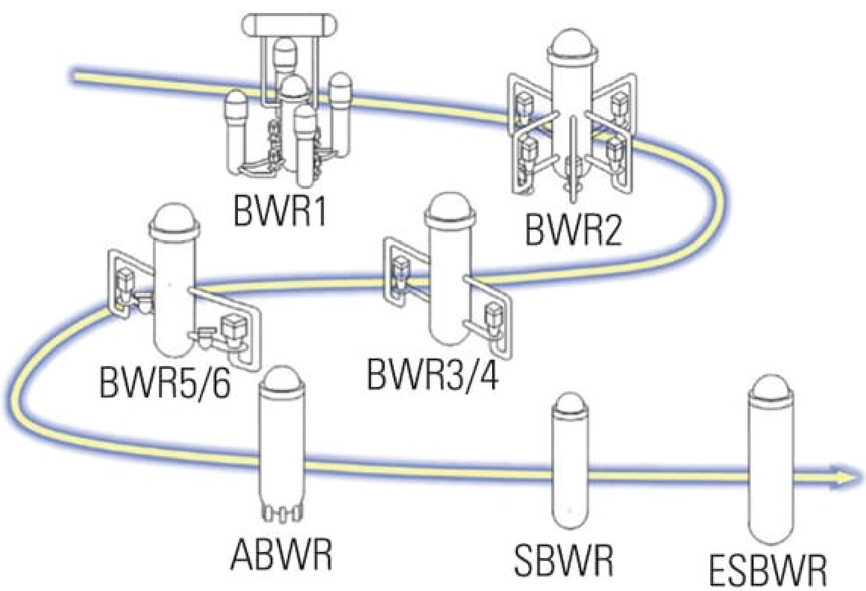

Figure 2-1: Evolution of Boiling Water Reactors (GE-Hitachi, 2011)

- **Boiling Water Reactor X-300 (BWRX-300), General Electric-Hitachi**: The BWRX-300 is a small modular reactor with a power output of 300 MWe. As shown in Figure 2-2, the BWRX-300 is a simpler and more compact design than the ESBWR, which eliminates several systems such as the suppression pool and the PCCS. The BWRX-300 design is still in development as of the publication date of this report, and as such the final design parameters are yet to be established. For the purposes of this study the critical fission product parameters are assumed to be bounded by the A-BWR and ESBWR parameters.

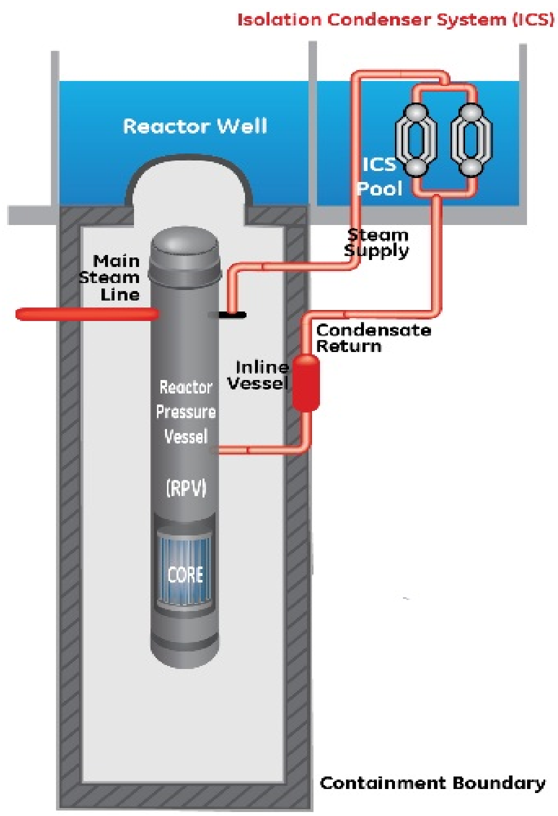

Figure 2-2: BWRX-300 Concept (GE-Hitachi, 2018)

A-BWR reactor types, and critical parameters associated with the reactor vessel (RV), drywell, wetwell, and related geometric characteristics were identified and documented in Table 2-1. Critical parameters are provided in Table 2-2, while the volume and related geometric characteristics are provided in Table 2-3.

Table 2-1: General information for the three A-BWR reactor types (GE-Hitachi, 2007) (GE-Hitachi, 2011) (GE-Hitachi, 2018)

Reactor type	ABWR	ESBWR	BWRX-300
Design Type	Gen III	Gen III+	Gen III+
Circulation	Forced + Natural	Natural	Natural
Primary Containment	• Reinforced Concrete • Smaller than Mark III • Integrated with reactor building • Design pressure 0.31 MPaG	• Similar to ABWR • Design pressure 0.31 MPaG • Accommodates Passive Containment Cooling System (PCCS)	Metal containment Concrete holder
Wetwell	Yes	Yes	No
Power	1350-1460 (1371) MWe	1600 MWe	300 MWe
Passive Safety Features	• Passive deposition phenomena in the drywell • Suppression pool present	• Passive deposition phenomena in the drywell • Suppression pool present • PCCS	• Passive deposition phenomena in the drywell • Passive cooling isolation condenser system (ICS)

Table 2-2: Reactor vessel parameters, drywell parameters, and wetwell parameters for the three A-BWR reactor types (GE-Hitachi, 2007) (GE-Hitachi, 2011)

Reactor type	ABWR	ESBWR	BWRX-300
Reactor Vessel Parameters			
Operating Pressure [MPa]	7.17	7.17	NA
Design Pressure [MPa]	8.62	8.62	NA
Operating Temperature [^{0}C]	287.5	287.5	NA
Drywell Parameters			
Operating Pressure [kPa]	104.1	104.1	NA
Design Pressure [kPa]	411.2	411.3	NA
Design Temperature [^{0}C]	171.1	171	NA
Operating Temperature [^{0}C]	NA	57.2	NA
Wetwell Parameters			
Operating Pressure [kPa]	104.1	104.1	NA
Design Pressure [kPa]	411.2	411.3	NA
Design Temperature [^{0}C]	103.9	NA	
Operating Temperature [^{0}C]	35	43.3	NA
NA – Information Not Available			

Table 2-3: Volume and related geometric characteristics for the three A-BWR reactor types

Reactor type	ABWR	ESBWR	BWRX-300
Safety Building Volume [m^3]	247,800	210,000	NA
Drywell Volume [m^3]	7350	7206	NA
Wetwell Volume [m^3]	5960	5350	NA
SP Volume [m^3]	3580	4424	N/A
Max SP Depth [m]	7	5.5	N/A
SP Depth (operation) [m]	5.45	5.45	N/A
NA – Information Not Available **N/A – Not Applicable**			

2.1 Description of Applicable Passive Deposition Phenomena of Interest

Aerosolized fission product behavior is significantly influenced by the environment within which thermal hydraulic and geometric elements exist that drive the deposition mechanisms. Hence, to develop a better understanding of the applicable passive deposition phenomena, the phenomena are categorized based on the environment in which they apply. The three A-BWR designs under consideration all have a drywell, while the ABWR and ESBWR also have a wetwell which houses a suppression pool that aids with passive aerosol decontamination. Thus, the environment in which aerosol processes occur are categorized into the following types:

- **Category 1**: Phenomena applicable to a gaseous environment, associated with the aerosols in the drywell that bypass the wetwell before deposition, and aerosols entering the dry region of the wetwell after escaping from the suppression pool, including:
    - Phenomenon P1: Sedimentation/Gravitational Settling
    - Phenomenon P2: Thermophoresis
    - Phenomenon P3: Diffusiophoresis
    - Phenomenon P4: Fluid Flow
    - Phenomenon P5: Agglomeration/Coagulation
    - Phenomenon P6: Impaction
    - Phenomenon P7: Aerosol Behavior during Pressure Transients
- **Category 2**: Phenomena applicable to a liquid environment, associated with aerosols flowing and depositing into the suppression pool housed inside the wetwell, including:
    - Phenomenon P8: Aerosol Behavior during Direct Contact Steam Condensation
    - Phenomenon P9: Aerosol Interaction with Bubble Processes
    - Phenomenon P10: Aerosol Behavior due to Effects of Suppression Pool Parameters

The phenomena and associated parameters are tightly coupled, and uncertainties exist in the behavior of the phenomena. Figure 2-3 illustrates the coupling of Category 1 phenomena, while Figure 2-4 illustrates the coupling of Category 2 phenomena. For example, referring to Figure 2-3 for Category 1 Phenomenon P6 (Aerosol Deposition by Impaction), it is seen that Phenomenon P6 is coupled with Phenomenon P4 (Aerosol Behavior due to Fluid Flow), and both are affected by the thermal gradient. For notational purposes, the primary parameters are defined as those parameters independent of the environment. The distinction between primary parameters and secondary parameters is that secondary parameters are calculated based on values of the primary parameters.

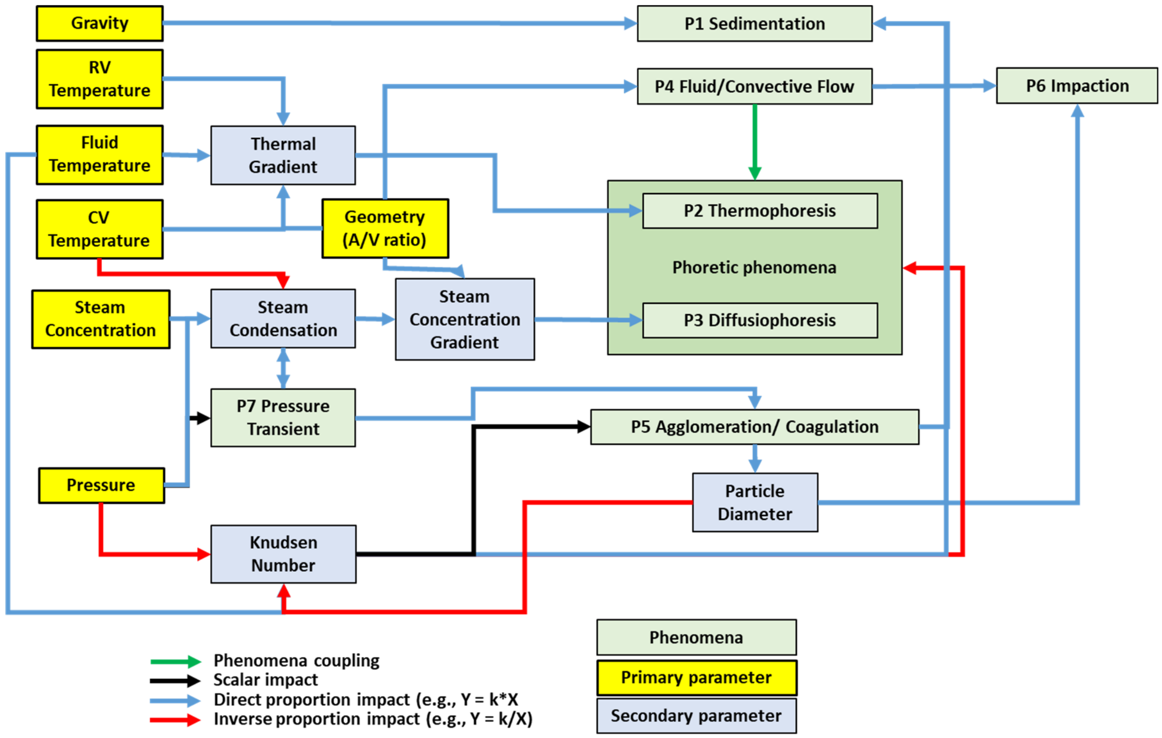

Figure 2-3: Category 1 (gaseous environment) phenomena coupling and uncertainties

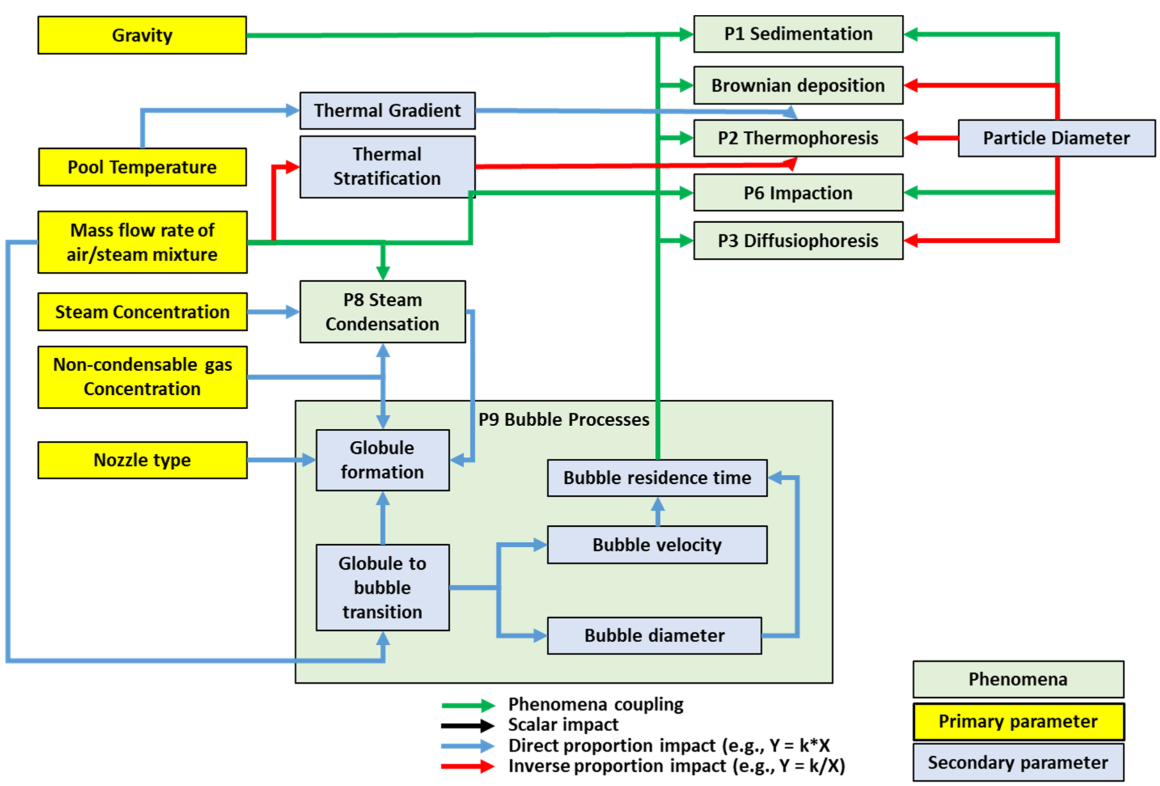

Figure 2-4: Category 2 (liquid environment) phenomena coupling and uncertainties

2.1.1 Category 1: Phenomena applicable to a gaseous environment

In the event of accidental steam release, the A-BWR drywell pressure and temperature will increase. The steam includes radionuclide particles, which are subject to various phenomena that affect their physical behavior and make them deposit on containment surfaces. These phenomena, applicable to a gaseous environment, are described as follows:

2.1.1.1 Phenomenon P1: Aerosol Behavior due to Sedimentation/Gravitational Settling

Sedimentation is the process of particle transport and deposition due to gravity. Sedimentation in iPWRs was studied experimentally and through CFD simulations with the Pittsburgh Technical Advanced Reactor Computational fluid dynamics Code (ARCC) model developed during Phase 2 of EPRI's iPWR aerosol study (EPRI, 2018a). It was confirmed that with increasing particle size, sedimentation is enhanced (EPRI, 2018b). A-BWR specific considerations for sedimentation as a deposition mechanism will be assessed as part of the current project. The equation to calculate the sedimentation velocity is given by (EPRI, 2018a):

$$v_g = -\frac{C_c \rho_p d_p^2 g}{18\mu_g} \qquad \text{Equation (2-1)}$$

2.1.1.2 Phenomenon P2: Aerosol Behavior due to Thermophoresis

Thermophoresis is the process of aerosol transport in the presence of a thermal gradient. This is due to an imbalance of forces caused by more energetic gas molecules striking a particle on the warmer side, than the less energetic molecules that are striking the particle's cooler side. In nuclear reactors, the thermophoretic deposition is due to the thermal gradient resulting from the temperature difference between the reactor vessel and containment vessel (CV) walls. The applicability of thermophoresis in iPWRs was studied experimentally and through CFD simulations with the ARCC model during Phase 2 of EPRI's iPWR aerosol study (EPRI, 2018a). While thermophoresis decreases marginally with increasing particle size, the depositional velocity attributable to thermophoresis is relatively low (EPRI, 2018b). It was also established that there is a coupling effect between the phoretic mechanisms of diffusiophoresis and thermophoresis that creates a higher combined velocity magnitude than the sum of their individual velocities (EPRI, 2018b). The applicability of thermophoresis as a deposition mechanism for A-BWRs will be analyzed during the current project. The equation to calculate thermophoresis velocity is given by (EPRI, 2018a):

$$v_t = -\frac{2\mu_g C_c M_s\left(\frac{k_g}{k_p}+C_t Kn\right)}{\bar{\rho}(1+3C_m Kn)\left(1+2\frac{k_g}{k_p}+2C_t Kn\right)}\frac{1}{T_p}\frac{\partial \tilde{T}}{\partial n} \qquad \text{Equation (2-2)}$$

2.1.1.3 Phenomenon P3: Aerosol Behavior due to Diffusiophoresis

Diffusiophoresis is the movement of a particle due to concentration gradients of the component gases in a gas mixture. In nuclear reactors, the diffusiophoretic deposition is due to the steam concentration gradient at the relatively cooler CV wall, where steam condensation takes place. This condensation creates a radial steam concentration gradient, with the highest steam concentration at the RV wall and the lowest steam concentration at the CV wall (where steam exists as water). The applicability of diffusiophoresis in iPWRs was studied experimentally and through CFD simulations with the ARCC model during Phase 2 of EPRI's iPWR aerosol study (EPRI, 2018a). While diffusiophoresis decreases marginally with increasing particle size, it is a powerful deposition mechanism, and is particularly useful for the deposition of smaller particles with negligible sedimentation velocities (EPRI, 2018b). The applicability of diffusiophoresis as a deposition mechanism for A-BWRs will be analyzed during the current project. The equation to calculate diffusiophoresis is given by (EPRI, 2018a):

$$v_d = -\frac{C_c\sqrt{M_s}}{X_s\sqrt{M_s}+X_a\sqrt{M_a}}\frac{\dot{m}''_{cond}}{\bar{\rho}} \qquad \text{Equation (2-3)}$$

2.1.1.4 Phenomenon P4: Aerosol Behavior due to Fluid Flow

Fluid flow inside the A-BWR drywell will influence the overall aerosol transport and deposition. During Phase 2 of EPRI's iPWR study, convective flow due to the temperature difference between the RV and CV walls and fluid buoyancy was observed inside the iPWR CV volume, both experimentally and through CFD simulations with the ARCC model. Convective flow was found to be a powerful aerosol transport and deposition mechanism, enhancing aerosol deposition by other mechanisms (EPRI, 2018b). Depending on the A-BWR vessel geometry and thermal-hydraulic parameters, the fluid flow inside the drywell will be analyzed as part of the current project. The drift-flux model, developed during Phase 2a of EPRI's iPWR aerosol study, can be used for coupling deposition velocities to the fluid flow velocity, thereby incorporating effects of fluid flow on aerosol deposition (EPRI, 2018a).

2.1.1.5 Phenomenon P5: Aerosol Behavior due to Agglomeration/Coagulation

Agglomeration is the process of inelastic particle collisions that result in the formation of a larger particle or agglomerate. An increase in particle size through agglomeration typically results in faster particle deposition due to the exponential relationship between sedimentation velocity and the particle diameter. Hence, theoretically, agglomeration results in an increase in particle mass (and/or volume/density), which increases decontamination rates. It should also be noted that agglomeration may occur without a net increase in density, due to the voids and interstitial spaces in the volume that may be created between particles in the agglomerate. Assumption of no agglomeration increases the conservatism associated with aerosol decontamination. It is therefore necessary to characterize the effects of this phenomenon for appropriate attribution of decontamination credit.

Agglomeration is applicable to the pressurization phase of the accident transient, where smaller particles may agglomerate to larger sizes. Nuclear aerosol codes typically assume inelastic particle collisions, resulting in particle growth which changes the aerosol size distribution and enhances the gravitational settling rate. Agglomeration has the potential to be very significant at high particle concentrations (NEA, 2009). Agglomeration depends on the Knudsen number (Dekkers & Friedlander, 2002), which in turn varies with particle diameter, temperature and pressure (NEA, 2009). Thermal-hydraulic parameters such as pressure, reduce the rate of agglomeration, while effects of temperature are not as pronounced (Dekkers & Friedlander, 2002).

Agglomeration can be classified into four types, based on the particle deposition mechanism that leads to the process: (1) Brownian diffusion, (2) Sedimentation, (3) Turbulent shear, and (4) Turbulent acceleration in eddies. These processes depend on the physical properties of the fluid and the particles. Due to the irregularity of these particles, agglomeration modeling is based on parameters such as the agglomeration/collision shape factor (γ), the dynamic shape factor (χ) and the spherical-equivalent particle diameter (d_p) (Sandia National Laboratories, 1997). Shape factors are necessary to characterize agglomeration due to the fractal nature of agglomerates (particle sizes not proportional to the cube root of the particle volume), which may affect particle behavior (NEA, 2009).

Agglomeration typically takes place when particle concentration is high (> 1 g/cc) since that increases the probability of inelastic particle collisions. It causes changes to the particle size distribution (which may change the overall decontamination characteristics), and consequently, particle concentration. The number concentration is therefore an important parameter, given by the following equation (NEA, State-of-the-art Report on Nuclear Aerosols, 2009):

$$N(t) = \frac{N_0}{1+N_0Kt} \qquad \text{Equation (2-4)}$$

Where, N_0 is the initial number concentration, $N(t)$ is the number concentration at time t, K (= 3.5e-10 cm^3/s for $d_p \geq 1$ μm) is the rate constant, and t is the time (s). The calculation of average particle diameter (given by the following equation) provides a measure of the agglomeration within time t:

$$d_p(t) = d_0\left(\frac{N_0}{N(t)}\right)^{1/3} \qquad \text{Equation (2-5)}$$

Where, $d_p(t)$ is the particle diameter at time t, and d_0 is the initial average particle diameter.

Growth of particles due to agglomeration leads to structures with similarities over a large range of scales (fractal nature of agglomerates). In such a case, the mass of these structure scales with their radius as given by the following equation (Jimenez, et al., 2003):

$$m \approx m_1\kappa\left(\frac{r}{r_1}\right)^{D_f} \qquad \text{Equation (2-6)}$$

Where, m_1 and r_1 are mass and radius of the primary particles, κ is an empirically derived constant of order unity, and D_f is the mass fractal dimension. This gives the radius r in terms of the other parameters, as follows:

$$r \approx r_1\left(\frac{m}{\kappa m_1}\right)^{\frac{1}{D_f}} \qquad \text{Equation (2-7)}$$

Small D_f values indicate open structures with large volumes. $D_f = 1$ indicates a linear chain of particles, while $D_f = 3$ corresponds to a solid sphere. The D_f value provides insights into the processes and mechanisms affecting particle structure.

Coagulation, which is a clustering of particles following vapor condensation, is a process related to agglomeration that also results in an increase in particle size (NEA, 2009). Coagulation can be classified into four types, based on the particle deposition mechanism that leads to the process (NRC, 1996): (1) Gravitational Coagulation (large particles that have exponentially larger gravitational settling velocities, may sweep out smaller particles along their flow path), (2) Brownian Coagulation (for small particles (< 1 μm), particles may intersect other particles across flow paths due to Brownian motion), (3) Turbulent Diffusion Coagulation (turbulent motion of the gas molecules may drive diffusion of particles), and (4) Turbulent Inertial Coagulation (slow moving particles that are unable to respond to acceleration of the gas phase, may cross streamlines of the flow and intersect other particles). Equations for the agglomeration kernels for the above mechanisms are provided in NRC NUREG 6189 (NRC, 1996).

This preliminary feasibility study has described agglomeration and coagulation as potential contributors to fission product transport and deposition. The relative significance of these phenomena will be established in future phases of this work scope, through empirical data and model simulation.

2.1.1.6 Phenomenon P6: Aerosol Deposition by Impaction

Impaction is a process by which aerosolized particles are removed from a fluid stream and deposited on the walls of the carrier vessel based on the momentum of the particle relative to the fluid. This relative motion may be due to the particle inertia, carrier fluid characteristics or geometry of the carrier vessel.

For impaction due to particle inertia, the process is called turbulent inertial deposition, which occurs in the turbulent diffusion eddy impaction regime, when the turbulence of the particles is high enough to penetrate the boundary layer. For impaction effects due to the carrier gas characteristics, the relevant parameters include the thermal gradient, system pressure, Knudsen number and boundary conditions such as a thermal gradient on the CV wall. For impaction due to carrier vessel geometry such as bends, the particle inertia may cause the particles to collide with the vessel walls due to an inability to stay in the stream (Peters & Leith, 2004).

Impaction has been studied experimentally; experiments range from calculation of the collection efficiency of a filter (Kasper, Schollmeier, Meyer, & Hoferer, 2009), impaction in industrial bends (Peters & Leith, 2004), impaction on a cylinder in turbulent cross-flow (Aarnes, Haugen, & Anderson, 2018), impaction on two square cylinders in laminar mixed-convection flow (Goharrizi & Sadeghi, 2009), and the safety assessment and the environmental impact statement for nuclear fuel cycle facilities (Sutter, Johnston, & Mishima, 1981). The Stokes number (Stk), which is the ratio of the characteristic times of a particle to the flow or obstacle, has been identified as a key parameter for most impaction studies. It was found that a Stokes number greater than 0.3 resulted in particle deposition by impaction (Kasper, Schollmeier, Meyer, & Hoferer, 2009).

A model for a duct flow with a Reynolds number (Re) lower than 10000 can be used to evaluate impaction efficiency for both laminar (Re < 3000) and moderately turbulent flow (3000 < Re < 10000). The Stokes and Reynolds numbers are calculated using the following equations (Sher & Hobbins, 2011):

$$Stk = \frac{\rho_p d_p^2 U_f}{18\mu_f d_c} \qquad \text{Equation (2-8)}$$

$$Re = \frac{\rho_f U_f d_c}{\mu_f} \qquad \text{Equation (2-9)}$$

Where, ρ_p is the particle density, d_p is the particle diameter, ρ_f is the fluid density, U_f is the fluid velocity, μ_f is the fluid dynamic viscosity, and d_c is the characteristic length for the fluid flow, which in this case is the width of the flow field. Based on the Reynolds number and the bend angle (φ), impaction efficiencies for laminar and turbulent flow are given by (Sher & Hobbins, 2011):

$$\varepsilon_{Laminar} = Stk\varphi \qquad \text{Equation (2-10)}$$

$$\varepsilon_{Turbulent} = 1 - 10^{(-1.412Stk\varphi)} \qquad \text{Equation (2-11)}$$

Impaction is highly dependent on the carrier gas flow, which is in turn dependent on the thermal gradient and the system pressure. Impaction is also dependent on particle diameter and velocities, which means that it is dependent on the Knudsen number, boundary conditions such as a thermal gradient on the CV wall, and agglomeration, which may serve to increase particle inertia by increasing particle diameter.

A mechanistic model to predict particle deposition on containment finned tube heat exchangers by modeling diffusiophoresis, sedimentation and impaction has been developed and implemented into the FORTRAN code TAEROSOL, using a Monte Carlo method (Munoz-Cobo, Pena, Herranz, & Perez-Navarro, 2005). Numerical simulation of particle deposition in turbulent boundary layers in duct flows has been performed to estimate deposition by impaction, which was found to be a significant deposition mechanism for a particle diameter range of 1-50 µm (Kallio & Reeks, 1988). CFD has been used to model deposition by impaction; this phenomenon has been incorporated in the CFD code Fuego by Sandia National Laboratories, with good agreement with experimental data (Rodriguez, Mueller, & Merryman, 2016).

Particle deposition by impaction was assessed during Phase 2a of EPRI's iPWR aerosol study (EPRI, 2018a). It was determined that impaction was likely to be minimal, and Phase 2b of EPRI's iPWR aerosol study demonstrated minimal impaction at the selected location, for both wet and dry environmental conditions (EPRI, 2018b). However, it is important to note that impaction is a location-specific phenomenon, and that low impaction at one location may not imply low impaction at other locations. Therefore, this phenomenon has significant sources of uncertainties due to the influence of other phenomena and conditions. Hence, to establish the contribution of impaction for the BWRX-300 design, the specific geometry and thermal hydraulic conditions should be emulated experimentally and simulated by applicable models. This should be included in future work scopes.

2.1.1.7 Phenomenon P7: Aerosol Behavior during Pressure Transients

Initial and overall pressure is an important thermal-hydraulic parameter that affects several other parameters. As observed during Phase 2b of EPRI's iPWR aerosol study, pressure affects the dew point of steam, which decreases with decreasing pressure (EPRI, 2018b). This results in lower steam condensation and fluctuation of the dew point plane, which affects the steam concentration gradient and consequently, diffusiophoresis (Biwalkar & Talabi, 2018). Incidentally, the cessation of diffusiophoresis was observed at low pressure, owing to an unfavorable environment for condensation on the CV wall, since the difference between the CV wall temperature and the dew point temperature affects the occurrence of condensation (EPRI, 2018b).

The pressure transient phase commonly occurs in the event of a Loss of Coolant Accident (LOCA), when highly pressurized water escapes from the primary circuit into the CV, transforming into steam in the process, due to the lower CV pressure. It is during this phase that aerosol formation takes place inside the containment. Pressure also influences key aerosol processes, such as agglomeration, the fluid flow regime, and steam condensation. Therefore, an assessment of the pressurization phase is necessary to determine the influence of pressure on aerosol formation, concentration and distribution.

Pressurization may occur due to several causes, such as an increase in fluid mass or temperature (as in a LOCA), or due to aerosol formation by a burst, which is a rapid process taking place when a vapor becomes supersaturated (Barrett & Clement, 1990). Characterization of the effect of various pressurization rates on aerosol formation, concentration and particle size will allow application of the current study to a wider range of accident scenarios (EPRI, 2018b). Pressurization may lead to a state in which the change in pressure could lead to more boiling and thus possible resuspension. Therefore, it is recommended to assess the effects of transient aerosol concentrations during pressurization.

For large A-BWRs, drywell pressurization due to a LOCA will result in opening of valves between the drywell and the wetwell, causing a mixture of air and steam to flow into the suppression pool (housed by the wetwell) and resulting in overall depressurization. However, there are uncertainties associated with the time in which this will happen, as well as the aerosols that bypass the suppression pool altogether. Therefore, it is important to consider the effects of pressurization on aerosol formation and deposition inside the drywell.

Depressurization is the process of pressure reduction inside the drywell, which may occur as a result of temperature decrease (due to heat loss) or loss of gaseous mass (due to steam condensation, containment leakage, flow of steam and air into the suppression pool). Depressurization may affect assumptions around the performance of the deposition phenomena and the decontamination factors. In Phase 2b of the referenced EPRI aerosol study, depressurization was observed experimentally and through CFD simulations (with the ARCC model) due to heat and gaseous mass loss during steam condensation. Depressurization results in a reduction in condensation rate, diffusiophoretic velocity, and consequently, aerosol deposition rates (EPRI, 2018b). Pressure can affect agglomeration and impaction as well. A decrease in pressure will increase the Knudsen number, but since temperature is directly proportional to pressure, the variation of the Knudsen number with pressure needs to be properly characterized in order to understand its effects on agglomeration. This is a major source of uncertainty in characterizing depressurization effects. Therefore, it is important to build on the knowledge gained from Phase 2b of EPRI's iPWR study for applicability to the current project.

2.1.2 Category 2: Phenomena applicable to a liquid environment (in large BWRs)

In the event of accidental steam release, the A-BWR drywell pressure and temperature will increase. The mixture of steam, non-condensable gases and radionuclide particles flows into the suppression pool (housed inside the wetwell) and is subject to various phenomena that affect aerosol deposition inside the pool. Aerosol deposition inside a suppression pool can be characterized based on decontamination coefficients (α_i) which can be defined for every aerosol deposition mechanism by the following equation:

$$\frac{dm(x)}{dx} = -\alpha_i m(x)$$ Equation (2-12)

Where, x [m] is the distance inside the pool above the point of particle entrance, and m(x) [kg] is the aerosol mass at distance x.

The pool decontamination factor (DF) is defined as:

$$DF = \frac{m_{in}}{m_{out}}$$ Equation (2-13)

Where, m_{in} [kg] is the aerosol mass entering the pool, and m_{out} [kg] is the aerosol mass leaving the pool. Both m_{in} and m_{out} (and consequently, the DF) are functions of the decontamination coefficients associated with different aerosol deposition mechanisms, which in turn depend on steam condensation, bubble processes (formation, size, shape, rise velocity), fluid properties (surface tension, viscosity), particle properties (size, distribution, density) and the suppression pool parameters (pool height, nozzle submergence depth, temperature). Steam condensation is enhanced when the pool is more subcooled due to the difference between the pool temperature and the boiling point of water. Therefore, the DF for subcooled pools is generally significant. The DF is also affected by the steam mass fraction within the inlet gaseous mixture.

The phenomena applicable to a liquid environment are described as follows.

2.1.2.1 Phenomenon P8: Aerosol Behavior during Direct Contact Steam Condensation

Underwater condensation of steam (directly in contact with water) is referred to as Direct Contact Condensation (DCC) (Chun, Kim, & Park, 1996). DCC takes place inside the suppression pool, when the steam entering the pool condenses and forms water. The process of steam condensation affects aerosol deposition inside the suppression pool, as well as key processes such as bubble formation, which are necessary in the determination of the decontamination factor (DF).

Experimentally, it has been found that the flow rate of the steam/non-condensable gas mixture and the steam mass flux determine the stability of DCC. Steam condensation in the inlet jet is stable in case of a large steam mass flux, while a low flow rate results in unstable condensation oscillation/cyclic condensation and chugging condensation (i.e. quick bubble pressurization). Therefore, to ensure stable steam DCC, a large steam mass flow rate is recommended (Pellegrini, et al., 2016). The unstable chugging condensation regime of steam condensation is characterized by the creation of a bubble at the end of the pipe, which quickly collapses and establishes a depressurization in the steam. This moves water backward into the pipe, until a new cycle is started over. This process, which involves large condensation and pressure spikes, creates instability.

Chugging condensation can be mitigated by the presence of air or non-condensable gases, due to an absence of large depressurization. It was also observed that a small discharge hole for the air/steam mixture while entering the suppression pool results in a jet/bubbling regime, while a larger hole gives rise to the chugging/oscillating regime. This leads to the inference that the fluid inlet velocity influences steam condensation as well.

Multiphase flow models are recommended for modeling of DCC, which makes it challenging. A study conducted at the POOLEX facility developed frequency and pattern recognition algorithms for DCC (Tanskanen, Jordan, Puustinen, & Kyrki-Rajamaki, 2013). The Particle Image Velocimetry (PIV) laser system has also been used to measure and evaluate the instantaneous fluid flow velocity fields during DCC (Cai, Jo, & Okamoto, 2015). Validation and development of DCC models that can capture interfacial condensation rate correctly using CFD is recommended.

In the current study, the modeling of DCC is an important consideration because the stability of the condensation regime affects aerosol deposition. Steam condensation enhances aerosol deposition, and the DF increases with aerosol carrier flow rate. Steam condensation moves particles to the surface of the suppression pool due to differences in vapor pressure (Escriche, 2017). Therefore, accurate characterization of steam condensation is necessary to understand its effects on aerosol deposition inside the suppression pool. In addition, it is also important to consider Brownian diffusion (random motion of particles suspended in a fluid) as an aerosol deposition mechanism in the context of particle-fluid interactions, since the liquid droplets can capture small aerosol particles by diffusion (Berna, Escriva, Munoz-Cobo, & Herranz, 2015).

2.1.2.2 Phenomenon P9: Aerosol Interaction with Bubble Processes

In the event of steam release due to a BWR accident, aerosols enter the suppression pool via a mixture of steam and non-condensable gases. Steam condensation takes place within the suppression pool, giving rise to bubble formation and particle entrainment inside the bubbles. Large bubbles first form at the inlet orifice, followed by detachment, disintegration into smaller bubbles, and rise through the pool in form of a plume (NRC, 1997). Particle entrainment inside bubbles can take place during transport to the suppression pool, bubble formation, bubble disintegration, and bubble rise. The entrained particles can deposit internally on the bubble surface by phenomena such as sedimentation, inertial impaction, and Brownian diffusion; these particles are then absorbed and retained in the liquid. The particles that are not absorbed escape to the dry region of the wetwell once the bubble breaks the pool surface (Sher & Hobbins, Aerosol Deposition Mechanisms, 2011).

Significant considerations for aerosol interaction with bubble processes are itemized as follows:

i. Active aerosol deposition mechanisms during bubble residence time are sedimentation, inertial impaction and Brownian diffusion (theoretical constructs presented herein).
ii. A higher bubble residence time results in more time for these deposition mechanisms to act on the particles entrained within the bubbles and making them deposit on the bubble wall, indicating a higher DF. However, the relative velocity of the bubble to the particle sedimentation velocity and inertia, may also contribute to higher deposition rates. By this logic, increasing bubble rise velocity (swarm velocity) may or may not decrease the DF.

iii. Bubble fragmentation increases the DF due to increased overall bubble surface area.
iv. The effect of particle-laden bubbles should be considered, which include:
   - A higher drag force, which may increase the residence time.
   - Dampening of the amplitude of the bubble rise velocity oscillations, which may affect inertial deposition rates within the bubble, due to relative motion.
   - To reflect the effects of particle-laden bubbles on aerosol deposition, it is proposed that future studies characterize a drag modification factor, which quantifies the drag influence of particles on the bubble velocity through a force analysis (Wang, Cilliers, Neethling, & Brito-Parada, 2019).
   - The partial pressure of water inside a bubble is lower than the equilibrium partial pressure of water inside the suppression pool. This results in a water vapor flux into the bubble, resulting in a Stefan flow which opposes particle transport to the bubble surface. Since the bubble contains a lower water vapor concentration than the pool, a diffusiophoretic force also acts on the particles inside the bubble in the same direction as the Stefan flow. The thermal gradient and thermophoresis are considered to be negligible. However, it has been shown from the prior iPWR study, that thermophoresis, when acting along with diffusiophoresis may create a net effect where the whole is larger than the sum of the parts. Hence, thermophoresis should be evaluated in the context of the potential coupling of other phoretic mechanisms to properly establish its significance.

The following equations can be used to calculate the deposition coefficients associated with Brownian diffusion, sedimentation, and inertial impaction, which are significant mechanisms assisting aerosol deposition on the bubble surface inside the bubble, which allows these aerosols to be absorbed and retained within the liquid:

(1) Brownian Diffusion

$$\alpha_{diff} = 1.8\sqrt{\frac{8u_{diff}}{\pi u_{rise} d_{bubble}^{3}}} \qquad \text{Equation (2-14)}$$

Where, α_{diff} [s^{-1}] is the decontamination coefficient associated with Brownian diffusion, u_{diff} [m/s] is the bubble rise velocity associated with Brownian diffusion, u_{rise} [m/s] is the terminal bubble rise velocity, and d_{bubble} [m] is the bubble diameter.

(2) Sedimentation

$$\alpha_{sed} = \frac{1.5 g u_{sed}}{g u_{rise} d_{bubble}} \qquad \text{Equation (2-15)}$$

Where, u_{sed} [m/s] is the sedimentation velocity.

(3) Inertial Impaction (spherical particles)

$$\alpha_{impact} = \frac{18 u_{rise} u_{sed}}{g d_{bubble}^{2}} \qquad \text{Equation (2-16)}$$

The DF during bubble rise (DF_{rise}) inside a suppression pool of height H [m] for a single particle size is given by the following equation:

$$DF_{rise} = \int_0^{t_{rise}} \int_A \left(\frac{u_n}{\pi a^2 b}\right) dA\, dt \qquad \text{Equation (2-17)}$$

Where, a, b are the major and minor radii of the bubble, t_{rise} (= H/u_{rise}) [s] is the bubble rise time, u_n (= $\sum u_i$) [m/s] is the overall bubble rise velocity, and A [m^2] is the bubble surface area. The overall DF is a product of the DF during bubble rise and the DF associated with bubble formation.

The PASSAM (Passive and Active Systems on Severe Accident source term Mitigation) experimental tests, conducted to estimate the suppression pool scrubbing efficiency while varying experimental conditions such as the mixture flow rate and suppression pool liquid, provide valuable insights on bubble formation and dynamics. Bubble size and velocity were found to be independent of nozzle diameter and mass flow rate. This implies that bubble flow is controlled by buoyancy. Two bubble regimes were observed; initially, the bubble distribution is bimodal, with two dominating bubble diameter ranges, following which disintegration of larger bubbles occurs, resulting in the bubble size distribution becoming lognormal. Bubble formation was also found to be dependent on the composition of the suppression pool water (Albiol , et al., 2017).

Current BWR aerosol safety analysis codes such as SPARC and BUSCA have different ways of modeling bubble dynamics, based on available experimental data at the time these models were developed. It is recommended that the assumptions made in these codes be reviewed, and the modeling be updated based on currently available experimental data. Advanced modeling of aerosol deposition due to bubble processes is recommended to align with experimental data more accurately.

2.1.2.3 Phenomenon P10: Aerosol Behavior due to Effects of Suppression Pool Parameters

Suppression pool parameters such as the pool height, nozzle submergence depth, and nozzle type affect aerosol deposition. A deeper pool, or a more submerged nozzle increases the distance a bubble needs to travel from the nozzle to the pool surface, thereby increasing residence time and subsequently, the DF (Dehbi , Suckow, & Guentay, 2001). The nozzle type (horizontal, vertical, T-type, X-type etc.) affects globule formation during steam condensation, which in turn affects aerosol behavior. Each nozzle type has unique initial globule sizes, which break into stable bubbles (NRC, 1991). For example, in horizontal nozzles, it is assumed that the DF during globule formation is negligible. Similarly, nozzle diameter and the number of holes in a nozzle also affect aerosol retention, since they affect the steam condensation regime.

Following steam condensation, the hot condensate flows upwards in the form of a narrow plume and spreads into a layer on the pool surface. If the plume momentum is insufficient to result in mixing, a stable thermal stratification (separation of the pool into hotter and cooler zones) is formed in the pool. This affects the steam partial pressure in the wetwell and impedes the pool's pressure suppression capacity (Li & Kudinov, 2010). Therefore, for efficient use of the suppression pool for aerosol retention, mixing is necessary to maintain homogeneity. The presence of nitrogen improves pool mixing and homogeneity by improving heat convection; a higher nitrogen concentration leads to better pool mixing and more stable condensation (Cai, Jo, & Okamoto, 2015). Therefore, it is important to optimize the values of steam mass flow rate and nitrogen concentration for better aerosol retention.

2.2 A-BWR Models and Codes Knowledge Base

Fission product transport and deposition models, including analytical codes, are specific to reactor types, which support fission product transport through various phenomenological processes. These phenomena are dependent on aerosol characteristics, geometry and thermal-hydraulic parameters. Existing safety analysis codes and models are largely verified and validated with data from prior experiments performed for current large light water reactors (LLWR), which have fission product attenuation parameters that may be different from small BWRs. These LLWR models, codes, and parameters are generally conservative for use in advanced reactors. However, it should be noted that there may be certain conditions that are not conservative, such as the potential for resuspension in smaller containment vessels, as observed in the related iPWR source term project (EPRI, 2018b).

Examination of A-BWR models and codes during this study may identify opportunities to modify existing codes for more specific and refined analyses of fission product deposition. An example is characterization of convective flow as an applicable fission product transport and deposition mechanism. Since convective flow has not been included as an applicable fission product removal mechanism in containment vessels. This study may provide the basis for attribution of this mechanism. The results could be factored into codes that use the similitude approach by inclusion of correlations for turbulence and impaction.

The knowledge base does not include application tools like the Predictive Capability Maturity Model (PCMM) (SNL, 2007) for the A-BWR models or codes. The PCMM provides a means of addressing six important elements of modeling and simulation (1) representation and geometric fidelity, (2) physics and material model fidelity, (3) code verification, (4) solution verification, (5) model validation, and (6) uncertainty quantification and sensitivity analysis (SNL, 2007). Prioritized phenomena are identified in a Phenomena Identification and Ranking Table (PIRT) assessment, which is performed as part of this study. The PIRT results are needed to initiate PCMM evaluations of A-BWR modeling and simulation capabilities. If required for further insights, PCMM evaluations of A-BWR modeling and simulation capabilities may be performed based upon the phenomena prioritization as part of a future research phase.

2.3 Gap Assessment of Current Suppression Pool Safety Analysis Codes

The purpose of the advanced BWR (A-BWR) gap assessment for suppression pool safety analysis computer codes is to (1) ascertain to what extent experimental data are used in the codes, (2) examine the codes and their computational framework, and (3) examine how the codes model A-BWR phenomena such as hydrodynamics, thermal-hydraulics, and aerosol deposition inside suppression pools. The gap assessment is an input for recommendations for code improvements or refinements. If the codes do not demonstrate a strong capability to model the A-BWR phenomena, this is defined as a gap which requires actions to include, but not limited to, identification of new code requirements or refinements to existing codes, development and demonstration of front-end inputs or interfaces to existing codes, demonstration of code performance for specific A-BWR phenomena, and test plan development for code verification and validation.

Several computer codes have been used for estimation of aerosol retention inside the suppression pool of a Boiling Water Reactor (BWR). Some of these codes include SPARC (Suppression Pool Aerosol Removal Code) (Owczarski & Burk, 1991), BUSCA (Bubble Scrubbing Algorithm) (Ramsdale, Guentay, & Friedrichs, 1995), SUPRA (Suppression Pool Retention Analysis) (Wassel, Mills, Bugby, & Oehlberg, 1984), and more recently, GOTHIC (Generation of Thermal-Hydraulic Information for Containments) (Lane, George, Claybrook, Zankowski, & Kindred, 2019), ASTEC (Albiol , et al., 2017), BMIX++ (Gamble, et al., 2000) and TRACG (Zhao, Zou, & Zhang, 2013). Of these, SPARC, BUSCA and SUPRA are the main codes that have been used for estimation of aerosol deposition inside suppression pools and have been examined in this document. The gaps associated with A-BWR suppression pool safety analysis computer codes SPARC, BUSCA, and SUPRA fall in three general areas, as follows:

1. **Gap Area 1, Lack of pertinent experimental data at the time of model development:** SPARC, BUSCA, and SUPRA were developed prior to 2000 using limited available experimental data. New data are currently available which can be incorporated into current codes for analyses or evaluations. Several assumptions are made in hydrodynamic modeling and bubble formation models due to lack of hydrodynamic experimental data.

2. **Gap Area 2, Application of recent empirical data to existing models:** Advances in empirical data availability and modeling techniques of specific suppression pool phenomena have occurred since initial code development. It is unclear if SPARC, BUSCA, and SUPRA have been updated based on current experimental data; while some models have been updated (Berna, Escriva, Munoz-Cobo, & Herranz, 2015), it is not clear if others have, as applicable. This gap is applicable to A-BWR thermal-hydraulics and aerosol characteristics. For example, empirical results indicate that the bubble distribution in a suppression pool following steam condensation and globule disintegration is first bimodal, then lognormal (Albiol , et al., 2017), while the current codes model bubble size distribution as initially lognormal, but not bimodal (Ramsdale, Guentay, & Friedrichs, 1995).

3. **Gap Area 3, Differences in computational framework:** Each code was developed by different code developers, with differences in the modeling and computational framework for several key phenomena. SPARC was developed by the Pacific Northwest National Laboratory (PNNL) (Owczarski & Burk, 1991), BUSCA by the Paul Scherrer Institute (Ramsdale, Guentay, & Friedrichs, 1995), and SUPRA by the Electric Power Research Institute (Fynbo, Haggblom, & Jokiniemi, 1990). For the same set of input conditions, there are no available comparisons of code performance and output ranges needed to examine or perform (1) representation and geometric fidelity, (2) physics and material model fidelity, (3) code verification, (4) solution verification, (5) model validation, or (6) uncertainty quantification and sensitivity analysis. SPARC assumes thermal equilibrium, while

BUSCA calculates it. Bubble dynamics is also analyzed differently in both codes. The sequences in which different phenomena occur are also different in both codes.

The above gap areas are important from the perspective of the accuracy of aerosol decontamination estimates predicted by the codes under consideration. Based on the complexity of the phenomena occurring inside suppression pools and the assumptions made, the code calculations may result in overly conservative estimates, while in some cases, it may be difficult to gauge the conservatism of the code prediction. It will be challenging to predict aerosol deposition for future A-BWRs which may rely more on naturally occurring passive decontamination phenomena. Current codes such as ASTEC and GOTHIC also have computational capabilities that were previously unavailable, which may make the reasons for certain modeling approaches and assumptions invalid or overly conservative. Therefore, it is important to gain a clear understanding of the gaps associated with the current codes in order to understand the kind of improvements that need to be made. The gaps associated with the SPARC, BUSCA and SUPRA codes are described in further detail in Appendix A: Gap Assessment.

3 Preliminary Analysis

3.1 A-BWR Reactors Knowledge Base

The A-BWR current knowledge base examines aerosol deposition attributes associated with the A-BWR designs under consideration. These include thermal-hydraulic parameters (pressure, temperature, steam concentration), geometry (size, shape, volume, A/V ratio for aerosol deposition) and aerosol characteristics (formation and deposition). Aerosol deposition is highly dependent on these attributes.

A thermal-hydraulics analysis identified the following general phenomena associated with A-BWRs:

- Passive aerosol decontamination mechanisms such as sedimentation, thermophoresis, diffusiophoresis, Brownian deposition and inertial impaction are applicable to the reactor drywell (GE-Hitachi, 2014).
- Phenomena such as agglomeration and pressure transient effects affect aerosol characteristics and deposition mechanisms.
- In the wetwell, phenomena affecting aerosol deposition inside the suppression pool (which has the major function to prevent over-pressurization of the containment vessel) such as steam condensation, bubble dynamics and pool parameters (nozzle shape, submergence depth, pool temperature and volume) were found to be applicable. It was inferred that the suppression pool was an important aspect for aerosol retention.

Analysis of geometry for the A-BWRs identified the following:

- The pool drywell and wetwell are connected through a set of nozzles, and drywell over pressurization is prevented by opening of the nozzles followed by steam condensation inside the suppression pool.
- The drywell shape and size affect passive deposition phenomena because different flow regimes are possible with different thermal-hydraulic parameters.
- There are reactor-specific systems (active and passive) to assist aerosol retention.
- Natural occurring aerosol deposition in pipes is significantly influenced by the geometry of the pipe. Phoretic mechanisms are influenced by the relatively high surface area to volume ratio, convective flow and turbulence are influenced by high aspect ratios, and impaction may be influenced by bends and the Stokes number.
- For containment vessels with smaller volumes, the reduction in volume may also be associated with a shorter radial distance between thermal gradients created by the different temperatures between the “hot” reactor vessel and “cool” drywell walls, or other cooler surfaces. Deposition phenomena such as thermophoresis and diffusiophoresis, which are driven by thermal and steam concentration gradients respectively, may be affected by this aspect of the geometry.
- Differences in geometry and thermal-hydraulics may result in phenomenological differences in fluid flow, and consequently, aerosol deposition and retention.

3.2 Conceptual A-BWR Designs

The A-BWR designs under consideration were used to develop a classification of generic A-BWR designs, since the differences in (1) thermal-hydraulic parameters (pressure, temperature, steam concentration), (2) geometry (size, shape, volume, depositional surface area to volume A/V ratio) and (3) aerosol characteristics (formation and deposition) lead to the inference that a classification of A-BWR designs is necessary for aerosol deposition analysis. Accordingly, the A-BWR classification into Types A and B is as illustrated in Table 3-1. The key discriminator is the presence or absence of a wetwell in the A-BWR.

Table 3-1: A-BWR Classification and Comparison

	Type A A-BWR	Type B A-BWR
Description	• Large reactor – both drywell and wetwell present • Passive deposition phenomena for both drywell and wetwell	• Small reactor – only drywell present, wetwell absent • Passive deposition phenomena for drywell only
Applicable reactors	ABWR, ESBWR	BWRX-300
Drywell	• Present – separate from the wetwell • Connected to wetwell through valves, which open in case of high pressure • Aerosol formation occurs inside the reactor vessel and may occur inside the drywell during pressurization • Passive aerosol deposition phenomena including thermophoresis, diffusiophoresis, impaction, sedimentation and fluid flow (possibly, convective flow) may apply for aerosols. Other aerosol processes such as agglomeration may also apply. • Phoretic phenomena and fluid flow depend on the thermal-hydraulic parameters (thermal gradient, pressure and steam concentration, etc.)	• Present • Aerosol formation occurs inside the reactor vessel and may occur inside the drywell during pressurization, governed by thermal-hydraulic parameters of concern • Passive deposition in the drywell is expected to be higher than in Type A reactors, due to the elimination of the wetwell • Need to consider that the smaller size (higher A/V ratio), enhanced fluid flow, potentially greater temperature difference between the RV and drywell walls than Type A reactors and enhanced deposition by thermophoresis and diffusiophoresis • The Type B reactor drywell may be similar to the iPWR containment vessel (CV) at SMART Center (EPRI, 2018b)
Path to wetwell	The wetwell is connected to the drywell through valves which open in case of pressurization.	Not applicable
Wetwell	• Suppression chamber, filled with water at the bottom section (pool) and an open free volume at the top • Aerosols flow into the suppression pool through a nozzle • Aerosol retention takes place based on steam condensation, bubble dynamics and suppression pool parameter effects	Not applicable

	Type A A-BWR	Type B A-BWR
	• Aerosols escape from the pool and are deposited in the dry region of the pool • Phenomena occurring in the drywell cause deposition in the dry region of the wetwell • Agglomeration and coagulation may also be applicable to the suppression pool	
Aerosol fraction bypassing wetwell	• Drywell deposition phenomena apply to aerosols that bypass the wetwell • Reactor-specific systems assist aerosol deposition in the drywell also apply	Not applicable
Reactor-specific passive aerosol deposition systems	• Passive deposition phenomena in the drywell • Suppression pool • ESBWR has a Passive Containment Cooling System (PCCS) assisting aerosol deposition by cooling the steam (containing aerosols) that flows through it	• Passive deposition phenomena in the drywell • BWRX-300 has Isolation Condenser System (ICS) which works similarly to the PCCS • Data is unavailable on the existence of other systems

3.3 Aerosol Transport Pathway: Characterization of the aerosol transport pathway for the two reactor types

Phenomena for both categories (discussed in Section 2.1) are influenced by the A-BWR Type (A or B), regions and components of the A-BWR, and reactor-specific systems as illustrated in Figure 3-1, which also forms a high-level definition of the aerosol transport pathway. For example, aerosol deposition due to phenomenon P8 (direct contact steam condensation) is affected by fluid flow and aerosol transport into the wetwell suppression pool. This process allows the wetwell aerosol bypass fraction to be considered, and deposition inside the drywell and the wetwell to be calculated separately and in the sequential order of the aerosol transport through the A-BWR components.

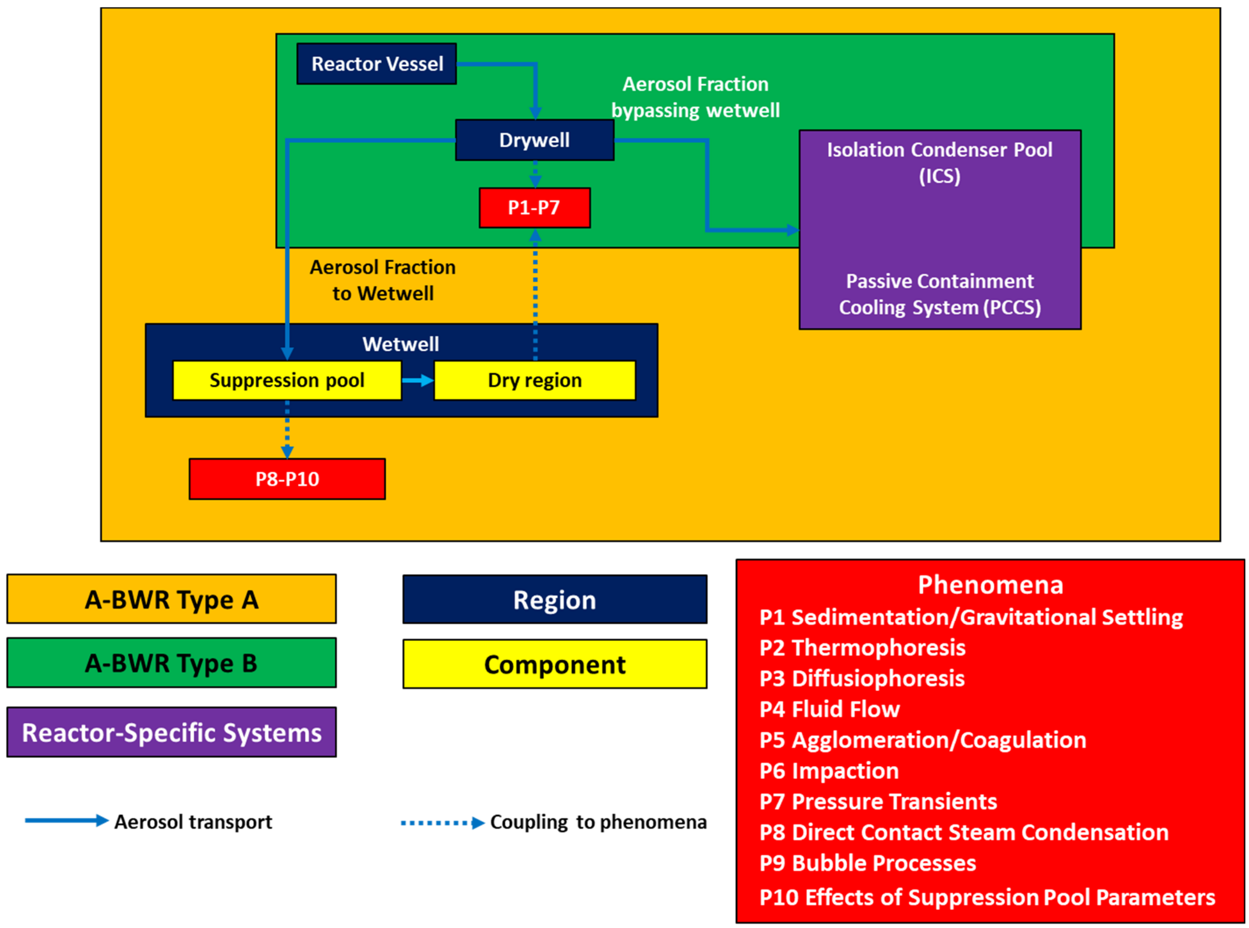

Figure 3-1: Applicable Phenomena for Type A and Type B A-BWRs

The aerosol transport pathway analysis, as applicable to Type A and Type B A-BWRs uses a serial approach, where aerosol deposition is characterized at various locations in the entire pathway. This is illustrated in Figure 3-2. For instance, aerosols entering the drywell may either deposit in the drywell due to passive deposition phenomena, or travel to the wetwell and deposit inside the suppression pool. Characterization of the fraction of aerosols bypassing the wetwell is therefore essential. Particles entrained inside bubbles formed within the suppression pool due to steam condensation may either be absorbed into the liquid water inside the pool or escape into the dry region of the wetwell once the bubble breaks the pool surface. The dry environment phenomena apply to these escaped aerosols, which may deposit on the wetwell walls as well as into the pool due to sedimentation. The current project proposes development of a procedure to characterize aerosol deposition in series to highlight the differences in the different A-BWR types.

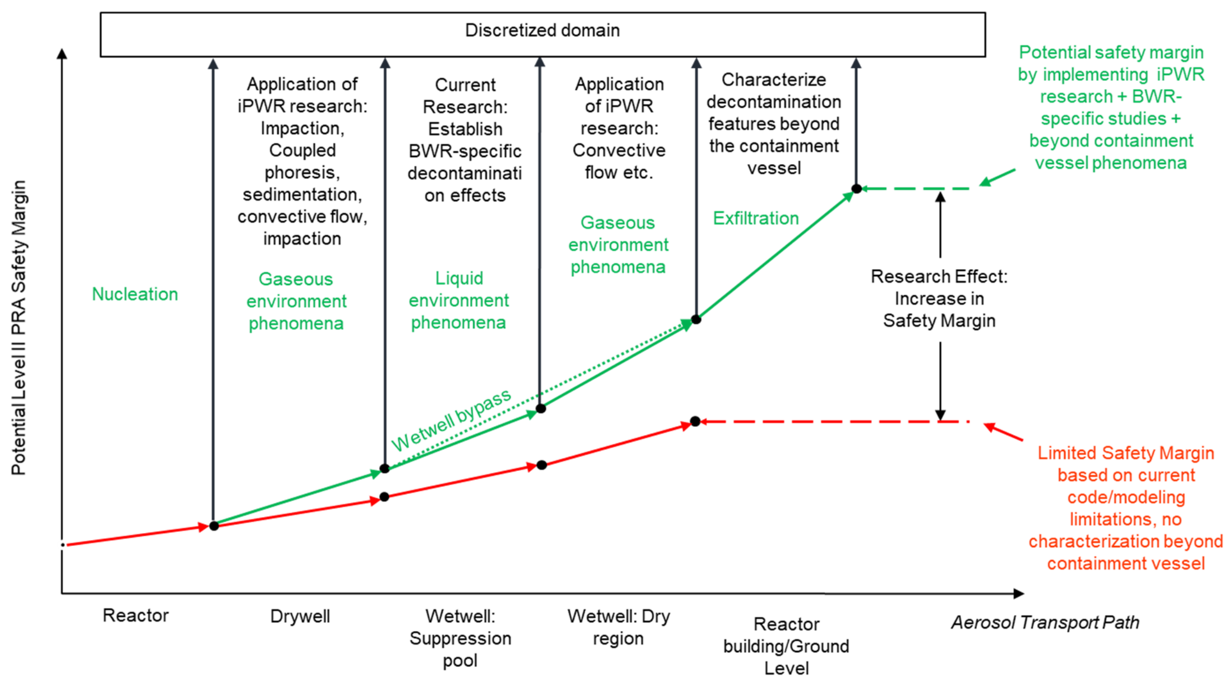

Figure 3-2: Improvement of Level II PRA Safety Margin for A-BWRs using the Aerosol Transport Pathway

An example of this characterization is provided with the following notional values and assumptions:

- Only the ex-vessel phase of a postulated accident is considered.
- 100 g of particles enter the drywell from the reactor vessel instantaneously.
- Aerosol leakage from the containment (drywell and wetwell) to the environment is zero; i.e. all aerosols eventually deposit in either the drywell or the wetwell (where applicable).
- Pressure rise inside the drywell opens the valves connecting the drywell to the wetwell, followed by depressurization. Depressurization rates affect aerosol deposition rates.
- The reactor-specific systems, such as the ICS and the PCCS, are not considered.

- The time taken for the analysis is 3 hours, which is the duration of a postulated ex-vessel phase of an accident (NRC, 1996).
- 80-90% of the aerosols in the drywell flow into the wetwell (where applicable), instantaneously at the start of the 3-hour time period.
- In 3 hours, about 65-75% aerosols in a Type A A-BWR drywell, and in the wetwell dry region, deposit on the walls. For the Type B A-BWR drywell, 90-95% aerosols deposit in 3 hours, an assumption which is made due to its more compact size and based on insights from the iPWR project.
- In 3 hours, about 10-15% of the aerosols from the suppression pool leak into the dry region of the wetwell.
- The DF definitions for different components are:
    - **Drywell**: Ratio of the initial aerosol mass to the sum of the final suspended aerosol mass in the drywell and the aerosol mass leaving the drywell
    - **Suppression pool**: Ratio of aerosol mass entering the pool to the aerosol mass leaving the pool
    - **Wetwell**: Ratio of aerosol mass entering the wetwell to the final aerosol mass suspended in the dry region of the wetwell
    - **Overall**: Ratio of initial aerosol mass to the final suspended aerosol mass in the drywell and the wetwell

Per the above assumptions, the aerosol deposition process for Type A A-BWRs is as shown in Figure 3-3. The following results can therefore be obtained through mass balance:

- 80-90% of the aerosols from the drywell flowing into the suppression pool gives a wetwell bypass fraction of 0.1-0.2.
- With the above numbers, the following results can be calculated for the 3-hour ex-vessel phase of the postulated accident:
    - DF(drywell) = 1.07-1.18
    - DF(suppression pool) = 6.67-10
    - DF(wetwell) = 19.05-45
    - DF(overall) = 8.93-21.05
- The range in the percentage of aerosol deposition at each stage of the process will lead to uncertainty in the DF estimation, which needs to be accurately characterized.

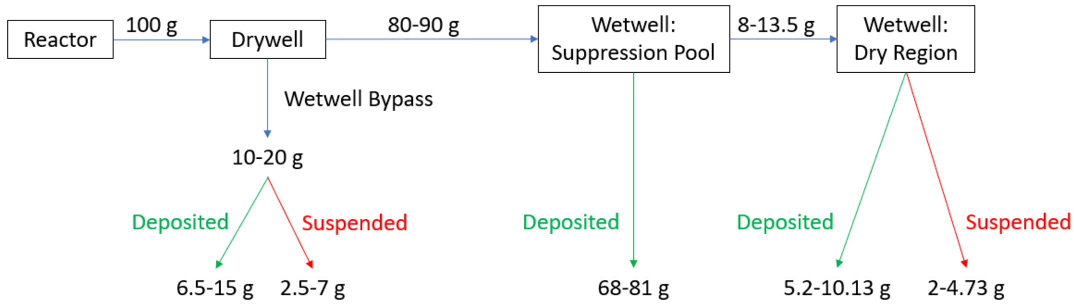

Figure 3-3: Type A A-BWR aerosol transport pathway with sample aerosol deposition calculations

A similar process can be used for Type B A-BWRs, where the suppression pool is absent, and the calculation only needs to be performed for the drywell. This is demonstrated in Figure 3-4.

- With the above numbers, the following results can be calculated for the 3-hour ex-vessel phase of the postulated accident:
  - DF(overall) = DF(drywell) = 10-20
- Variations in drywell thermal-hydraulic parameters will affect the Type B DF value more than the Type A DF value, due to the more compact and smaller Type B drywell.

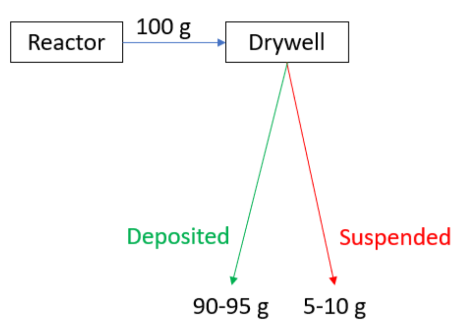

Figure 3-4: Type B A-BWR aerosol transport pathway with sample aerosol deposition calculations

Based on the above example, it is important to consider Type A and Type B A-BWR aerosol deposition calculations separately, since the aerosol deposition pathway is different for both A-BWRs.

3.4 PIRT Analysis

3.4.1 Summary

This section supports the development of a framework and roadmap to achieve improved source term characterization for advanced BWRs. A source term Phenomena Identification and Ranking Table (PIRT), denoted as the A-BWR PIRT, will be used to evaluate and prioritize phenomena related to A-BWR fission product transport and deposition in gaseous and liquid environments. The steps of the A-BWR PIRT process are presented in Figure 3-5. The A-BWR PIRT is a two-stage process; the Identification Stage consists of Steps 1 through 6, and provides background information for the Ranking Stage accomplished in Steps 7 through 9. The A-BWR PIRT relies on the form and structure of previous PIRT efforts (Diamond, 2006), (Bales, 2018), (Nowlen, Olivier, Dreisbach, & Salley, 2008), (NRC, 2008), (NEA, 2018). This section provides the relevant information for Steps 1 to 6 and for Steps 7 to 9.

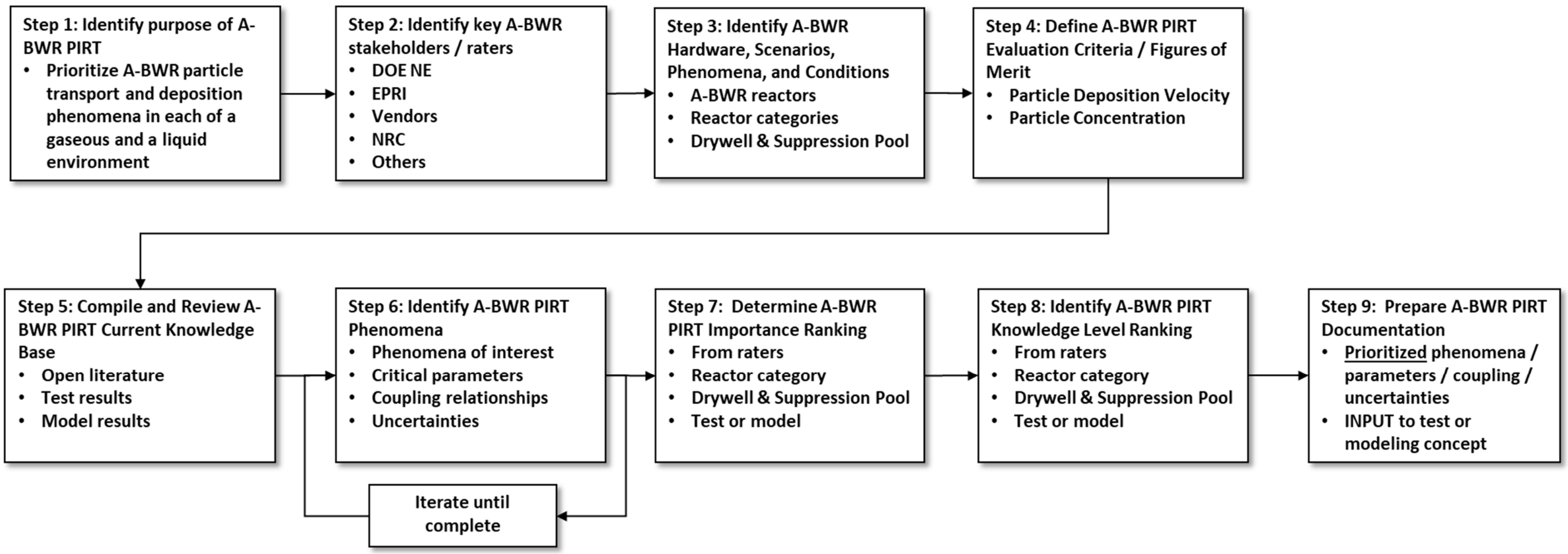

Figure 3-5: A-BWR PIRT Process

The PIRT development steps are as shown in Table 3-2.

Table 3-2: PIRT Development: Steps

Step	Title
1	Purpose of the A-BWR PIRT
2	Identify Key A-BWR Stakeholders/Raters
3	Identify A-BWR Reactor-types
4	Define A-BWR PIRT Evaluation Criteria/Figures of Merit
5	Compile and Review A-BWR PIRT Current Knowledge Base
6	Identify A-BWR PIRT Phenomena
7	Determine A-BWR PIRT Importance Ranking
8	Identify A-BWR PIRT Knowledge Level Ranking
9	Prepare A-BWR PIRT Documentation

3.4.2 Step 1: Purpose of the A-BWR PIRT

The purpose of the A-BWR PIRT is to prioritize A-BWR fission product transport and deposition phenomena in gaseous and liquid environments associated with advanced BWRs. A-BWR PIRT results are used to:

- **Identify data requirements to improve current modeling approaches:** This includes a gap assessment of the current modeling approaches, as shown in Section 2.3.
- **Identify experimentation requirements to develop the required data:** This includes identifying specific equipment to emulate thermal-hydraulic environments and to collect data for A-BWRs.
- **Develop optimal research strategies by leveraging knowledge and resources across similar source-term investigation research projects:** This includes evaluation of findings from similar research efforts for applicability to the A-BWR research.
- **Develop specific recommendations to improve modeling and simulation capabilities for current BWR aerosol safety analysis codes, including but not limited to the following codes:**
  - Modular Accident Analysis Program (MAAP – Suppression Pool Retention Analysis (SUPRA) module)
  - Advanced Reactor Computational fluid dynamics Code (ARCC) (Developed by Pittsburgh Technical during Phase 2a of EPRI's iPWR aerosol study (EPRI, 2018a))
  - Suppression Pool Aerosol Removal Code (SPARC)
  - BUbble SCrubbing Algorithm (BUSCA)

- Generation of Thermal-Hydraulic Information for Containments (GOTHIC)

Based on the A-BWR types and the environment in which the aerosol deposition phenomena apply, three A-BWR PIRT evaluations need to be performed. These evaluations are denoted as 1A, 1B, and 2 and are provided in Table 3-3.

Table 3-3: A-BWR PIRT Evaluation Structure

A-BWR PIRT Evaluations	**A-BWR Type**	
Environment Category	**Type A: A-BWR with a wetwell**	**Type B: A-BWR without a wetwell**
Category 1: Phenomena applicable to a gaseous environment	1A	1B
Category 2: Phenomena applicable to a liquid environment	2	*Not applicable (liquid environment requires the presence of a suppression pool inside a wetwell)*

The applicable A-BWR phenomena have been discussed in detail in Section 2.1.

3.4.3 Step 2: Identify Key A-BWR Stakeholders/Raters

The stakeholders are project participants from DOE-Nuclear Energy (NE), Nuclear Regulatory Commission (NRC), Pittsburgh Technical, Electric Power Research Institute, Inc. (EPRI), Carnegie Melon University (CMU), and industry stakeholders, which include General Electric, GE-Hitachi Nuclear Energy Americas LLC, and Hitachi-GE Nuclear Energy. Raters provide the importance and knowledge information used for the A-BWR PIRT prioritization.

3.4.4 Step 3: Identify A-BWR Reactors

A-BWR reactor types, reactor vessel (RV) parameters, drywell parameters, wetwell parameters, and volume and related geometric characteristics were identified during review of open and vendor literature. General information for the three A-BWR reactor types, as well as vendor-provided inputs has been compiled in Section 2.

3.4.5 Step 4: Define A-BWR PIRT Evaluation Criteria/Figures of Merit

Figures of Merit (FOM) are quantitative measures that represent the outputs from tests or models. The A-BWR phenomena of interest are assessed relative to the FOM for the critical parameters of each phenomenon, the coupling between phenomena, time phases of phenomena, and the uncertainties in measurement/estimation of the phenomena/parameters. Two FOM are examined in the A-BWR PIRT:

- **FOM 1: Particle Deposition Velocity [mm/s]** – This FOM is a basic unit that is directly proportional to the volumetric fission product deposition rate. The quantification of the particle deposition velocities is based on the vectoral resultant of deposition velocities for decontamination mechanisms such as sedimentation, thermophoresis, diffusiophoresis, impaction etc. Particle deposition velocity is denoted as v_n.

- **FOM 2: Decontamination Factor [dimensionless]** – This FOM is based on the quantification of the aerosol decontamination rate as a function of time, based on post-accident environmental conditions including transient thermal-hydraulic and geometric parameters. The Decontamination Factor is denoted as DF.

3.4.6 Step 5: Compile and Review A-BWR PIRT Current Knowledge Base

The current knowledge base for the A-BWR PIRT, based on the nuclear reactors under consideration as well as the modeling approaches used, has been complied in Sections 3.1 and 2.2 respectively.

3.4.7 Step 6: Identify A-BWR PIRT Phenomena

A detailed description of the aerosol deposition phenomena applicable to all three A-BWR PIRT evaluations has been provided in Section 2.1.

3.4.8 Step 7: Determine A-BWR PIRT Importance Ranking

Importance of the phenomenon or condition and its impact on the FOM is assessed by A-BWR stakeholders and team members. This is accomplished for A-BWR PIRT evaluations 1A, 1B, and 2, discussed earlier.

A five-point scale of phenomenon importance (very high, high, moderate, low, and very low) is used, with allowance for an unknown importance rating. The phenomenon is described in terms of key parameters, coupling of parameters, and uncertainties. Table 3-4 identifies the phenomena importance scales used in the A-BWR PIRT Worksheet for models or simulations.

Importance is assessed by asking the question, "How important is the phenomena on the FOM including parameter coupling and uncertainties?"

Table 3-4: Importance Measurement Scale

Importance		
The importance of the A-BWR phenomena to the FOM based on the parameters, coupling, and uncertainties describing the phenomena is <meaning>		
Score	**Meaning**	**Interpretation as understood within the A-BWR community**
Very High (VH)	Very High Importance	The highest importance to the FOM. There is a definite need for model results for the FOM.
High (H)	High Importance	High to moderately high importance to the FOM. Significant need for model results for the FOM.
Moderate (M)	Important	Of less importance than high or very high importance to the FOM, but still important. There is a need for model results for the FOM.
Low (L)	Moderate importance	Secondary importance to the FOM. There is some need for model results for the FOM.
Very Low (VL)	Low importance	Negligible importance to the FOM. Not necessary to model the phenomenon.
Unknown (UNK)	Unknown	Potentially important. Importance should be explored through sensitivity studies, exploratory or models, or additional PIRT exercises.

3.4.9 Step 8: Identify A-BWR PIRT Knowledge Level Ranking

Current knowledge of the phenomenon or condition and its impact on the FOM is assessed by A-BWR stakeholders and team members. This is accomplished for A-BWR PIRT evaluations 1A, 1B, and 2 discussed earlier.

A three-point scale of phenomenon current knowledge (high, moderate, and low) is used with allowance for an unknown knowledge rating. This assessment represents the knowledge level of the phenomenon or condition based on whether information for the phenomenon was obtained from tests or models.

Knowledge level measurement scales for models or simulations are provided in Table 3-5. For models or simulations, the knowledge level is assessed by asking the question, “What degree or level of knowledge exists for results from verified and validated (V&V) models or simulations?” Model or simulation representativeness and whether verification and validation has been accomplished or not, are key knowledge aspects for models or simulations.

Table 3-5: Knowledge Measurement Scale for Models or Simulations

Knowledge for Models or Simulations		
What degree or level of knowledge exists for results from models or simulations?		
Score	**Meaning**	**Interpretation within the A-BWR community**
High (H)	A great deal	Information from model/ simulation results strongly supports identification of new research questions. The models/ simulations are demonstrably verified or validated. The information results in readily acceptable inferred results.
Moderate (M)	Somewhat	Information from model/ simulation results moderately supports identification of new research questions. The models/ simulations are partially verified or validated. The credibility of inferred results would still need to be considerably enhanced.
Low (L)	Very limited	Information from model/ simulation results is insufficient to support identification of new research questions. The models/ simulations are either partially or not at all verified or validated. Evidence-based solutions, explanations of coupling and uncertainties, decisions, and process improvement alternatives cannot be credibly identified and drawn.
Unknown (UNK)	Unknown	It is not known if model or simulation results from verified or validated models or simulations are available for this phenomenon.

Knowledge level measurement scales for experiments or tests are provided in Table 3-6. For experiments or tests, the knowledge level is assessed by asking the question, “What degree or level of knowledge exists for empirical data obtained from experiments or tests?” Experimental or test results and facilities are examined in terms of their fidelity representativeness of A-BWR. Data acquisition systems used for the test results or in-place at the test facility are examined in terms of potential to assess particle concentration change, measurement precision and accuracy for test data. Data acquisition has improved considerably since the safety analysis computer codes that use inputs from these facilities were developed. Since the codes were developed at a time when experimental data availability was scarce, it is unclear whether observations and insights from more recent experimental studies have been incorporated into these codes.

Table 3-6: Knowledge Measurement Scale for Experiments or Tests

Knowledge for Experiments or Tests		
What degree or level of knowledge exists for empirical data obtained from experiments or tests?		
Score	**Meaning**	**Interpretation within the A-BWR community**
High (H)	A great deal	Available information from experiments or tests strongly supports identification of new research questions. Test facilities are high fidelity representations of the A-BWR. Data acquisition systems offer precise particle tracking and measurements. The information results in readily acceptable inferred results.
Moderate (M)	Somewhat	Information from experiments or tests moderately supports identification of new research questions. Test facilities are moderate fidelity representations of the A-BWR. Data acquisition systems are sufficient for particle tracking but limited in precision. The credibility of inferred results would still need to be considerably enhanced.
Low (L)	Very limited	Information from experiments or tests is insufficient to support identification of new research questions. Test facilities are low fidelity representations of the A-BWR. Data acquisition systems are not state of the art for particle tracking or measurements. Evidence-based solutions, explanations of coupling and uncertainties, decisions, and process improvement alternatives cannot be credibly identified and drawn.
Unknown (UNK)	Unknown	It is not known if empirical data are available for this phenomenon.

3.4.10 Step 9: Prepare A-BWR PIRT Documentation

Results have identified the prioritization for the ten phenomena associated with BWR particle transport and deposition phenomena in gaseous and liquid environments. The prioritization aids in understanding parameter coupling and how to reduce uncertainties associated with the phenomenon. The prioritization is also helpful in identification of supplemental requirements in existing codes. Table 3-7 and Table 3-8**Error! Reference source not found.** show the prioritization of the phenomenon and its impact on the FOM for all combinations of phenomena categories and A-BWR types, for modeling and experimentation respectively, based on stakeholder input. The intent is to provide a clear delineation between phenomena, so that model refinement and test data collection requirements can be identified, which forms the basis for future phases of this project.

Table 3-7: Results of A-BWR PIRT prioritized phenomenon for models

<table>
<tr><th colspan="3">Prioritized Phenomena for A-BWR Models</th></tr>
<tr><th>1A
Phenomena applicable to a gaseous environment for A-BWR with a wetwell</th><th>1B
Phenomena applicable to a gaseous environment for A-BWR without a wetwell</th><th>2
Phenomena applicable to a liquid environment for A-BWR with a wetwell</th></tr>
<tr><td colspan="3">Very High Importance and Low Knowledge</td></tr>
<tr><td>P4 Fluid Flow</td><td>P4 Fluid Flow
P6 Impaction</td><td></td></tr>
<tr><td colspan="3">Very High Importance and Moderate Knowledge</td></tr>
<tr><td>P3 Diffusiophoresis
P4 Fluid Flow
P6 Impaction
P7 Pressure Transients
P8 Direct Contact Steam Condensation
ADDED: Assess deposition in buildings adjacent to containment vessel</td><td>P2 Thermophoresis
P3 Diffusiophoresis
P4 Fluid Flow
P6 Impaction
P7 Pressure Transients
ADDED: Assess deposition in buildings adjacent to containment vessel</td><td>P4 Fluid Flow
P10 Effects of Suppression Pool Parameters</td></tr>
<tr><td colspan="3">High Importance and Low Knowledge</td></tr>
<tr><td>P5 Agglomeration/Coagulation
P10 Effects of Suppression Pool Parameters</td><td>P5 Agglomeration/Coagulation</td><td>P8 Direct Contact Steam Condensation
P9 Bubble Processes</td></tr>
<tr><td colspan="3">Unknown Importance and Unknown Knowledge</td></tr>
<tr><td>P9 Bubble Processes</td><td>P8 Direct Contact Steam Condensation
P9 Bubble Processes
P10 Effects of Suppression Pool Parameters</td><td>P7 Pressure Transients</td></tr>
</table>

Table 3-8: Results of A-BWR PIRT prioritized phenomenon for tests

Prioritized Phenomena for A-BWR Tests		
1A **Phenomena applicable to a gaseous environment for A-BWR with a wetwell**	**1B** **Phenomena applicable to a gaseous environment for A-BWR without a wetwell**	**2** **Phenomena applicable to a liquid environment for A-BWR with a wetwell**
Very High Importance and Low Knowledge		
P4 Fluid Flow	P4 Fluid Flow P7 Pressure Transients	
Very High Importance and Moderate Knowledge		
P7 Pressure Transients P8 Direct Contact Steam Condensation ADDED: Assess deposition in buildings adjacent to containment vessel	P2 Thermophoresis P6 Impaction ADDED: Assess deposition in buildings adjacent to containment vessel	P10 Effects of Suppression Pool Parameters
High Importance and Low Knowledge		
P9 Bubble Processes P10 Effects of Suppression Pool Parameters	P4 Fluid Flow	P8 Direct Contact Steam Condensation P9 Bubble Processes
Unknown Importance and Unknown Knowledge		
	P8 Direct Contact Steam Condensation P9 Bubble Processes P10 Effects of Suppression Pool Parameters	P7 Pressure Transients

4 Analysis

4.1 Applicability of Existing Decontamination Factor Correlations for BWR Drywells and Wetwells

This section provides an assessment of the applicability of existing aerosol deposition correlations to the Type A (wetwell present; e.g. ABWR (GE, 1997), ESBWR (GE-Hitachi, 2014)) and Type B (wetwell absent; e.g. BWRX-300 (GE-Hitachi, 2018)) A-BWRs. This assessment provides the applicability of the existing referential bases for A-BWR aerosol deposition analysis, which includes applicability of methods, models and codes. This is achieved by identifying applicable regulatory references for aerosol deposition analysis for each of the major segments in the aerosol deposition pathway. Table 2-1 to Table 2-3 are useful for these considerations.

4.1.1 Applicability of correlations for the A-BWR drywell

4.1.1.1 Aerosol decontamination coefficient correlation

The decontamination coefficient is a parameter that is evaluated as a function of time for different phases of a reactor accident and is used to calculate the Decontamination Factor (DF). This study is focused on the ex-vessel phase of the accident.

The correlation for evaluating the drywell aerosol decontamination coefficient due to naturally occurring phenomena (λ [hr^{-1}]) for the BWR ex-vessel release accident phase (9000-19800s) is as follows:

$$\lambda(90) = 0.756 + 3.5 * 10^{-6} * P \qquad \text{Equation (4-1)}$$

Where P, is the rated thermal power [MWth] and $\lambda(90)$ is the 90^{th} percentile value. This correlation, as provided in Table 44 of NUREG 6189 (NRC, 1996), was developed through a stochastic assessment of the uncertain range of variables for critical fission product deposition parameters for BWRs with power outputs in a 1500-3500 MWth range.

To evaluate the applicability of this correlation to the A-BWRs under consideration, their rated thermal power needs to be considered. For the Advanced Boiling Water Reactor (ABWR) and the Economic Simplified Boiling Water Reactor (ESBWR), the rated thermal power values are:

- P(ABWR) = 3926 MWth
- P(ESBWR) = 4500 MWth

Clearly, both reactors fall outside the power output range of the above correlation for the decontamination coefficient. However, the applicability of this correlation will be assessed based on thermal-hydraulic and geometric considerations as well.

4.1.1.2 Surface area to volume ratio calculation

Reactor geometry can be well-characterized based on the deposition surface area to drywell volume ratio. The following correlation from NUREG 6189 is used for calculation of the A/V ratio in BWR Mark I, Mark II and Mark III containments (NRC, 1996):

$$\frac{A_E}{V} = 0.469 - (2.43 * 10^{-5})V \pm 0.0225 \quad \text{Equation (4-2)}$$

Where A_E is the envelope area [m^2], and V is the drywell volume [m^3]. Applying this correlation to calculate the nominal A/V ratio for the A-BWR and ESBWR containments, the values obtained are as shown in Table 4-1 for comparison.

Table 4-1: A/V ratios for BWR containment vessels (NRC, 1996)

Containment Type	**Drywell Volume [m^3]**	**A/V ratio [m^{-1}] (ft^{-1})**
Mark I	4500	0.36 (0.11)
Mark II	6500	0.31 (0.094)
Mark III	7650	0.28 (0.085)
A-BWR	*7350*	*0.29 ± 0.0225 (0.088 ± 0.007)*
ESBWR	*7206*	*0.29 ± 0.0225 (0.088 ± 0.007)*

For the purposes of the current analysis, the A/V ratio values obtained from the above correlation places the Type A A-BWRs (ABWR, ESBWR) in a similar geometric regime as the Mark III containment. In addition, the ABWR and ESBWR also house a suppression pool, similar to the Mark III containment.

4.1.1.3 Thermal-hydraulic parameter range

Similarities in thermal-hydraulic post-accident regimes between older BWR and newer A-BWR drywells can be established based on design, thermal-hydraulic parameter values, and upper and lower limits for post-accident conditions. The upper limits for post-accident pressure and temperature values in the ex-vessel phase for typical BWRs and the Mark III containment are given in Table 16 of NUREG 6189. The upper limits for post-accident containment thermal-hydraulic conditions for the ESBWR in case of a LOCA are given in Table 6.2-5, chapter 6, of the ESBWR DCD document (GE-Hitachi, 2014). These conditions are summarized in Table 4-2 for comparison. The thermal-hydraulic conditions for the A-BWRs appear to be in a somewhat similar range (below the containment design pressure and temperatures) as the Mark III containments.

Table 4-2: Drywell thermal-hydraulic parameter ranges (NRC, 1997) (GE, 1997) (GE-Hitachi, 2014)

Parameter	**Typical BWR**	**Mark III**	**ESBWR (LOCA)**	**ESBWR (rated)**	**ABWR (rated)**
Pressure [kPa]/(atm) upper limit	1195/11.8	489/4.83	397.45/3.92	411.3/4.06	411.2/4.06
Temperature [K]/[^{o}C] upper limit	850/577	432/159	416.46/143.46	444/171	444.1/171.1

Thus, thermal-hydraulically, the ESBWR and ABWR post-accident conditions are similar to the Mark III containment post-accident conditions, and well below the upper limits for typical BWRs.

4.1.1.4 Overall DF Calculations

From the above items, while the BWR aerosol decontamination coefficient correlation may not be applicable to the Type A A-BWRs, the geometric and post-accident thermal-hydraulic conditions are similar enough for using this correlation to estimate a nominal drywell decontamination coefficient value for both Type A A-BWRs. These values are as follows:

- DF(ABWR) = 2.309
- DF(ESBWR) = 2.315

Both values have been calculated using the correlation for λ under Item 1 (multiplied by 3 since t = 3 hr.), for the ex-vessel phase of the accident.

It is important to note that the BWRX-300 has a rated power output of 300 MWe. This, with an assumed overall efficiency range of 30-50%, places the thermal power output at P = 600-1000 MWth, which is also outside the 1500-3500 range of the decontamination coefficient correlation. However, the geometry of this reactor is different due to the absence of a wetwell/suppression pool. Data on thermal-hydraulic post-accident conditions is unavailable. It can therefore be assumed that due to differences in geometry and components, the referenced NUREG 6189 correlation does not apply to the BWRX-300. To further assess the applicability of the correlation, the estimated DF with the correlation was compared to an empirically derived DF for PWR SMRs. The estimated DF with the correlation yielded a value of DF(BWRX-300) = 2.27, while the empirically derived DF for PWR SMRs was 19.7 (EPRI, 2018b). It should be noted that prior to the PWR SMR empirical inquiry, the estimated DF based on prior art, including existing correlations, similarly yielded a DF of approximately 2 (EPRI, 2014).

4.1.2 Applicability of correlations for the A-BWR wetwell

This section is relevant to the Type A A-BWRs, which have a wetwell and a suppression pool. NUREG 6153 (NRC, 1997) provides correlations to calculate the total suppression pool DF (ratio of mass entering the suppression pool to the mass exiting the suppression pool throughout the accident phase). It is, however, important to note the following:

- The DF is calculated based on the nozzle submergence depth.
- Per Table 1 of NUREG 6153 (NRC, 1997), the reactors from which these correlations are developed have thermal power ratings between 2894-3833 MWth. Both ABWR and ESBWR thermal power ratings are outside this range. Therefore, a further assessment of similarities between the ABWR and ESBWR suppression pool parameters is required to determine the applicability of these correlations.
- Different suppression pool pressure upper limits have different correlations. If applicable, the correlations for pressures under 5 atm (505 kPa) should be used, since the wetwell

design pressures are 411.2 kPa (ABWR) and 411.3 kPa (ESBWR) i.e. lower than 5 atm (GE, 1997) (GE-Hitachi, 2014).

- Correlations have been evaluated for nozzle submergence depths ranging from 100 cm (1 m) to 700 cm (7 m). These may be applicable to the Type A A-BWRs, since their maximum pool depths (nozzle submergence depth is less than pool depth) are 7 m (ABWR) and 5.5 m (ESBWR).
- The upper limits of the pool volumes, design pressures and design temperatures for the reactors used to develop the suppression pool DF correlations, as well as the wetwell design pressure and temperature for the Type A A-BWRs are summarized in Table 4-3.

Table 4-3: Wetwell thermal-hydraulic parameter ranges (NRC, 1997) (GE, 1997) (GE-Hitachi, 2014)

Parameter	Mark I	Mark II	Mark III	ESBWR	ESBWR
Wetwell design Pressure [kPa]/(atm) upper limit	425.6/4.2	385/3.8	101.3/1	411.3/4.06	411.2/4.06
Wetwell design Temperature [K]/[°C] upper limit	427/154	411/138	358/85	394/121	376.9/103.9
Pool volume [m^3] upper limit	3483	4383	3851	4424	3580

- Correlations are provided for T-type and X-type quenchers only. The nozzle type for the ABWR and ESBWR is unclear; these correlations would not be applicable to calculate the DF if the nozzle type is different from the T and X-types.

Per the above considerations, assuming applicability of the DF correlation, the best estimate of the suppression pool DF for pressures not exceeding 5 atm is given by (NRC, 1997):

$$DF(total) = 10^{1.752+0.00192H} \quad \text{Equation (4-3)}$$

Where H = nozzle submergence depth (cm). Using the H values as maximum suppression pool depth values, the DF best estimate values for the suppression pools of both reactors can be calculated.

4.1.3 Miscellaneous considerations

- Per NUREG 6189, the naturally occurring deposition phenomena for the BWR drywell and the PWR containment vessel are similar (NRC, 1996). Therefore, the following improvements made to the theoretical constructs of these phenomena during the iPWR Phase 2 project should apply to the BWR drywell phenomena:
  - Consideration of the Cunningham Slip Correction factor for diffusiophoresis.
  - Use of local gradients to calculate thermophoresis and diffusiophoresis velocities.

- Characterization of fluid flow inside the containment.
- Coupling of phenomena with the fluid flow inside the containment.

4.1.4 Inferences

- NUREG 6189 correlations are not directly applicable to the Type A A-BWRs for estimating decontamination inside the drywell. However, considering the thermal hydraulic parameters are similar, from a phenomenological standpoint, existing methods and models may be applicable, with certain corrections to reflect updated knowledge. An example of this would be the application of the Cunningham correction factor to the diffusiophoresis deposition velocity for the discrete analysis method.
  The correlations from NUREG 6153 can be applicable to the Type A A-BWRs if certain assumptions are made, and certain conditions are applicable.
  The drywell DF correlations may not be applicable to the BWRX-300.

4.2 Uncertainty Analysis

The USNRC established the Best Estimate Plus Uncertainty (BEPU) approach as an alternative analysis and qualification method to the conservative or deterministic approach (NRC, 1989). The BEPU approach includes best estimate calculations and uncertainty analysis based on NRC methods described in regulatory guide 1.203 (RG1.203). The code scaling and uncertainty evaluation (CSAU) approach is used to quantify the uncertainty. The CSAU methodology was developed by the NRC to address issues related to scaling capability of a best-estimate code, to ensure applicability to safety analysis scenarios. The uncertainty quantification requires the identification of figures of merit (FOM) and the prioritization of critical parameters using a PIRT (Section 3.4).

The uncertainty analysis examines parameter identification, probability density functions (PDF), and values used to describe each PDF for the parameters. The term PDF is used interchangeably with the term probability distribution in this discussion. Identification of key uncertainties in parameters and aerosol deposition phenomena are derived from the following references:

- Liquid environment: NUREG/CR-6153 (NRC, 1997)
- Gaseous Environment: NUREG/CR-6189 (NRC, 1996)

4.2.1 Uncertainty analysis associated with NUREG/CR-6153

NUREG/CR-6153 (NRC, 1997) describes phenomena that can decontaminate aerosol-laden gases sparging through steam suppression pools of boiling water reactors and the associated uncertainties in aerosol properties, aerosol behavior in gas bubbles, and bubble behavior in plumes. Parameters that characterize boundary and initial conditions, aerosol properties and behavior uncertainties, and bubble behavior are discussed. Using probability density functions in Monte Carlo simulations, uncertainty distributions and error propagation are performed. These are discussed in Appendix A of NUREG/CR-6153.

For the parameters identified in NUREG/CR-6153, empirical data is required to update and validate the input ranges and the PDF. Model evaluation is not performed in NUREG/CR-6153 and is a requirement for future research.

The relevance of the NUREG/CR-6153 uncertainty discussion is cross-walked to the prioritized PIRT phenomena applicable to a wet (liquid) environment for A-BWRs with or without a wetwell. This focuses the examination of the uncertainties identified in NUREG/CR-6153 with the A-BWR phenomena of interest.

FOM affected by these phenomena are particle deposition velocity, v (mm/s) and the DF. Since both of these FOM are functionally affected by particle diameter, d_p, this parameter is also examined in this discussion. The prioritized PIRT phenomena for A-BWR in a wet (liquid) environment (A-BWR with a suppression pool) are presented in Table 4-4.

Table 4-4 Prioritized PIRT phenomena applicable to A-BWR wet environments

PIRT Requirement	**Prioritized PIRT Phenomena applicable to a wet environment for A-BWRs with a wetwell**	
Enhanced Models	Primary	P4 Fluid Flow P10 Effects of Suppression Pool Parameters
	Secondary	P8 Direct Contact Steam Condensation P9 Bubble Processes P7 Pressure Transients
Further Tests	Primary	P10 Effects of Suppression Pool Parameters
	Secondary	P8 Direct Contact Steam Condensation P9 Bubble Processes P7 Pressure Transients

Parameters and uncertainties from NUREG/CR-6153 are identified in Table 4-5. A combination of empirical data and subjective assessments were used by the report authors to define the PDF for the parameters and specific values (means, ranges, distribution, etc.) for each parameter. Analytic or computational fluid dynamics (CFD) models may be useful to update selected parameters derived from correlations.

Gap release, in-vessel release, ex-vessel release, and late in-vessel conditions are significantly different, and this requires examination of parameter uncertainty ranges during these phases of severe accident conditions. Input / boundary condition uncertainties are due to BWR variability and thermal hydraulic environment variability during the severe accident phases.

Aerosol behavior uncertainties are also identified and reflect uncertainties in removal of aerosols. These are highlighted in NUREG/CR-6153 in the introduction to Section V, Uncertainty in Prediction of Aerosol Removal in Steam Suppression Pools is the statement "… there is another type of uncertainty. This is the uncertainty in the physical model used to describe the [aerosol] process or phenomenon. It is not obvious how this type of uncertainty can be reduced to a parametric quantity …" Model evaluation is not performed in NUREG/CR-6153 and is a requirement for future research.

Table 4-5 NUREG/CR-6153 parameters and uncertainties applicable to A-BWR wet environment (NRC, 1997)

ID	**Parameter**	**Input range and Probability Density Function (PDF)**	**Reference in NUREG/CR-6153, Section V, Uncertainty in Prediction of Aerosol Removal in Steam Suppression Pools, B Uncertainty Models, Inputs, and Parametric Conditions**	**Comment**
W1	Pool depth	Range: 100-700 cm; PDF: uniform	Section 1, Input and Boundary conditions, Table 22 and pages 268 - 279	Assumed to be known
W2	Orifice size	Range: 59.7-69.8 cm; PDF: uniform	Section 1, Input and Boundary conditions, Table 22 and pages 268 - 279	Uncertainty due to number of orifices not considered to be very high.
W3	Wetwell Pressure	Range: 1 atm-P_fail; PDF: uniform	Section 1, Input and Boundary conditions, Table 22 and pages 268 - 279	P_fail is different for Mark I, II and III containments
W4	Particle diameter	Range: 1.1-7 micron; PDF: lognormal	Section 1, Input and Boundary conditions, Table 22 and pages 268 - 279	This is an approximation; it is likely that an aerosol has aged sufficiently such that deviations of particle diameter from lognormal distributions have been eliminated.
W5	Particle density	Range: 2.9-5.65 g/cc; PDF: uniform	Section 1, Input and Boundary conditions, Table 22 and pages 268 - 279	Based on calculated severe accident results
W6	Shape factor - primary particle diameter	Range: 0.001-0.1; PDF: log-uniform	Section 1, Input and Boundary conditions, Table 22 and pages 268 - 279	Based on primary particle diameter ranges
W7	Shape factor – fractal	Range: 1.5-2.2; PDF: uniform	Section 1, Input and Boundary conditions, Table 22 and pages 268 - 279	Based on fractal dimension of agglomerates
W8	Gas flow rate	Ranges: 100-300 mol/s (Mark I), 150-1100 mol/s (Mark II, III); PDF: uniform	Section 1, Input and Boundary conditions, Table 22 and pages 268 - 279	Higher for Mark II and III because of higher degassing of concrete

ID	Parameter	Input range and Probability Density Function (PDF)	Reference in NUREG/CR-6153, Section V, Uncertainty in Prediction of Aerosol Removal in Steam Suppression Pools, B Uncertainty Models, Inputs, and Parametric Conditions	Comment
W9	Steam production rate	Range: 50-500 mol/s; PDF: uniform	Section 1, Input and Boundary conditions, Table 22 and pages 268 - 279	Small portion for Mark I, higher for mark II and III
W10	Bubble formation - David Schular model coefficient	Range: 0.976-1.722; PDF: uniform	Section 2, Phenomenological Uncertainties in Bubble Behavior, Table 23 and pages 279 – 288	Correlation has not been validated; data is scarce. Coefficient part of correlation to calculate bubble volume
W11	Equilibrium distance	Range: 2-10 bubble diameters; PDF: unknown	Section 2, Phenomenological Uncertainties in Bubble Behavior, Table 23 and pages 279 – 288	All mechanisms responsible for aerosol removal have not been characterized/identified quantitatively.
W12	Initial bubble size	Range: Uncertain, calculated from correlation (logarithm of bubble size); PDF: Students' t	Section 2, Phenomenological Uncertainties in Bubble Behavior, Table 23 and pages 279 – 288	Bubble size itself is an uncertain quantity
W13	Bubble shape parameter	Range: 0-1; PDF: uniform	Section 2, Phenomenological Uncertainties in Bubble Behavior, Table 23 and pages 279 – 288	The parameter decides the selection of the model to calculate bubble shape
W14	Bubble slip velocity parameter	Range: 0-1; PDF: uniform	Section 2, Phenomenological Uncertainties in Bubble Behavior, Table 23 and pages 279 – 288	Uncertainty depends on void fraction; uniformly distributed parameter used to calculate slip velocity based on void fraction and rise velocity
W15	Bubble rise velocity correlation parameters	Various uncertainties; PDF: Students' t	Section 2, Phenomenological Uncertainties in Bubble Behavior, Table 23 and pages 279 – 288	There are three such parameters, with different ranges for the parameter H which is calculated using another correlation.
W16	Plume parameters - entrainment coefficient	Range: From correlation; PDF: Students' t	Section 2, Phenomenological Uncertainties in Bubble Behavior, Table 23 and pages 279 – 288	Derived from experimental values with a least squares fit
W17	Plume parameters -	Range: 1.1-2.8; PDF: lognormal	Section 2, Phenomenological Uncertainties in Bubble	Range is based on comparison to data

ID	Parameter	Input range and Probability Density Function (PDF)	Reference in NUREG/CR-6153, Section V, Uncertainty in Prediction of Aerosol Removal in Steam Suppression Pools, B Uncertainty Models, Inputs, and Parametric Conditions	Comment
	momentum amplification factor		Behavior, Table 23 and pages 279 – 288	
W18	Plume parameters - size parameter ratio	Range: 0.7-1; PDF: lognormal	Section 2, Phenomenological Uncertainties in Bubble Behavior, Table 23 and pages 279 – 288	Based on relation between radial distributions of void fraction and liquid velocities
W19	Radial mixing fraction	Range: 0-1; PDF: uniform	Section 2, Phenomenological Uncertainties in Bubble Behavior, Table 23 and pages 279 – 288	Based on equilibrium of bubbles coalescing and disintegrating; a fraction of bubbles in a radial node exchanges with that of the next node.
W20	Inertial impaction efficiency - molar volume of surface agents	Range: 40-1000; PDF: log-uniform	Section 3, Phenomenological Uncertainties in Aerosol Behavior, Table 24 and pages 288 – 302	This is for inertial impaction of bubble walls, depending on circulation of gases in a rising bubble.
W21	Inertial impaction efficiency - surface active agent concentration	Range: 1e-10-1e-4; PDF: log-uniform	Section 3, Phenomenological Uncertainties in Aerosol Behavior, Table 24 and pages 288 – 302	The surface agent immobilizes the bubble interfaces and makes particles stick to bubble walls.
W22	Brownian diffusion deposition - Sherwood number	Range: 14.6-17.66; PDF: uniform	Section 3, Phenomenological Uncertainties in Aerosol Behavior, Table 24 and pages 288 – 302	Calculated for a bubble in vortex flows.
W23	Slip correction - momentum accommodation coefficient uncertainty parameter	Range: 0-0.6; PDF: uniform	Section 3, Phenomenological Uncertainties in Aerosol Behavior, Table 24 and pages 288 – 302	Based on available data; momentum accommodation coefficient decreases with temperature
W24	Slip correction - temperature accommodation coefficient	Range: 0-1; PDF: uniform	Section 3, Phenomenological Uncertainties in Aerosol Behavior, Table 24 and pages 288 – 302	Temperature accommodation coefficient does not exceed the momentum

ID	Parameter	Input range and Probability Density Function (PDF)	Reference in NUREG/CR-6153, Section V, Uncertainty in Prediction of Aerosol Removal in Steam Suppression Pools, B Uncertainty Models, Inputs, and Parametric Conditions	Comment
	uncertainty parameter			accommodation coefficient
W25	Oscillation capture - onset criterion	Range: 2.96-4.24; PDF: uniform	Section 3, Phenomenological Uncertainties in Aerosol Behavior, Table 24 and pages 288 – 302	Oscillations sweep out aerosol particles
W26	Oscillation capture - onset criterion	Range: 0-1; PDF: uniform	Section 3, Phenomenological Uncertainties in Aerosol Behavior, Table 24 and pages 288 – 302	
W27	Oscillation capture - onset criterion	Range: 0-1; PDF: uniform	Section 3, Phenomenological Uncertainties in Aerosol Behavior, Table 24 and pages 288 – 302	Abrupt variation in impaction efficiency is seen with particle size; alternative model is proposed to show less variation by using this interpolation factor.
W28	Oscillation capture - onset criterion	Range: 0-1; PDF: uniform	Table 24. Uncertainties in phenomena affecting aerosol behavior	Convective deposition efficiency (capture of particles through convective motion of gases within the bubble) depends on both inertial impaction and convective mass transport.

A simplified model of decontamination by steam suppression pools is developed given an understanding of these uncertainties and correlation based on a Monte Carlo simulation. The DF(total) and the mean and (geometric) standard deviation of particle diameter, dp, are produced as outputs in the form of scaling (correlation) functions for the 10th percentile (10%-tile), the best estimation (the median or the 50%-tile), the mean, and the 90%-tile. These four measures serve to bound DF and d_p.

Using the simplified model in Section VII of NUREG-6153 (NRC, 1997) for situations at 5 atm or less, the following outputs are obtained. For the DF(total), the scaling function is a linear form log10(DF total) = a + b x H(cm), where a is the intercept, b is the slope, and H is the quencher depth in cm. Type A A-BWR specify a maximum pool depth of 550 cm for ESBWR and 700 cm for ABWR, and these values are used for the quencher depth.

Figure 4-1 illustrates the DF(total) values obtained by the simplified scaling model for each of the A-BWR at their maximum pool depth. Per the caveat for DF estimation, calculated DF values over 1E+06 are assigned 1E+06 as the DF value.

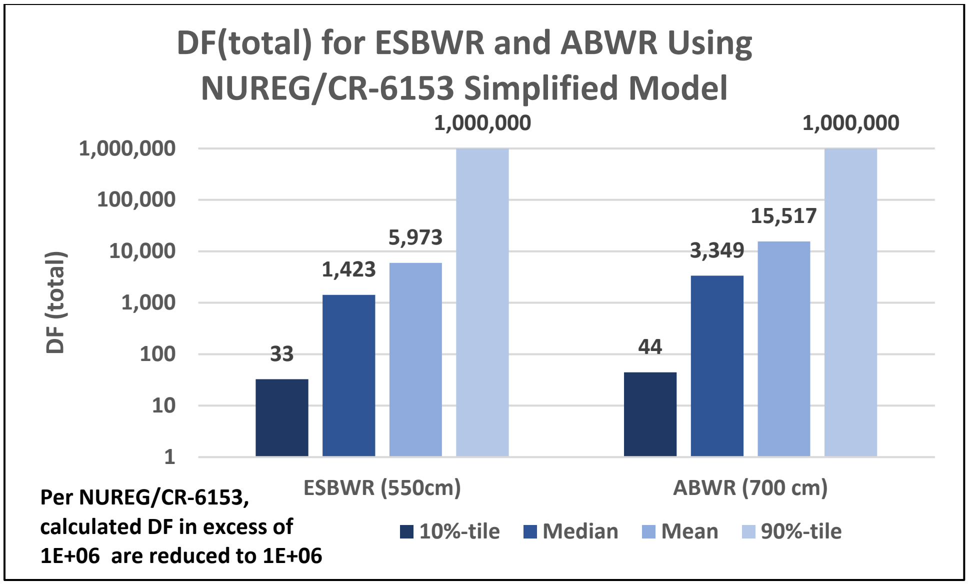

Figure 4-1 DF(total) for ESBWR and ABWR using NUREG/CR-6153 simplified model

There appears to be a linear relation between the scaled output of the 10%-tile, the median (most likely), and the 90%-tile for each of the log-scale ESBWR DF and the ABWR DF. This is demonstrated by the nearly straight line between the 10%-tile, the median, and the 90%-tile. For example, the linear relationship for (value, %-tile) in log-scale is [(33, 10%). (1,423, 50%), (1,000,000, 90%) for ESBWR.

To fit the data to a PDF requires a hypothesis that the data fits or does not fit a PDF. A statistical goodness of fit test is used to conclude the data follows, or does not follow, the hypothesized PDF. There are insufficient data to perform such a statistical test. There are three (n=3) observations corresponding to the scaled output values for the 10%-tile, the median, and the 90%-tile. A statistical Goodness-of-Fit (GOF) test for the scaled output is not performed and an assumed PDF is identified.

Table 4-6 provides the expected DF(total) and the 90%-tile under the assumption of a log-triangular PDF (logarithm base 10) for each of the ESBWR DF and the ABWR DF. Palisade @Risk simulation software is used to simulate this PDF (Palisade Corporation, 2018). For both the ESBWR DF and the ABWR DF values, the 10%-tile and the median can be used directly for the PDF simulation; however, the 90%-tile is decreased by ~30% to compensate for adjustable upper bounds when simulating a triangular PDF using percentiles rather than an absolute maximum value.

Table 4-6: DF(total) for ESBWR and ABWR fit as a log-triangular PDF

Summary statistics associated with DF(total) using a log(10)-triangular PDF	**Median (50%-tile)**	**Expected DF (Mean)**	**90%-tile**
ESBWR (550cm)	2,873	3,599	70,815
ABWR (700 cm)	4,761	5,294	81,974

Under the simplifying assumption of a log-triangular PDF for the ESBWR and ABWR DF(total), a bias reduction of 2,374 in the mean for the ESBWR is observed (5,973 to 3,599) and a similar bias reduction of 10,223 in the mean for the ABWR is observed (15,517 to 5,249). The 90%-tile values under a log-triangular PDF are considerably reduced from 1E+06 to 70,815 and 81,974 for the ESBWR and the ABWR, respectively. The realism of these values obtained by the simplified model is unconfirmed.

The simplified model in NUREG/CR-6153 provides scaling equations for the particle diameter, d_p, as illustrated in Figure 4-2. For the d_p, the scaling function is a linear form d_p (mm)= a + b x H(cm), where a is the intercept, b is the slope, and H is the quencher depth in cm. Type A A-BWR specify a maximum pool depth of 550 cm for ESBWR and 700 cm for ABWR, and these values are used for the quencher depth.

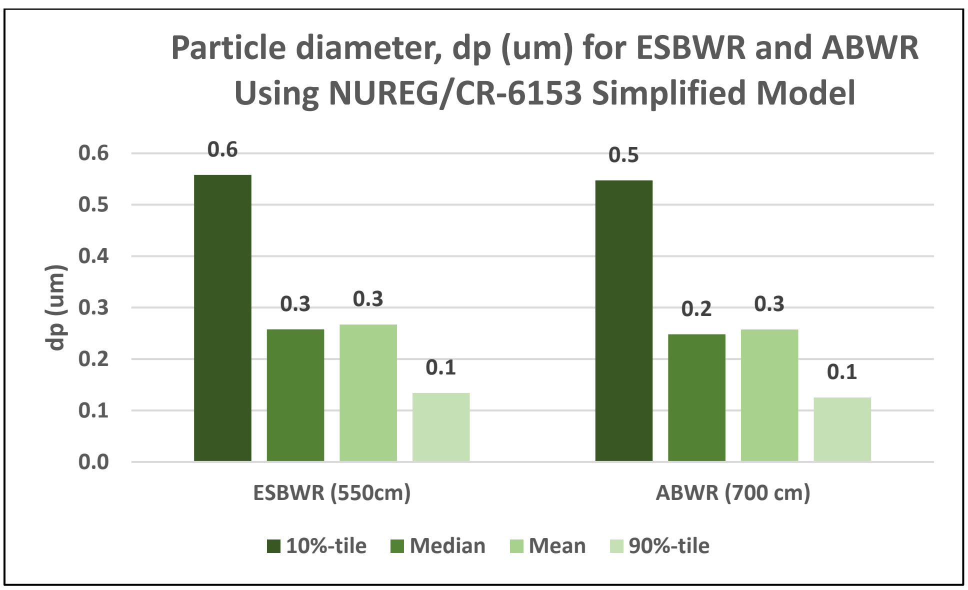

Figure 4-2: Particle diameter d_p (mm) for ESBWR and ABWR using NUREG/CR-6153 simplified model

4.2.2 Uncertainty Analysis Associated with NUREG/CR-6189

NUREG/CR-6189 (NRC, 1996) provides simplified formulae for estimating aerosol decontamination that can be achieved by natural processes in the containments of pressurized water reactors and in the drywells of boiling water reactors under severe accident conditions. These simplified formulae were derived by correlation of results of Monte Carlo uncertainty analyses of detailed models of aerosol behavior under accident conditions.

As stated earlier, NUREG 6189 correlations are not directly applicable to the Type A A-BWRs for estimating decontamination inside the drywell. It is unknown if newer methods and models are applicable

The relevance of the NUREG/CR-6189 uncertainty discussion is cross-walked to the prioritized PIRT phenomena applicable to a dry (gaseous) environment for A-BWR without a wetwell. This focuses the examination of the uncertainties identified in NUREG/CR-6189 with the A-BWR phenomena of interest. FOM affected by these phenomena are particle deposition velocity, v (mm/s) and the DF. Since both of these FOM are functionally affected by particle diameter, d_p, this parameter is also examined in this discussion. The prioritized phenomena are identified in Table 4-7.

Table 4-7: Prioritized PIRT Phenomena Applicable to A-BWR Dry (Gaseous) Environment

PIRT Requirement	**Prioritized PIRT Phenomena applicable to a dry (gaseous) environment for A-BWR with or without a wetwell**	
Enhanced Models	Primary	P4 Fluid Flow P6 Impaction
	Secondary	P2 Thermophoresis P3 Diffusiophoresis P7 Pressure Transients P5 Agglomeration/Coagulation
Further Tests	Primary	P4 Fluid Flow P7 Pressure Transients
	Secondary	P6 Impaction P8 Direct Contact Steam Condensation P2 Thermophoresis P3 Diffusiophoresis P9 Bubble Processes

Parameters and uncertainties associated with a gaseous environment for A-BWRs without a wetwell are identified in Table 4-8.

Table 4-8 NUREG/CR-6189 Parameters and Uncertainties Applicable to A-BWR Dry (Gaseous) Environment (NRC, 1996)

ID	**Parameter**	**Input range and Probability Density Function (PDF)**	**Reference in NUREG/CR-6189**	**Justification and Assumptions**
D1	Particle density	Range: 2.9-5.65 g/cc; PDF: uniform	Table 12, Uncertain quantities, range of values and subjective probability distributions	Based on experimental data from accident sequences.
D2	Particle diameter (initial)	Range: 0.02-0.2 micron; PDF: log-uniform	Table 12, Uncertain quantities, range of values and subjective probability distributions	There is a high level of uncertainty in particle diameter values, which is why the assumption is made. Basis is not provided.
D3	Steam Condensation rates	Constant steady state rate defined; PWR accident sequence analyzed based on steady state conditions	d. Late In-Vessel Release Phase, Page 114	Steady state assumed

ID	Parameter	Input range and Probability Density Function (PDF)	Reference in NUREG/CR-6189	Justification and Assumptions
		during each accident phase		
D4	Thermal gradient and steam conc gradient	Uncertainty coefficients for heat and mass transfer coefficient correlations; PDF: uniform		
D5	Heat and mass transfer length scale	Uncertainty parameter calculated from correlations; PDF: log-uniform		Used for gradient calculations
D6	Fluid velocity	Unknown		
D7	Particle thermal conductivity	Range: 2e-6-5e-4; PDF: log-uniform	Table 12, Uncertain quantities, range of values and subjective probability distributions	Calculated based on correlations. There is high uncertainty; particles are assumed to have higher diameter after agglomeration, and the porous regions are filled with water.
D8	Fluid density	Unknown		
D9	BWR drywell A/V ratio	Range: 0.28-0.36 m^{-1} with a continuous distribution; PDF: Students t	Table 12, Uncertain quantities, range of values and subjective probability distributions	Correlation derived from Mark I, II, III containment volumes.
D10	Temperature	Range: T_low = 0-850 K; T_high = T_sat (= 457.8 K at P = 11 atm); PDF: uniform	Table 12, Uncertain quantities, range of values and subjective probability distributions	Calculations performed with Source Term Code Package. The upper limit should be lower than the design temperature.
D11	Pressure	Range: P_low = 1.16-5.52 atm; P_high = 8-11 atm; PDF: uniform	Table 12, Uncertain quantities, range of values and subjective probability distributions	Calculations performed with Source Term Code Package. The upper limit should be lower than the design pressure.
D12	Decontamination coefficient for flow into suppression pool	Calculated from drywell P, T, V, flow rate (f) and gas constant R		Quasi steady heat transfer conditions are assumed for calculations.
D13	Containment surface temperature	Unknown		Weighted average of all drywell surface temperatures

ID	Parameter	Input range and Probability Density Function (PDF)	Reference in NUREG/CR-6189	Justification and Assumptions
D14	ε term in the particle Collision efficiency equation	Range: 0.1-1; PDF: lognormal	1. Uncertainty in the Collision Efficiency, Page 122	
D15	Shape factors	Calculated from packing efficiency (which is calculated from primary and final particle diameter) and density	4. Uncertainty in the Aerosol Shape Factors, Page 124	
D16	Fluid viscosity	Calculated from Fluid temperature		There exists a correlation for this calculation.
D17	Fluid thermal conductivity	Calculated from correlation		There exists a correlation for this calculation.

4.2.3 Example #1 of uncertainty reduction

Probabilistic distributional analyses using PDF of A-BWR allow data, which may be derived from a model or a test, to be represented compactly using only a few parameters such as the mean, standard deviation, and minimum, most likely and maximum values. Exploratory analysis of the model or test data offers insights to the underlying physical mechanisms involved in generating the data and vice-versa. Additionally, the analysis permits data to be generated which are outside the range of historically observed data, which can be useful for examination of a broader range of geometric or thermal hydraulic conditions. Hence, a broader range of reactor types may be assessed along with a wider range of thermal hydraulic conditions, which may include “extreme events”. Theoretical distributions may be preferable to the use of empirical distributions when the data are limited, the fit of the theoretical distribution to the data is good, and there is a theoretical or mechanistic basis that supports the chosen parametric distribution.

This leads to the tasks of (1) selecting candidate PDF theoretical distributions to determine which general families appear to be appropriate to use on the basis of the shape, summary statistics, and simple distributional plots, (2) estimating intrinsic parameters of the candidate distributions to define the specific distribution, and (3) assessing the quality of the resulting fit by examining how closely they represent the true underlying distributions for the data of interest and using statistical GOF tests. In both NUREG/CR-6189 and NUREG/CR-6153, a combination of empirical data and subjective assessments were used to define the PDF for the parameters.

Uncertainty reduction associated with the PDF based on updated tests or models may be achieved by adjusting the bias of the mean value, refining estimates of the variance of the parameter, or refining the correlation models previously determined for the parameters. For example, in NUREG/CR-6153 (NRC, 1996) the statement is made (p273-274):

> *"the deposition processes are often quite dependent on the aerosol particle size and tend to preferentially extract particles larger than 1 to 2 mm. Based on this reasoning, the mean aerosol particle size during the in-vessel phase of an accident is taken to be lognormally distributed around 1.6 mm with a geometric standard deviation for the distribution of the mean taken to be 2. Then, the 5 and 95 percentiles of the mean are about 0.5 and 5.0 mm. The geometric standard deviation of the aerosol size distribution is expected to be large. Here it is assumed to be uniformly distributed over the range of 1.8 to 3.8."*

Assuming the driver for uncertainty reduction is the geometric standard deviation, modeling or empirical data can be used to reduce the interval associated with the 5 and 95 percentiles of the mean.

Refinement in the values of the range of the geometric standard deviation can either increase or decrease the uncertainty in the 5%-tile or 95%-tile mean aerosol particle size. Such a refinement is accomplished using more granular models or test conditions.

The PDF as a cumulative distribution function for the mean aerosol particle size for changes in the geometric standard deviation is illustrated in Figure 4-3**Error! Reference source not found.**. For fixed or random values of the geometric standard deviation, the three cases appear similar, however, examining the behavior of the PDF for the 5%-tile and for the 95%-tile of the mean aerosol particle size illustrate the significance of changing the geometric standard deviation**Error! Reference source not found.**.

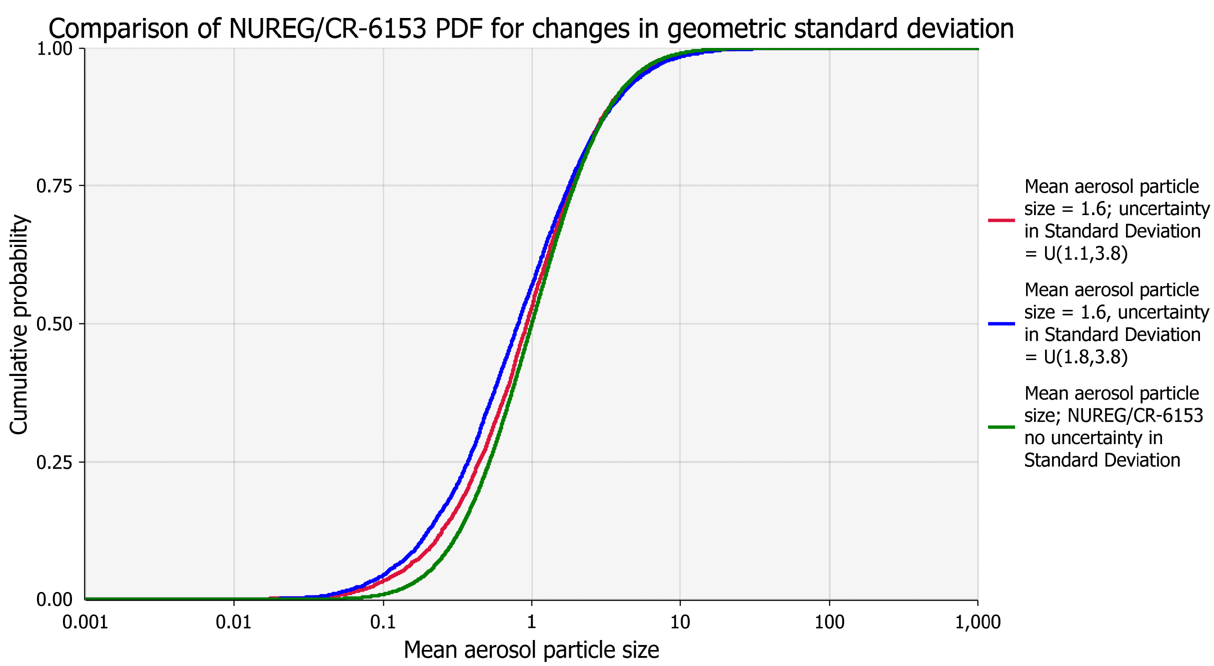

Figure 4-3 Comparison of NUREG/CR-6153 PDF for changes in geometric standard deviation

Figure 4-4**Error! Reference source not found.** illustrates the uncertainty reduction on (a) the 5%-tile mean aerosol particle size and (b) the 95%-tile mean aerosol particle size when changes in the geometric standard deviation are made. When the geometric standard deviation is a fixed value of 2 mm, the 5%-tile mean aerosol particle size is 0.20 mm and (b) the 95%-tile mean aerosol particle size is 4.9 mm. Assuming the geometric standard deviation is uniformly distributed over the range of 1.8 mm to 3.8 mm rather than a fixed value of 2 mm, the 5%-tile value mean aerosol particle size is approximately 0.11 mm (a 47% reduction from the case with a fixed geometric standard deviation) and the 95%-tile value is 5.44 mm (a 10% increase from the case with a fixed geometric standard deviation). If the minimum of the geometric standard deviation is reduced from 1.8 mm to 1.1 mm and is uniformly distributed over the range of 1.1 mm to 3.8 mm, the 5%-tile mean aerosol particle size is 0.13 mm (a 35% reduction from the case with a fixed geometric standard deviation) and the 95%-tile mean aerosol particle size is approximately 5.11 mm (a 4% increase from the case with a fixed geometric standard deviation).

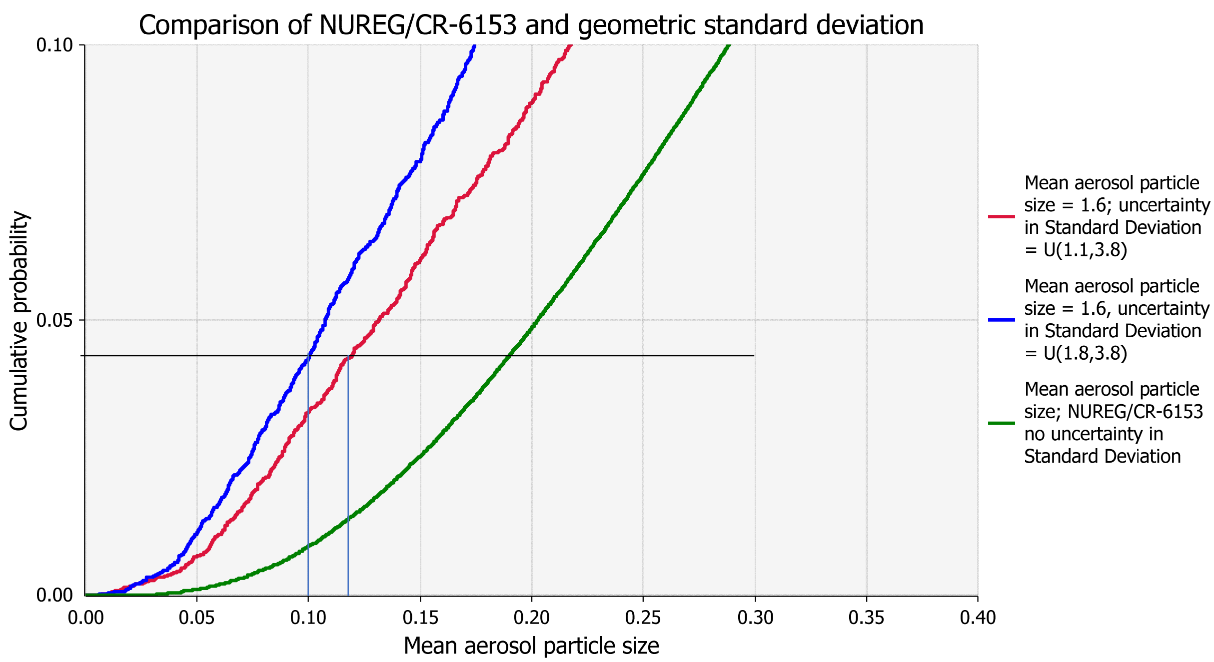

(a)

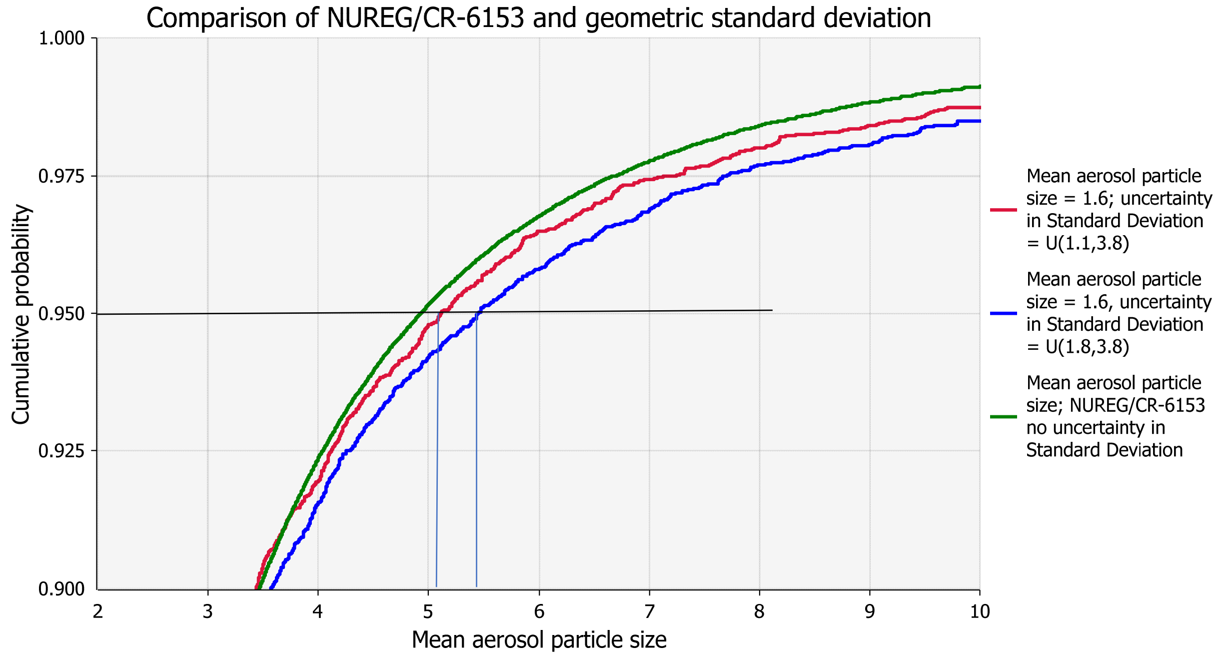

(b)

Figure 4-4: Illustration of uncertainty reduction of (a) 5%-tile and (b) 95%-tile

4.2.4 Example #2 of uncertainty reduction

A previous example provided deterministic overall DF values for 100 g for 16 cases associated with (1) percent aerosol mass remaining in the drywell after aerosol transport to the suppression pool (10%, 20%), (2) percent aerosol mass deposited in the drywell (65%, 75%), (3) percent aerosol mass transfer out of suppression pool (10%, 15%), and (4) percent aerosol mass deposited in the wetwell dry region (65%, 75%).

Although the DF values are numerically different for the cases, they are not statistically different. Since the percentages are considered continuous variables with unknown random effects on DF, **Error! Reference source not found.** a non-parametric density statistical approach can be used to illustrate this. The benefit of this approach is that no assumption of the distribution of the percentages is required. Figure 4-5 shows the examination of the DF as a function of percentage of aerosol mass in the drywell and suppression pool. Contours indicate the quantile densities (red indicates 10% of the data, purple indicates 90% of the data, and the color scale indicates values between 10% and 90%). The red line is the overall average DF = 13.8 for the 16 cases, the standard deviation is 3.32 indicating a relatively small relative standard error of deviation 24%, and the standard error of the mean is quite small, 0.83. The overlap in the contours for each of the percentages visually demonstrates the similarity of the cases.

The single point that stands out corresponds to the DF = 21.05 for (1) percent aerosol mass remaining in the drywell after aerosol transport to the suppression pool = 10%, (2) percent aerosol mass deposited in the drywell = 75%, (3) percent aerosol mass transfer out of suppression pool = 10%, and (4) percent aerosol mass deposited in the wetwell dry region = 75%. It is not an outlier but is simply a large value.

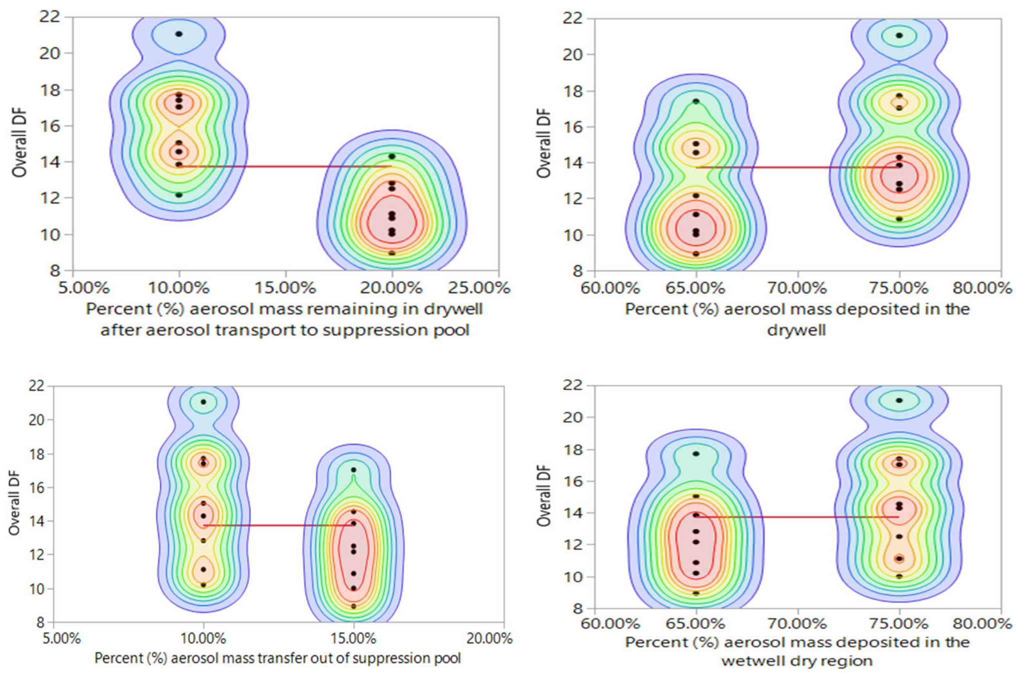

Figure 4-5: Examination of DF as a function of percentage of aerosol mass in drywell and suppression pool

To illustrate the impact of changing values in PDFs and PDFs themselves, consider a base case of (1) percent aerosol mass remaining in drywell after aerosol transport to suppression pool (uniformly distributed between 10% and 20%), (2) percent aerosol mass deposited in the drywell (uniformly distributed between 65% and 75%), (3) percent aerosol mass transfer out of suppression pool (uniformly distributed between 10%, and 15%), and (4) percent aerosol mass deposited in the wetwell dry region (uniformly distributed between 65% and 75%). The expected DF for the base case is 13.0 which is bounded by the 10%-tile of 11.1 and the 90%-tile of 15.8.

The first sensitivity case is defined in two parts. First, there is no change in (1) percent aerosol mass remaining in drywell after aerosol transport to suppression pool (uniformly distributed between 10% and 20%), (2) percent aerosol mass deposited in the drywell (uniformly distributed between 65% and 75%), and (3) percent aerosol mass transfer out of suppression pool (uniformly distributed between 10%, and 15%). Second, the PDF is changed from a uniform PDF to a triangular PDF for (4) percent aerosol mass deposited in the wetwell dry region (triangular distributed with minimum 65%, most likely 74%, and maximum 75%). The expected DF for the base case is 13.3 which is bounded by the 10%-tile of 11.3 and the 90%-tile of 15.9.

A second sensitivity is defined as the same as the first except the maximum for (4) percent aerosol mass deposited in the wetwell dry region is increased to 80%. The expected DF for the base case is 15.5 which is bounded by the 10%-tile of 8.8 and the 90%-tile of 45.8.

The change of the PDF from uniform to triangular and increasing the maximum for (4) percent aerosol mass deposited in the wetwell dry region from 75% to 80% increases the DF and provides a considerably greater 90%-tile than the base case and the initial sensitivity.

4.2.5 Use of experimental designs in modeling or testing to measure and reduce uncertainties

Experimental designs (or test matrices) can be developed based on the analytical models developed based on parameters that influence gravitational, diffusiophoretic and thermophoretic deposition and how these phenomena affect the DF in ABWR and ESBWR drywell and the wetwell air volume above the suppression pool.

Five of the key parameters and ranges of the parameters are presented in Table 4-9. Some of these parameter values are not independent and will be considered as coupled in an experimental design for modeling or testing

Table 4-9: Five key parameters for phenomena affecting DF in ABWR and ESBWR drywell and wetwell air volume

Parameter	Meaning	Values for models or tests	Units
Afloor/V	Area of floor divided by volume	0.12, 0.16, 0.21, 0.66, 0.86	1/m
x	Steam mole fraction	0.25, 0.50, 0.75	none
D_p	Particle diameter	1, 5, 10	mm
T_g	Operating temperature	35, 43.3, 57.2, 103.9, 171	C
T_w	Temperature	25, 33.3, 47.2, 93.9, 161	C
P_g	Operating pressure	104.1, 411	kPa

Assuming each of the six parameters has three possible values (low, moderate, high), an experimental design could be constructed that has 3^6 = 729 possible combinations. This is prohibitive in terms of schedule and cost of model runs or tests. A staged approach is recommended for development of experimental designs for model runs or tests as identified in

Table 4-10.

Table 4-10 Staged approach for experimental deigns for models or tests

Stage	ID	Steps	Data sources
Set Up	SU-1	Identify the FOM to be examined (DF, v)	Model or test objectives and PIRT
Screening	S-1	Identify the key parameters required to determine the FOM	Analytical modeling, model/ test and statistical planning
Screening	S-2	Identify maximum number of runs which can be performed	Analytical modeling, model/ test and statistical planning
Screening	S-3	Identify any nesting or dependency of the key parameters	Analytical modeling, model/ test and statistical planning
Screening	S-4	Determine whether a key parameter is a continuous or categorical variable. During preliminary experimental design efforts, continuous parameters may be considered as categorical.	Analytical modeling, model/ test and statistical planning
Screening	S-5	Determine values for key parameters (low and high)	Model/ test and statistical planning
Screening	S-6	Construct screening experimental designs with maximum number of runs included and allowable aliasing of parameters (fractional designs or main effects). Construct specialized design if required.	Model/ test and statistical planning
Screening	S-7	Select test matrix/design based on confidence achievement, power analysis, estimated variance profile, estimation efficiency, and correlation analysis	Model/ test and statistical planning
Screening	S-8	Perform modeling or perform tests using selected test matrix/design	Modeling or simulation or test execution including instrumentation
Screening	S-9	Determine which parameters drive the variance associated with the FOM	Modeling or simulation or test analysis of results
Detailed modeling or testing	Same as S-1 through S-9	Given understanding of parameters and FOM responses obtained through models or tests, developed detailed designs and test matrices to examine finer levels of parameter values	• Analytical modeling • Model/ test and statistical planning • Modeling or simulation or test execution • Analysis of results

4.3 Sample Decontamination Factor Calculations for the 1A PIRT Evaluation

Per Table 2-1, the 1A PIRT evaluation pertains to aerosol deposition phenomena applicable to a dry environment for Type A A-BWRs, which are defined in this report as A-BWRs with a wetwell (e.g. ABWR, ESBWR). Sample calculations for deposition velocities due to sedimentation and phoretic phenomena have been presented in the 1A PIRT evaluation to obtain qualitative trends for the variation of the DF with respect to the particle diameter and steam concentration. The following assumptions have been made for this evaluation:

1. Vessel wall temperature is assumed to be 10°C less than the air temperature inside the vessel.
2. The air inside the drywell vessel is assumed to be stagnant.
3. The air will lose momentum when it passes through the suppression pool and reaches the SP surface with a relatively insignificant air velocity.
4. DF of SP will be calculated during subsequent phases of the project (assuming stakeholder concurrence).
5. DF in the wetwell's air volume section above the SP is calculated for the gravitational, diffusiophoretic and thermophoretic deposition mechanisms.
6. Nickel particles are used in DF and deposition velocity calculations (ρ_p=8900 kg/m^3).
7. A/V values used in DF calculations for drywell and wetwell vessels are given in the following Table 4-11.

Table 4-11: A/V Values of Drywell and Wetwell Containment Vessels (GE-Hitachi, 2007) (GE-Hitachi, 2011)

Vessel Parameters	ABWR Drywell	ESBWR Drywell
V (Volume) [m^3]	7350	7206
$A_{envelope}/V$ [1/m]	0.29	
$A_{envelope}=A_{Side}+A_{floor}+A_{dome}$ [m^2]	2132	2090
H (Height) [m]	≈15	≈15.3
D (Diameter) [m]	≈25	≈24.5
A_{floor}/V (for gravitational DF)	0.67	0.65
	0.66 (used average value for both ABWR & ESBWR calculations)	
A_{side}/V (for phoretic DFs)	0.16	
Vessel Parameters	**ABWR Wetwell Air Volume Section Above SP**	**ESBWR Wetwell Air Volume Section Above SP**
V (Wetwell Volume – SP Volume) [m^3]	5960 - 3580 = 2380	5350 - 4424 = 926
$A_{envelope}/V$ [1/m]	0.29	
$A_{envelope}=A_{Side}+A_{floor}+A_{dome}$ [m^2]	2132	2090
H (Height) [m]	≈4.65	≈1.15
D (Diameter) [m]	≈25.5	≈32
A_{floor}/V (for gravitational DF)	0.21	0.87
A_{side}/V (for phoretic DFs)	0.16	0.12

For brevity, the sample DF calculations with the above assumptions and parametric values have been provided for the ESBWR, for the drywell as well as the dry region in the wetwell. The deposition velocity trends agree qualitatively with theory, and the trends seen during Phase 2 of EPRI's iPWR project. Broadly, the sedimentation velocity increases while the phoretic velocities decrease with increasing particle diameter. The presence of steam enhances both thermophoresis (due to lower overall mixture density) and diffusiophoresis (due to stronger condensation). These trends for the ESBWR have been shown from Figure 4-6 to Figure 4-11 for the operating conditions, as shown in Table 4-11.

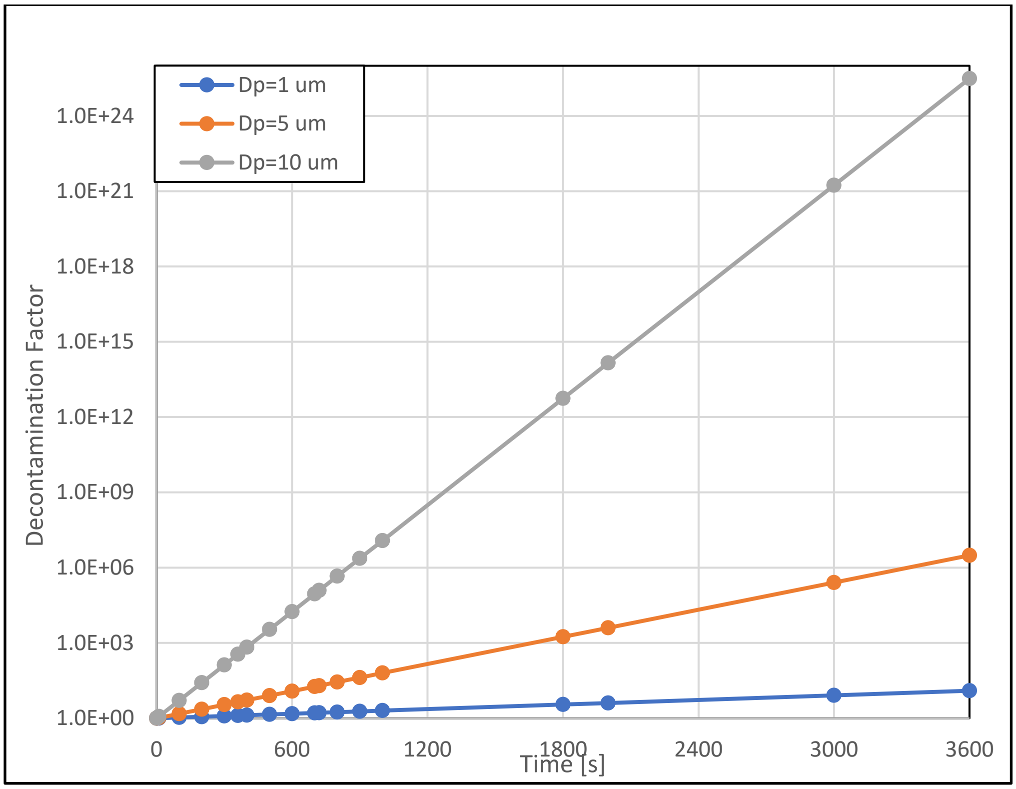

Figure 4-6: Sedimentation DF for ESBWR Drywell (A_{floor}/V=0.66 m^{-1})

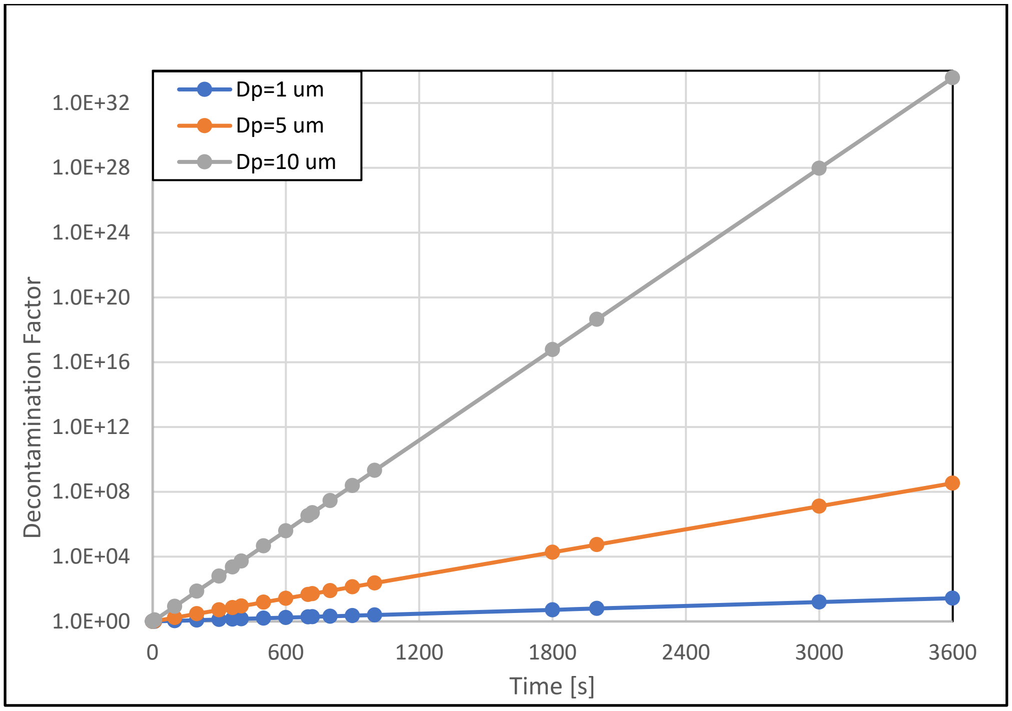

Figure 4-7: Sedimentation DF for ESBWR Wetwell Air Volume Above Suppression Pool ($A_{floor}/V=0.87\ m^{-1}$)

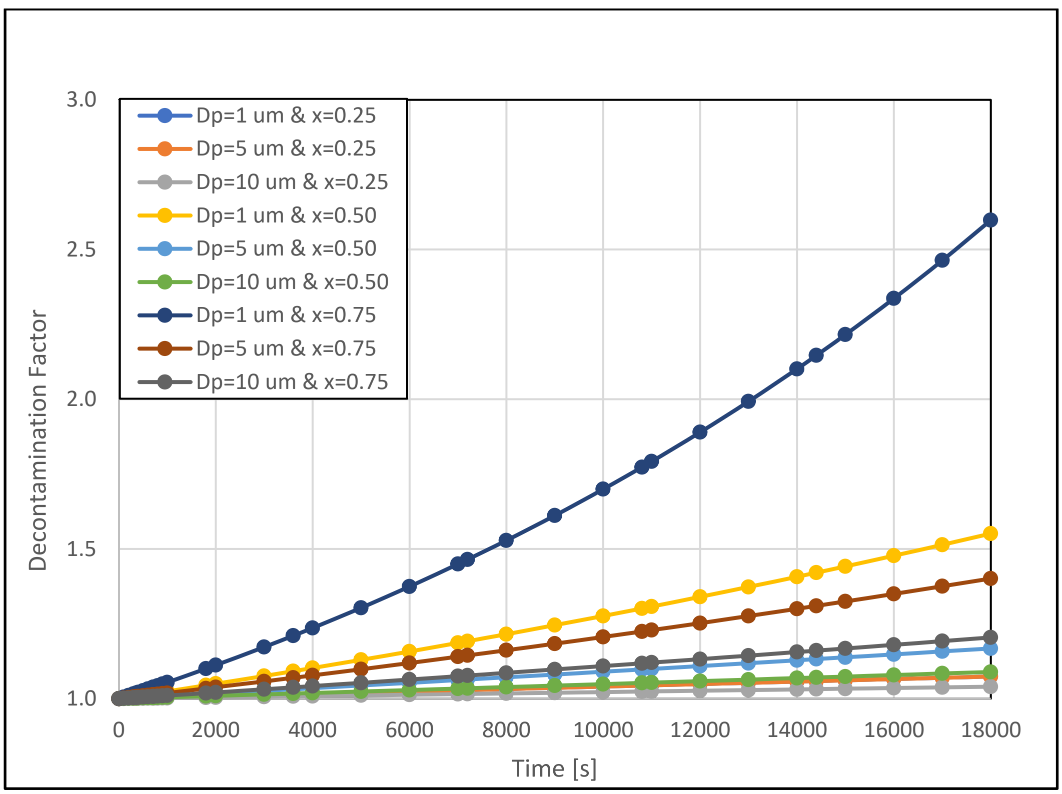

Figure 4-8: Thermophoretic DF for ESBWR Drywell ($A_{side}/V=0.16\ m^{-1}$)

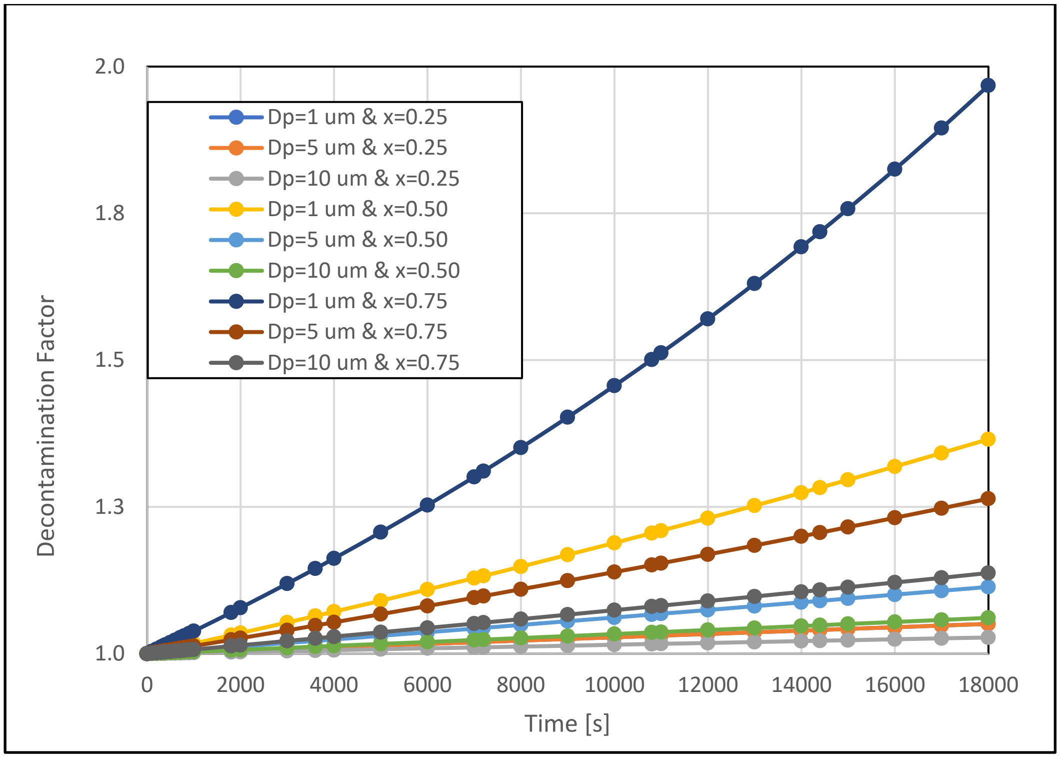

Figure 4-9: Thermophoretic DF for ESBWR Wetwell Air Volume Above Suppression Pool ($A_{side}/V=0.12\ m^{-1}$)

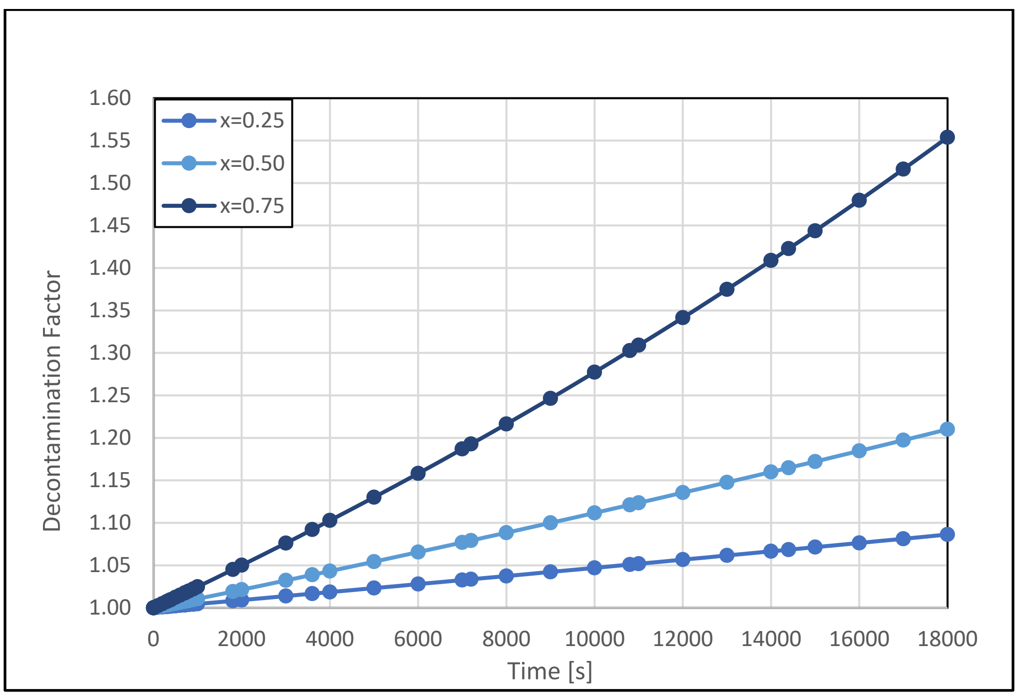

Figure 4-10: Diffusiophoretic DF for ESBWR Drywell ($A_{side}/V=0.16\ m^{-1}$)

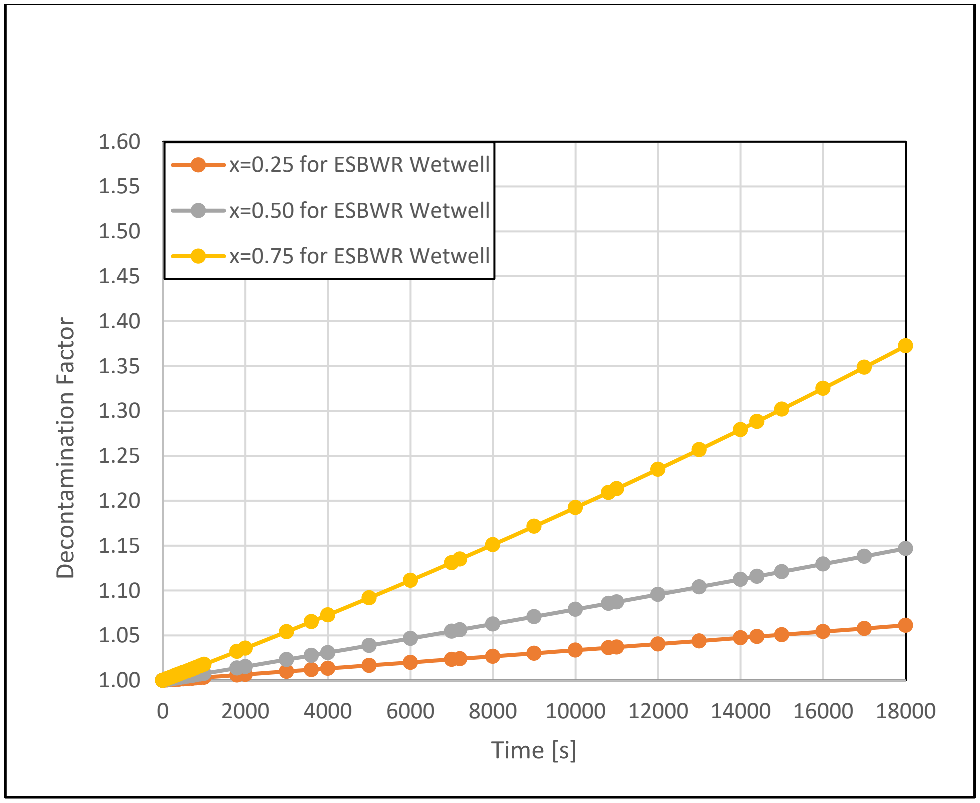

Figure 4-11: Diffusiophoretic DF for ESBWR Wetwell Air Volume Above Suppression Pool ($A_{side}/V = 0.12\ m^{-1}$)

5 Experimental Verification of Fission Product Deposition Phenomena Effects on Decontamination Factors in the Severe Accident Regime of Advanced Boiling Water Reactors

This section provides a summary of the major test assumptions and input parameters for the required A-BWR source term reduction project experiments. The experiments will quantify critical parameters for fission product deposition processes for a range of conditions that are representative of ABWR designs. Note that input from critical stakeholders has been incorporated into this document. Additional feedback will be considered and incorporated as practicable within the future follow-on scopes of work.

As described in prior sections of this report, the technical basis for the proposed experimental work includes an assessment of ABWR accident conditions, a gap assessment of available experimental data, and a PIRT assessment of the significance of fission product deposition processes. Prior work, notably the iPWR Aerosol Containment Experiments was referenced based on the relative similarities, to make the planned experiments more efficient.

The test plan will describe a set of physical experiments to investigate and verify theoretical models of fission product decontamination under simulated accident conditions for A-BWR designs. The test plan focuses on known aerosol-behavior data gaps under severe accident conditions.[1] The project involves the experimental evaluation of aerosol deposition processes for a range of conditions that are appropriate for A-BWR. There are four major integrated work streams that will be used to successfully execute the experiments, and these include Stakeholder Communication, Analysis, Test Loop Design and Experimentation. The activities in each work stream and their interrelations are described subsequently.

Stakeholder Communication: This process will ensure that the experimental work performed adequately addresses stakeholder requirements. It will include structured, periodic communication with the stakeholders where input and feedback on specific questions will be elicited. The required input from vendors includes design dimensions, thermal hydraulic operating parameters and radionuclide particle inventories, amongst other inputs.

Analysis: The analysis scope is required to support the planning, experimental design, effective execution and interpretation of results. Specifically, the analysis will include the following steps:

- Characterize and establish agreement on the critical fission product retention parameters for Type A and B A-BWRs.
- Define generic A-BWR containment models.
- Define assumptions around accident progression.
- Define assumptions for aerosol composition.
- Define generic containment environment properties.

[1] Note that severe accidents are specifically identified because these include potential radionuclide particle release, which is the subject of the study.

- Develop A-BWR specific correlations that can be used to model severe accident aerosol behavior.

Test Loop Design: This work scope is required to develop an experimental test loop that represents A-BWR geometries and thermal hydraulic parameters. Specifically, this work scope will include the following items:

- Design test loop with varying test chamber dimensions: The parametric study will require dimensional variability to capture a range of planned and potential A-BWR geometries.
- Determine test periods: This will be based on representative accident scenarios and sequences.
- Secure appropriate aerosol radionuclide particle simulants.
- Procure equipment for temp, pressure, humidity, heat flux, and steam condensation rate measurements: These will be used to simulate the thermal hydraulic conditions.
- Assemble test loop for various tests.

Experimentation: The experiments will be conducted in three phases which include:

- Experiment Phase I: Calibration and benchmarking, including confirmation of particle sizes.
- Experiment Phase II:
    - Establish decontamination factors due to critical phenomena of interest, which include phoretic, gravitational, convective flow and wet-well related mechanisms.
    - Perform experiments with varying reactor vessel configurations to achieve various surface area to volume ratios.
    - Establish the significance of convective flow and its effect on deposition velocities.

5.1 Derivation of Appropriate Simulant for Aerosolized Radionuclide Particles

NUREG/CR-6189 provides a range of aerosol material densities for various release phases of large LWR severe accidents. The material density in the ex-vessel phase is estimated to be between 3.50 to 6.15 g/cm^3 due in part to the “vigorous interaction between core debris and concrete”. After this initial phase, the material density of the aerosols reduces to a range of 2.1 to 3.90 g/cm^3 (U.S. Nuclear Regulatory Commission, 1996). Considering there is no concrete in the BWRX-300 containments under consideration, the aerosol material density is expected to be higher than this range. It is recommended that the subsequent phase of this study includes a characterization of the constitution of the aerosol for BWRX-300.

5.2 Test Dimensions to Model Generic SMR Containments

Dimensional variability is required to capture a range of geometric parameters that are representative of A-BWR designs. The critical parameter of interest is the containment surface area to volume ratio.

$\frac{A_E}{V} = 0.469 - (2.43 * 10^{-5})V \pm 0.0225$ Equation (4-2) is used for calculation of the A/V ratio in BWR Mark I, Mark II and Mark III containments (NRC, 1996), with the values as shown in Table 5-1.

Table 5-1: A/V ratios for BWR containment vessels

Containment Type	Drywell Volume [m^3]	A/V ratio [m^{-1}] (ft^{-1})
Mark I	4500	0.36 (0.11)
Mark II	6500	0.31 (0.094)
Mark III	7650	0.28 (0.085)
A-BWR	7350	0.29 (0.088 ± 0.007)
ESBWR	7206	0.29 (0.088 ± 0.007)
BWRX-300	TBD	TBD

5.3 Assumptions for Containment Vessel Thermal Hydraulic Parameters

The temperature values that would be selected for the experiments are based on considerations for two scenarios; an Early (prescriptive) Release based on current regulatory guidance (NRC Regulatory Guide 1.183)[2] and advanced BWR-specific Late (Mechanistic) Release. The Early Release scenario assumes the occurrence of a large pipe break and hence immediate drainage that results in core exposure in less than one hour, and which results in a containment vessel atmosphere temperature increase. The Late Release scenario assumes the elimination of the large pipe break scenario for the BWRX-300 and hence results in a range of time to core exposure that would be significantly longer (with specific estimates yet to be provided). Given the phoretic forces are proportional to thermal and steam gradients between the 'hot' reactor vessel and 'cold' containment vessel, it is conservative to assume a lower temperature gradient for the experiments, which is experienced in the mechanistic case. Hence, to capture both the mechanistic and prescriptive scenarios, the temperature range for the containment vessel atmosphere will include both assumptions.

5.4 System Description: Pit-Tech Experimental Test Loop and System Overview

The Pit-Tech fission product deposition testing system is comprised of three vessels that represent the CV and variable-sized RVs, which are inserted into the CV. These vessels are removable and interchangeable. The CV diameter is 80 inch and includes a dimpled water jacket to simulate immersion in water and control the interior wall temperature as specified by the conditions for a given test. The water in the dimpled jacket is circulated to a heat exchanger and chiller system.

[2] U.S. Nuclear Regulatory Commission, 2000. Regulatory Guide 1.183, "Alternate Radiological Source Terms for Evaluating Design Basis Accidents and Nuclear Power Plants," Rev 0, U.S. NRC.

Each of the reactor vessels has a matched top cover that will provide an interface and seal with the containment vessel. The top cover will also house an array of ports for optical access. Pressure conditions for the containment vessel, interior volume and annulus will be controlled using compressed air and a pressure gauge. Pressure values will range between 20 to 200 psi.

5.5 System Description: Thermal Hydraulic Loop

The thermal hydraulic loop includes the following major components: steam generator, vacuum recirculation pump, compressors, chiller, piping, connectors and various control valves. The loop also includes measurement and control devices that include flow meters, thermocouples and pressure transducers. The thermal hydraulic system is designed to supply steam at variable concentrations into the containment vessel. The maximum steam temperature and pressure are respectively 500°F and 200 psi.

5.6 System Description: Non-Invasive Measurement Access with Glass Ports for the Laser Measurement System

Aerosol deposition velocities and concentration change will be measured with particle image velocimetry using specialized lasers. The position of the lasers was determined based on requirements to focus on the most important regions of interest within the CV volume. The CV volume can be described as having three discrete steam concentration regions; the superheated region which is closest to the RV, the condensation region which is in the immediate vicinity of the CV wall and the superheated region which is between the saturated and condensation regions. Hence, for diffusiophoresis, which is driven by a steam concentration gradient, measurement points were selected in the superheated and condensation regions. Hence the measurement points indicated in Table 3 were determined with consideration of the radial distance between the CV and RV based on the following dimensions:

- RV Outer Diameter: D_{RV} = 4″, 26″, and 36″
- CV Inner Diameter: D_{CV} = 80″

5.6.1 Radial locations the laser transmitter glass access port

Sample points for each elevation are shown as radial locations from the CV wall.

Table 5-2: Laser Sample Points Location from Top View

RV Radius	**Case 1**	**Case 2**	**Case 3**
	2″	13″	18″
Annulus Distance between RV & CV	38″	27″	22″
$R_{RV} + \Delta R$	40″		
1st, 3rd, and 5th sample points R_1, R_3, and R_5 (CV wall is reference)	2.5″		
2nd, 4th, and 6th sample points R_2, R_4, and R_6 (CV wall is reference)	7″		

5.6.2 Vertical locations for the laser transmitter glass access port

In order to measure the particle concentration and velocities at 3 different vertical locations (height of CV shell), the following view ports are required.

Table 5-3: Laser Sample Points Location from Side View

CV Shell Height = 96″	Desired Height from Top	Glass Access Port Sizes for Transmitter and Receiver Laser Beams (circular)
Height of 1st and 2nd Sample points	24″	4 Ports with D_{port}=80 mm
Height of 3rd and 4th Sample points	48″	4 Ports with D_{port}=80 mm
Height of 5th and 6th Sample points	72″	4 Ports with D_{port}=80 mm

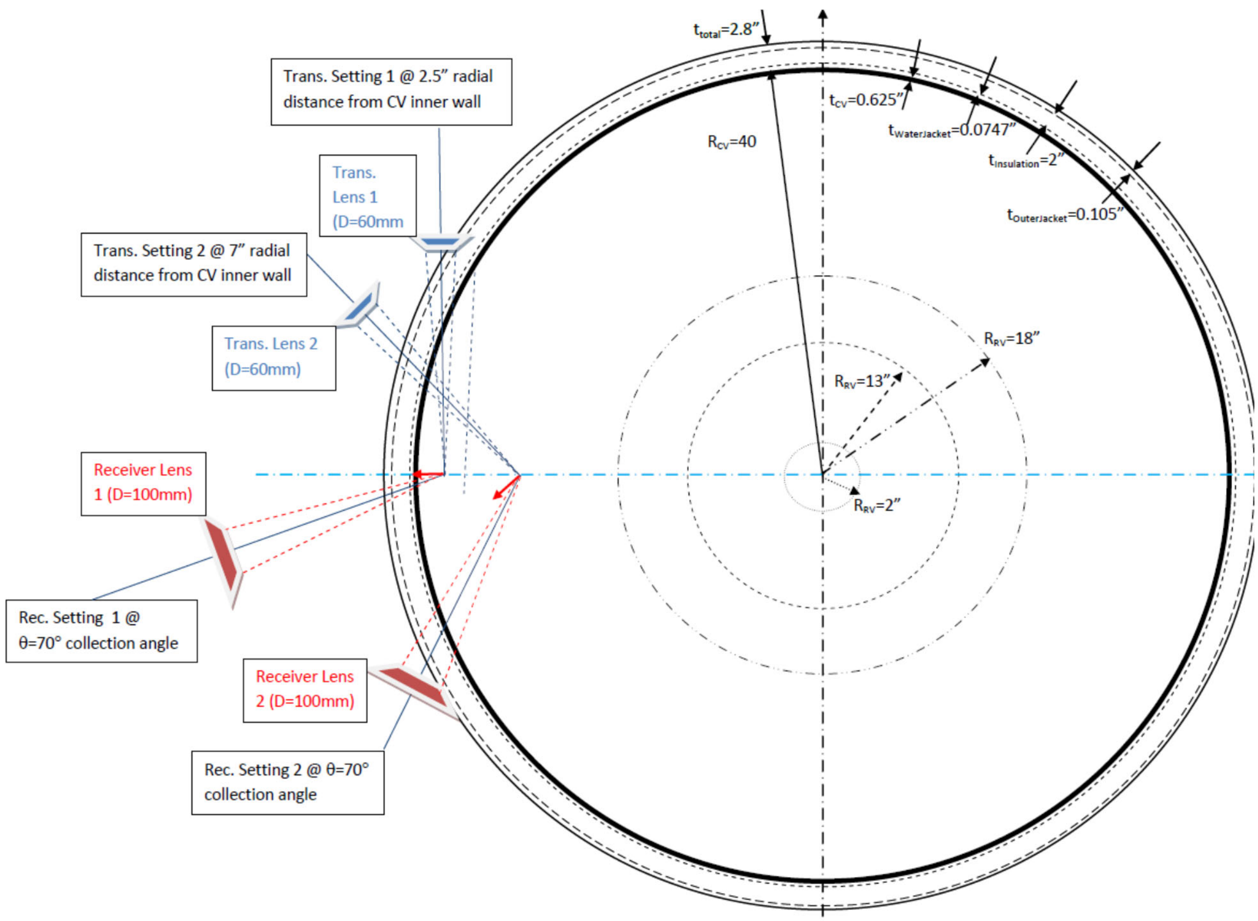

Figure 5-1: Laser Sight Access Locations from Top View

6 Conclusions and Recommendations

6.1 Conclusions

Major takeaways from each section

1. Section 1: Introduction
    a. The current assumptions for BWR in-containment fission product removal may not be appropriate for SMR type BWRs.
    b. Examination of A-BWR models and codes has identified opportunities to modify existing codes for more specific and refined analyses of fission product deposition.
    c. The existing correlations for aerosol decontamination estimates may not be directly applicable to advanced BWRs.
    d. Improvements made to the theoretical constructs of drywell deposition phenomena during the iPWR Phase 2 project should apply to the BWR drywell phenomena as well.
2. Section 2: Literature review
    a. Deposition phenomena can be categorized into two categories – phenomena applicable to a gaseous environment, and those applicable to a liquid environment.
    b. Assessment of the effects of coupling between parameters and phenomena should be considered during the modeling of these phenomena.
    c. There are gaps in current BWR safety analysis codes, which are identified in this document and that need to be addressed before they can be applied to A-BWR studies.
3. Section 3: Preliminary analysis
    a. The A-BWRs can be classified into two types – with and without a wetwell; this classification can take into account the differences in size, volume, thermal-hydraulics, geometry and aerosol characteristics between the two A-BWR types.
    b. The aerosol transport pathway characterization allows consideration of the A-BWR aerosol deposition processes in series (at different locations) and as a whole. Different pathways apply to different A-BWR types.
    c. Three PIRT analyses based on the phenomena categories and A-BWR types are needed to understand the phenomena which are more important in each case.
4. Analysis
    a. Current correlations may not be applicable to the given A-BWRs. However, there exist similarities in thermal-hydraulics and geometry.
    b. Uncertainty characterization at each stage of the calculation is important and can be done by enhancing and building on the Monte Carlo analyses given in existing NUREGs.
    c. Sample DF calculations show the DF values calculated with 1D modeling. The qualitative trends are consistent with the physics.
5. Test plan considerations

    a. Two major areas of testing identified: BWRX-300 drywell, and ABWR and ESBWR suppression pool.
    b. Changes need to be made to the current testing facility in order to perform experiments for this project.
6. Miscellaneous conclusions
    a. Established a roadmap to improve the characterization of source terms for A-BWRs.
    b. Roadmap leverages prior research findings and lessons learned from a similar related iPWR program.
    c. Verified that there is a potential for significant reduction in the estimated A-BWR source term, if the recommended roadmap is further executed and completed.
    d. Identified critical geometric, thermal hydraulic, aerosol characteristics and systemic parameters that influence fission product behavior and deposition.
    e. The most critical parameters were identified by stakeholder input through a PIRT exercise, modeling, and uncertainty analysis.
    f. Additional experimental data needs and analytical correlation requirements to properly model unique design features and transient containment post-accident thermal-hydraulic behavior were identified.
    g. Identified the need to separately assess small and large A-BWRs due to the different geometric and thermal hydraulic regimes in which their depositional phenomena occur.

6.2 Phase 2 recommendations

- For SMR-Type Advanced BWRs:
    - Current assumptions for BWR in-containment fission product removal may not be appropriate for SMR type BWRs.
    - Specifically, critical parameters for fission product retention analysis, which include aerosol characteristics, thermal hydraulic environment, geometry and systemic features are significantly different for the BWRX-300 design.
    - Phase 2 Scope: Include characterization of the constitution of the aerosolized radionuclides for BWRX-300.
    - By assessing large advanced boiling water reactors, that generally have parameters that conservatively bound the expected BWRX-300 parameters, a qualitative statement can be made that the BWRX-300 has characteristics that would support higher fission product deposition rates, similar to the iPWR design.
    - Based on the similarities, the BWRX-300 and other potential future BWR SMR designs may adopt the approach used to characterize and quantify the iPWR passive fission product retention capabilities.
    - This will leverage prior analytical work and model development. An example of this is the use of the drift flux model to simulate and measure radionuclide deposition velocities.

- Closure of existing gaps:
    - Identify methods to close existing gaps with modeling.
    - Examination of A-BWR models and codes has identified opportunities to modify existing codes for more specific and refined analyses of fission product deposition. An example is characterization of convective flow as an applicable fission product transport and deposition mechanism. Considering convective flow has not been included as an applicable fission product removal mechanism in containment vessels, this study may provide the basis for attribution of this mechanism. The results could be factored into codes that use the similitude approach by inclusion of correlations for turbulence and impaction.
    - Support the enhancement of existing codes by developing analytical inputs that improve the existing frameworks, model fidelity and confidence associated with outputs. An example of this is the development of drag modification factors that can be included in existing codes. To reflect the effects of particle-laden bubbles on aerosol deposition, it is proposed that future studies characterize a drag modification factor, which quantifies the drag influence of particles on the bubble velocity through a force analysis.

- Applicability of existing regulatory-recognized analytical frameworks and correlations to advanced boiling water reactors:
    - Existing correlations for aerosol decontamination estimates may not be directly applicable to advanced reactors.
    - Existing correlations as described in references such as NUREG 6189 relate power to decontamination estimates, and the power ranges for the advanced reactors are outside of the range of applicability described in NUREG 6189.
    - However, there are thermal hydraulic parameters that are similar. Hence, on a phenomenological basis, similar methods and models may be used to perform deposition estimates between the reactor types.
    - For application of the simplified models provided in NUREG 6153 and 6189, there is a need to establish specific correlations for the advanced reactors based on their power range.

References

1. Aarnes, J. R., Haugen, N. E., & Anderson, H. I. (2018). Inertial particle impaction on a cylinder in turbulent cross-flow at modest Reynolds numbers. *International Journal of Multiphase flow*.
2. Albiol , T., Herranz , L., Riera, E., Dalibart, C., Lind, T., Del Corno, A., . . . Cantrel, L. (2017). *Passive and Active Systems on Severe Accident source term Mitigation (PASSAM project).* NUCLEAR FISSION AND RADIATION PROTECTION.
3. Bales, M. (2018). *Michelle Bales, Phenomena Identification and Ranking Tables WHY and HOW.* Nuclear Regulatory Commisson.
4. Barrett, J. C., & Clement, C. F. (1990). AEROSOL CONCENTRATIONS FROM A BURST OF NUCLEATION. *Journal of Aerosol Science*.
5. Berna, C., Escriva, A., Munoz-Cobo, J. L., & Herranz, L. E. (2015). Enhancement of the SPARC90 code capabilities for pool scrubbing under jet injection regimes. In *Computational Methods in Multiphase Flow.*
6. Biwalkar, R. M., & Talabi, S. M. (2018). Sensitivity of Aerosol Removal Mechanisms to Varying Thermal-hydraulic Parameters in Intergated Small Modular Reactors. *ANS Winter Meeting.* Orlando, FL.
7. Cai, J., Jo, B., & Okamoto, K. (2015). Effect of non-condensable gas on thermal stratification and flow patterns in suppression pool. *Nuclear Engineering and Design*.
8. Chan, C. K., & Lee, C. K. (1980). A regime map for direct contact condensation. *International Journal of Multiphase Flow*.
9. Chun, M.-H., Kim, Y.-S., & Park, J.-W. (1996). AN INVESTIGATION OF DIRECT CONDENSATION OF STEAM JET IN SUBCOOLED WATER. *Int. Comm. Heat Mass Transfer.*
10. Dehbi , A., Suckow, D., & Guentay, S. (2001). Aerosol retention in low-subcooling pools under realistic accident conditions. *Nuclear Engineering and Design*.
11. Dekkers, P. J., & Friedlander, S. K. (2002). The Self-Preserving Size Distribution Theory: I. Effects of the Knudsen Number on Aerosol Agglomerate Growth. *Journal of Colloid and Interface Science*.
12. Diamond, D. J. (2006). Experience Using Phenomena Identification and Ranking Technique (PIRT) for Nuclear Analysis. *PHYSOR-2006 Topical Meeting.* Brookhaven National Laboratory.
13. EPRI. (2014). *Integrated Pressurized Water Reactor (iPWR) Containment Aerosol Deposition Behavior.* Electric Power Research Institute.

14. EPRI. (2018a). *Advanced Nuclear Technology: Integrated Pressurized Water Reactor (iPWR) Containment Aerosol Deposition Behavior - Phase 2a: Technical Basis and Test Plan for Experimental Testing and Computational Fluid Dynamics Analysis (EPRI 3002010491)*. Electric Power Research Institute.

15. EPRI. (2018b). *Advanced Nuclear Technology: Integrated Pressurized Water Reactor (iPWR) Containment Aerosol Deposition Behavior - Phase 2b: Results and Analysis (EPRI 3002013032)*. Electric Power Research Institute.

16. Escriche, C. B. (2017). *ESTIMATION OF THE RADIOACTIVE AEROSOLS CAPTURE IN ACCIDENTAL SEQUENCES OF NUCLEAR POWER PLANTS.*

17. Fynbo, P., Haggblom, H., & Jokiniemi, J. (1990). *Aerosol Transport in Severe Reactor Accidents.* Nordic Liaison Committee for Atomic Energy.

18. Gamble, R. E., Nguyen, T. T., Shiralkar, B. S., Peterson, P. F., Greif, R., & Tabata, H. (2000). Pressure suppression pool mixing in passive advanced BWR plants. *Nuclear Engineering and Design*.

19. Gao, S., Fu, Y., Sun, D., Mei, Q., Pan, N., Zhang, S., & Huang, G. (2017). COMPARISON RESEARCH ON DIFFERENT AEROSOL POOL SCRUBBING MODELS (ICONE25-66540). *International Conference on Nuclear Engineering.*

20. GE. (1997). *ABWR Design Control Document: Rev. 4, Chapter 6: Engineered Safety Systems.* General Electric Nuclear Energy.

21. GE-Hitachi. (2007). *The ABWR Plant General Description.* GE-Hitachi.

22. GE-Hitachi. (2011). *The ESBWR Plant General Description.* GE-Hitachi.

23. GE-Hitachi. (2014). *ESBWR Design Control Document Tier 2, Chapter 6: Engineered Safety Features.* GE-Hitachi Nuclear Energy Americas LLC.

24. GE-Hitachi. (2018). *BWRX-300 Fact Sheet.* General Electric Hitachi Nuclear Energy.

25. Goharrizi, A. S., & Sadeghi, R. (2009). Thermophoretic deposition of aerosol particles in laminar mixed-convection flow in a channel with two heated built-in square cylinders. *Advanced Powder Technology*.

26. Hashimoto, K., Soda, K., Uno, S., & Nakatani, H. (1988). *EFFECT OF POOL SCRUBBING OF INSOLUBLE AEROSOL IN TWO PHASE FLOW IN A PIPE.* IAEA.

27. Herranz, L. E., Escudero, M. J., Peyres, V., Polo, J., & Lopez-Jimenez, J. (1996). *Review and assessment of pool scrubbing models.* Instituto de Tecnología Nuclear.

28. Hujala, E., Tanskanen, V., & Hyvarinen, J. (2018). Frequency analysis of chugging condensation in pressure suppression pool system with pattern recognition. *Nuclear Engineering and Design*.

29. Jimenez, J. L., Bahreini, R., Crocker III, D. R., Zhuang, H., Varutbangkul, V., Flagan, R. C., . . . Hoffmann, T. (2003). New particle formation from photooxidation of diiodomethane (CH2I2). *Journal of Geophysical Research*.
30. Kallio, G. A., & Reeks, M. W. (1988). A NUMERICAL SIMULATION OF PARTICLE DEPOSITION IN TURBULENT BOUNDARY LAYERS. *International Journal of Multiphase Flow*.
31. Kasper, G., Schollmeier, S., Meyer, J., & Hoferer, J. (2009). The collection efficiency of a particle-loaded single filter fiber. *Journal of Aerosol Science*.
32. Lane, J. W., George, T. L., Claybrook, S. W., Zankowski, J. A., & Kindred, T. (2019). APPLICABILITY OF GOTHIC 8.3(QA) FOR NON-LWR SIMULATION, AEROSOL MODELING & HYDROGEN MANAGEMENT. *NURETH*.
33. Li, H., & Kudinov, P. (2010). EFFECTIVE APPROACHES TO SIMULATION OF THERMAL STRATIFICATION AND MIXING IN A PRESSURE SUPPRESSION POOL. *Division of Nuclear Power Safety*.
34. Munoz-Cobo, J. L., Pena, J., Herranz, L. E., & Perez-Navarro, A. (2005). Steam condensation on finned tubes, in the presence of non-condensable gases and aerosols: Influence of impaction, diffusiophoresis and settling on aerosol deposition. *Nuclear Engineering and Design*.
35. NEA. (2009). *State-of-the-art Report on Nuclear Aerosols.* NEA.
36. NEA. (2018). *Phenomena Identification and Ranking Table: R&D Priorities for Loss-of-Cooling and Loss-of-Coolant Accidents in Spent Nuclear Fuel Pools.* Nuclear Energy Agency.
37. Nowlen, S., Olivier, T., Dreisbach, J., & Salley, M. (2008). *A Phenomena Identification and Ranking Table (PIRT) exercise for Nuclear Power Plant Fire Model Applications.* ANS PSA 2008 Topical Meeting, Knoxville, TN, Sept. 7-11, 2008, (SAND2008-4176C).
38. NRC. (1991). *SPARC-90: A Code for Calculating Fission Product Capture in Suppression Pools (NUREG CR 5765).* Nuclear Regulatory Commission.
39. NRC. (1995). *Accident Source Terms for Light-Water Nuclear Power Plants.* U.S. Nuclear Regulatory Commission.
40. NRC. (1996). *A simplified model of aerosol removal by natural processes in reactor containments.* U.S. Nuclear Regulatory Commission.
41. NRC. (1997). *A Simlified Model of Decontamination by BWR Steam Suppression Pools.* U.S. Nuclear Regulatory Commission.
42. NRC. (2008). *A Phenomena Identification and Ranking Table (PIRT) Exercise for Nuclear Power Plant Fire Modeling Applications (NUREG/CR-6978).* Office of Nuclear Regulatory Research.

43. Owczarski, P. C., & Burk, K. W. (1991). *SPARC-90: A Code for Calculating Fission Product Capture in Suppression Pools (NUREG/CR--5765)*. NUREG.

44. Palisade Corporation. (2018). *@Risk, Risk Analysis Add-in for Mictrosoft Excel, Version 7.6.1.* Ithaca, New York: Palisade Corporation.

45. Pellegrini, M., Araneo, L., Ninokata, H., Ricotti, M., Naitoh, M., & Achilli, A. (2016). Suppression pool testing at the SIET laboratory: experimental investigation of critical phenomena expected in the Fukushima Daiichi suppression chamber. *Nuclear Science and Technology*.

46. Peters, T. M., & Leith, D. (2004). Particle Deposition in Industrial Duct Bends. *Annals of Occupational Hygiene*.

47. Pitts, J. H. (1980). Steam Chugging in a Boiling Water Reactor Pressure-Suppression System. *International Journal of Multiphase Flow*.

48. Ramsdale, S. A., Guentay, S., & Friedrichs, H.-G. (1995). *BUSCA-JUN91 Reference Manual.* Paul Scherrer Institut.

49. Rodriguez, S., Mueller, C., & Merryman, B. (2016). *Lagrangian 3D CFD Simulation of Turbulent Aerosol Experiments.* Sandia National Laboratories.

50. Sandia National Laboratories. (1997). *NUREG/CR-653: Code Manual for CONTAIN 2.0: A Computer Code for Nuclear Reactor Containment Analysis.* Sandia National Laboratories.

51. Sher, R., & Hobbins, R. (2011). Aerosol Deposition Mechanisms. In *Transport and Removal of Aerosols in Nuclear Power Plants Following Severe Accidents.* American Nuclear Society.

52. Sher, R., & Hobbins, R. R. (2011). Transport and Removal of Aerosols in Nuclear Power Plants Following Severe Accidents. American Nuclear Society.

53. SNL. (2007). *Predictive Capability Maturity Model for Computational Modeling and Simulation (SAND2007-5948).* Sandia National Laboratory.

54. Sutter, S. L., Johnston, J. W., & Mishima, J. (1981). *NUREG/CR-2139: Aerosols Generated by Free Fall Spills of Powders and Solutions in Static Air.* NRC.

55. Tanskanen, V., Jordan, A., Puustinen, M., & Kyrki-Rajamaki, R. (2013). CFD simulation and pattern recognition analysis of the chugging condensation regime. *Annals of Nuclear Energy*.

56. Wang, P., Cilliers, J., Neethling, S., & Brito-Parada, P. (2019). The behavior of rising bubbles covered by particles . *Chemical Engineering Journal*, 111-120.

57. Wassel, A. T., Mills, A. F., Bugby, D. C., & Oehlberg, R. N. (1984). ANALYSIS OF RADIONUCLIDE RETENTION IN WATER POOLS. *Nuclear Engineering and Design*.

58. Youn, D. H., Ko, K. B., Lee, Y. Y., Kim, M. H., Bae, Y. Y., & Park, J. K. (2003). The Direct Contact Condensation of Steam in a Pool at Low Mass Flux. *Journal of Nuclear Science and Technology*.

59. Zhao, H., Zou, L., & Zhang, H. (2013). Simulation of thermal stratification in BWR suppression pools with one dimensional modeling method. *Annals of Nuclear Energy*.

Appendix A: Gap Assessment

The roadmap for this section is as follows:

- Background information on the computer codes used for BWR suppression pool safety analysis.
- Overview of recent experimental data available to supplement Gap Area 1 and 2.
- Summary of suppression pool safety analysis computer codes.
- Discussion of SPARC (including SPARC B/98 and SPARC 90 Jet), BUSCA, and SUPRA code-specific gaps, issues and limitations demonstrating Gap Area 3 from Section 2.3.

Background

For the advanced BWR (A-BWR) project, with the objective of providing recommendations towards source-term reduction for A-BWRs, aerosol deposition inside suppression pools forms an important part of the overall analysis. A-BWR designs such as the Advanced BWR (ABWR) and Economic Simplified BWR (ESBWR) have suppression pools housed inside their wetwells. Thus, for the purposes of this study, the capacity of the following computer codes: (1) SPARC, (2) BUSCA, and (3) SUPRA to predict aerosol retention inside suppression pools is analyzed, along with an assessment of existing gaps/approximations that may need to be addressed. The gap analysis is performed based on the modeling of the following aspects: (1) hydrodynamic modeling, (2) thermal-hydraulic modeling, and (3) aerosol deposition modeling. Insufficient modeling, parametric uncertainties, and lack of characterization of some additional phenomena pertaining to aerosol retention reduce the accuracy of deposition velocity calculations and consequently, aerosol retention. This document summarizes the gaps in the above codes, along with the recommendation that in order to provide more accurate results, these gaps need to be addressed.

Recent Experimental Data

For the purpose of this gap assessment, experimental data on suppression pools were studied from recent experiments. The technical basis for selecting these experiments is the applicability of the data, observations and insights gathered from these experiments, which improves the understanding of the parameters and passive aerosol deposition phenomena inside suppression pools. These experiments include

- The Passive and Active Systems on Severe Accident source term Mitigation (PASSAM) project focusing on pool scrubbing under various conditions such as jet injection and hydrodynamics (Albiol , et al., 2017).
- The Societa Informazioni Esperienze Temoidrauliche (SIET) laboratory tests to examining degradation of suppression pool characteristics under the discharge of steam and non-condensable gases through vent pipes, and steam through several quencher different geometries to represent vent pipes and reactor core isolation cooling (RCIC) exhaust pipes (Pellegrini, et al., 2016).

- The POSEIDON tests conducted at the Paul Scherrer Institute (PSI) in Switzerland investigating aerosol scrubbing in low subcooling pools for provision of date to assist predictive model development (Dehbi , Suckow, & Guentay, 2001).
- Experiments involving Direct Contact Condensation (DCC) (Youn, et al., 2003), (Tanskanen, Jordan, Puustinen, & Kyrki-Rajamaki, 2013), (Chan & Lee, 1980), (Chun, Kim, & Park, 1996), (Pitts, 1980).

Experimental data collected after 2000 are candidate data sources for the SPARC, BUSCA, and SUPRA codes; however, it is unclear if code updates have used the more recent data. Background information and observations and insights from these experiments are discussed in the following subsections.

PASSAM Project

The suppression pool experiments conducted as part of the PASSAM project (Albiol , et al., 2017) focus on pool scrubbing under various conditions such as jet injection and hydrodynamics. In addition, two-phase flow inside tube bundles is investigated at the TRISTAN (Tube Rupture In Steam generaTor: multi-phAse-flow iNvestigations) hydrodynamic facility, which was designed and constructed at the Paul Scherrer Institute (PSI).

Background Information

1. The effects of the gas/steam mixture flow rate into the suppression pool on aerosol scrubbing are characterized through the Weber number (We: ratio of inertia and surface tension forces) and gas saturation ratio.
2. 1 µm diameter SiO_2 particles are used for testing.
3. Scrubbing efficiency is defined by particle retention inside the suppression pool.
4. Three suppression pool liquids are considered, namely water, seawater and water with a surfactant (to vary surface tension).
5. Bubble formation and velocities are observed.

Observations and Insights

- **Pool scrubbing efficiency:**
  - The pool scrubbing efficiency increases as the mixture flow rate increases.
  - It is not noticeably affected by the steam volume fraction or the temperature difference between steam and pool.
  - It is high when jet injection is well-developed (We > 1.0E6).
  - Inertial impaction is dominant when We > 2.0E6.
- **Bubble dynamics:**
  - Bubble size and velocity was found to be independent of the nozzle diameter and mass flow rate. This implies that flow is controlled by buoyancy.
  - Depending on the injection flow rate and nozzle type, both bubble and churn-turbulent structures were seen during the injection phase.
  - Two bubble regimes were observed during the experiment. Initially, the bubble distribution is bimodal, with two dominating bubble diameter ranges, following

which disintegration of larger bubbles occurs, resulting in the bubble size distribution becoming lognormal.
  - Bubble formation is dependent on water composition.
  - The void fraction (fraction of the volume occupied by the gas phase, i.e. bubbles) depends on injection velocity and nozzle size.
- **Decontamination Factor (DF):**
  - The DF is defined as amount of a pollutant upstream divided by pollutant downstream from a filtering device.
  - The DF was observed to be double for a pool containing seawater and water with a surfactant when compared to a pool containing normal water.
  - Active deposition mechanisms during bubble residence time are sedimentation, centrifugal impaction and Brownian diffusion. A high residence time gives rise to a high DF.
  - Bubble fragmentation increases the DF due to increased bubble surface area. Therefore, addition of obstacles/grids is recommended to aid bubble fragmentation and thereby enhance the DF.
- **Summary of study:**
  - Pool hydrodynamics for Steam Generator Tube Rupture (SGTR) conditions is studied at the TRISTAN facility.
  - The analysis showed that following jet injection, bubble residence times are smaller and bubble diameters are larger than those assumed by the codes, which predict a larger DF.
  - The interfacial area of the bubble determines the mass transfer from gas to liquid.
- **Recommendations from study:**
  - Detailed bubble size, shape, interfacial area and velocity data will allow more credible estimates of the multiphase phenomena than corresponding models in existing low injection regime codes.
  - Multiphase flow modeling is recommended for accurate results. For Jet injection, three phase modeling (gas, solid particles, and bubbles) is recommended.
  - It was also recommended that simple models and correlations can be developed from the experimental data, and implemented into severe accident analysis codes, such as ASTEC, which is used for modeling.

Societa Informazioni Esperienze Temoidrauliche (SIET) Laboratory Tests

Experimentation at the Societa Informazioni Esperienze Temoidrauliche (SIET) laboratory includes the study of degradation of suppression pool characteristics under the discharge of steam and non-condensable gases through vent pipes, and steam through several quencher different geometries to represent vent pipes and reactor core isolation cooling (RCIC) exhaust pipes.

Background Information

1. Degradation of suppression pool characteristics under discharge of gas/steam mixture, behavior of steam at the quencher mouth is observed (Pellegrini, et al., 2016).
2. Pool water temperature is measured at different locations.

3. A high-speed imaging camera used to gather experimental data.

Observations and Inferences

1. A large steam mass flux results in stable condensation in the inlet jet. A low flow rate results in unstable condensation oscillation/cyclic condensation, known as chugging condensation (i.e. quick bubble pressurization). For a very low flow rate, condensation takes place fully within vent pipe.
2. The chugging condensation regime of steam condensation is characterized by the creation of a bubble at the end of the pipe, which quickly collapses and establishes a depressurization in the steam. This moves up lot of water backward into the pipe, until a new cycle is started over. It is an unstable process which involves large condensation and pressure spikes.
3. Pipe diameter influences chugging condensation.
4. While entering the suppression pool, a small hole for the air/steam mixture results in a jet/bubbling regime, while a larger hole gives rise to the chugging/oscillating regime.
5. Chugging condensation can be mitigated by the presence of air or non-condensable gases, due to no large depressurization. A mass flow rate of air which is about 3% of steam mass flow rate is sufficient to stabilize the chugging condensation regime.
6. During the chugging condensation process, a bubble grows (in case of pure, saturated steam), then collapses. A 3-D analysis tool recommended for proper analysis.
7. Pool mixing is enhanced by presence of air and is also dependent on size and shape of the pool. This is an important insight for two-phase CFD modeling.

POSEIDON Tests

The POSEIDON-II experiments have been conducted at the Paul Scherrer Institute (PSI) in Switzerland to investigate aerosol scrubbing in low subcooling pools for provision of date to assist predictive model development. In addition, severe accident research on passive containment coolers and aerosol retention is conducted at the PSI.

Background Information

1. Experiments consist of 17 tests to determine dependence of the DF on pool height, steam mass fraction of inlet gas, pool and inlet gas temperature, and particle diameter (Dehbi , Suckow, & Guentay, 2001).
2. SnO_2 aerosols are used, with lognormal inlet and outlet size distributions.
3. BUSCA results are used for comparison with experimental data.

Observations and Insights

1. DF increases with pool height (low pool height results in higher rate of aerosol escape from the pool).
2. Pool retention capacity decreases as its temperature nears the saturation temperature, due to decreasing rate of steam condensation in the pool. However, experimental data from the POSEIDON-II tests shows that aerosol retention takes place in low subcooling (hot) pools. Therefore, the assumption that hot pools provide zero decontamination is conservative.

3. DF increases significantly with steam mass fraction and flow rate. Also, DF increases with particle size.
4. Comparison of experimental data with the BUSCA code results showed good agreement for DF values lower than 10, but BUSCA overpredicted larger DF values by two orders of magnitude.

Direct Contact Condensation (DCC) Experiments

DCC Experiments Examined

Direct contact condensation (DCC) is the underwater condensation of steam (directly in contact with water) (Chun, Kim, & Park, 1996). Since the flow of a gaseous mixture containing, steam, non-condensable gases and fission product aerosols into the suppression pool is an important occurrence in the drywell depressurization process, experiments analyzing DCC form an integral part of suppression pool analysis. Experiments have been conducted with the In-Containment Refueling Water Storage Tank (IRWST) at the (Korea Next Generation Reactor (KNGR) (Youn, et al., 2003), the PPOOLEX facility at the Lappeenranta University of Technology (LUT) (Tanskanen, Jordan, Puustinen, & Kyrki-Rajamaki, 2013), and by Chan et al. (Chan & Lee, 1980), Chun et al. (Chun, Kim, & Park, 1996), and Pitts (Pitts, 1980). The key observations and insights regarding DCC have been presented below.

Observations and Insights

1. Three distinct DCC regimes were initially observed based on varying steam flow rates (Chan & Lee, 1980); frequency and pattern recognition algorithms for DCC have been developed at PPOOLEX facility (Tanskanen, Jordan, Puustinen, & Kyrki-Rajamaki, 2013).
2. It is now possible to collect and analyze experimental data with newer and better measurement techniques, such as high-speed cameras, data processing, and pattern recognition algorithms. Comparison of experimental data with Computational Fluid Dynamics (CFD) simulations can also be performed (Hujala, Tanskanen, & Hyvarinen, 2018).
3. Validation and development of condensation models that can capture interfacial condensation rate correctly using CFD is recommended.
4. Two-phase flow with CFD is challenging. Currently, CFD is unable to perfectly model DCC.
5. It was also found that the presence of nitrogen removes thermal stratification in the suppression pool and enhances mixing. The DCC regime becomes the External Chug with Encapsulated Bubble (ECEB) regime (Cai, Jo, & Okamoto, 2015).

Summary of Computer Code Models

The thermal-hydraulic and aerosol retention models in SPARC, SPARC-B/98, BUSCA and SUPRA are summarized in Table A-1, which has been adapted using Tables 1 and 2 from a study by Gao et al., comparing computer codes for suppression pool modeling (Gao, et al., 2017). The technical basis for selecting these codes is their prevalence in use for suppression pool aerosol deposition calculations.

Table A-1: Comparison of thermal-hydraulic and aerosol retention models in SPARC, BUSCA and SUPRA (Gao, et al., 2017)

Model	SPARC/SPARC-90	SPARC/SPARC-	BUSCA	SUPRA
Thermal-hydraulic models				
Jet region	Not considered	Not considered	Not considered	Immersed jet modeled for high injection velocity
Primary bubble volume	SPARC'S horizontal vent, downcomer and quencher correlation	SPARC'S horizontal vent, downcomer and quencher correlation	Not considered	Not considered
Rising bubble size	Single diameter which depends on the steam fraction in injected gas	Superposition of two lognormal size distributions	Ramakrishnan et al's theoretical model; EPRI's horizontal and vertical vent correlations	Ramakrishnan et al's theoretical model; Surface tension / buoyancy balance correlation
Bubble shape	oblate ellipsoid	oblate ellipsoid	Lognormal size distribution	Leibson et al. Correlation
Relative velocity of rising bubble	Two correlations based on Haberman et al's data	Two correlations based on Haberman et al's data	Sphere; oblate ellipsoid; spherical cap	Sphere; oblate ellipsoid; spherical cap
Swarm rise velocity	Data from Paul et al and GE company	New correlations that considers the influence of finite water pool size	Correlation of the Five Wallis Regimes – Spherical, oblate ellipsoid, spherical cap bubble shape respectively	Correlation of Haberman and Morton; correlation of the Five Wallis Regimes
Condensation on aerosol particles	Modified form of Mason's equation	Modified form of Mason's equation	GEC cluster model; Colder cluster model; Sjoen plume	Not considered
Temperature of bubble interface	Different from pool and bubble gas temperature, calculated additionally	Different from pool and bubble gas temperature, calculated additionally	Modified form of Mason's equation	Not considered
Aerosol Removal Models				
Immersed Jet at injection zone	Not considered	Impaction, droplet interception, molecular and turbulent diffusion, condensation, diffusiophoresis,	Not considered	Not considered

Model	SPARC/SPARC-90	SPARC/SPARC-	BUSCA	SUPRA
Bubble formation at injection zone	Condensation, sedimentation, inertial impaction, Brownian diffusion, centrifugal deposition	Condensation, diffusiophoresis, thermophoresis, sedimentation, inertial impaction, Brownian diffusion, centrifugal deposition	Impaction	Impaction, centrifugal deposition
Bubble rising zone	Diffusiophoresis, sedimentation, Brownian diffusion, centrifugal deposition	Diffusiophoresis, sedimentation, Brownian diffusion, centrifugal deposition	Diffusiophoresis, thermophoresis, sedimentation, Brownian diffusion, centrifugal deposition	Diffusiophoresis, thermophoresis, sedimentation, Brownian diffusion, centrifugal deposition

Overview of SPARC

The SPARC (Suppression Pool Aerosol Removal Code) safety analysis computer code was developed by the Pacific Northwest National Laboratory (PNNL) to calculate the capture of aerosol particles by the wetwell i.e. the pressure suppression pool inside a BWR, in the event of a postulated accident where aerosols are forced into the pool. Typical inputs include the suppression pool parameters (pressure, temperature), vent parameters (number of holes, vent type, cross-section area), various hydrodynamic parameters (inlet gas temperature, flow rates for various gases etc.), and aerosol characteristics (size distribution etc.). Typical outputs include the DF, particle number flow rate, dry and wet particle mass flow rates, along with up to 37 other output variables. This code contains several models for aerosol particle retention and thermal-hydraulics (Owczarski & Burk, 1991). In this section, the working of SPARC is briefly outlined, followed by the gaps present in the code.

SPARC Characteristics

SPARC provides a computational framework to model various aspects of phenomena associated with hydrodynamics, thermal-hydraulics, and aerosol retention.

Modeling of Hydrodynamics

1. Gas injection is modeled under the "globule regime", i.e. the formation of globules followed by their disintegration into bubbles when a mixture of air and steam enters the suppression pool. The size of initial globule depends on vent type and mixture composition (condensable vs non-condensable gases) (Escriche, 2017).
2. Aerosol size distribution at the gas inlet is assumed to be lognormal.
3. Thermal-hydraulic conditions of the suppression pool and injected gas are required for modeling.

4. Aerosol deposition processes modeled:
    a. Convective flow from steam condensation
    b. Growth of soluble particles by water vapor sorption
    c. Gravitational settling (sedimentation)
    d. Inertial deposition due to circulation of the bubble surface
    e. Diffusional deposition

Modeling of Thermal-hydraulics

1. The thermal-hydraulic model consists of two parts (Escriche, 2017):
    a. **Model for the equilibrium pool temperature:** This is the steady-state temperature of the pool in thermal and vapor equilibrium with the gas leaving the pool.
    b. **Model for steam evaporation into the bubble as it rises:** Incoming steam (into the bubble) is the result of the steam maintaining vapor equilibrium as the bubble rises. This steam influx retards all particle deposition mechanisms, and it is especially important in pools near the boiling point.
2. Calculation aspects of thermal-hydraulics:
    a. Heat transfer to/from the gas phase
    b. Mass transfer to/from the gas phase
    c. Work of the expanding gas phase as the bubble rises
3. The thermal hydraulics of these pool/gas interactions also affects particle capture mechanisms.
4. Entering gas attains equilibrium with pool temperatures
    a. **Hot/dry entering gas (low steam concentration):** Evaporates water from the pool and hinders particle capture.
    b. **High steam concentration:** Enhances particle capture.
5. Bubble rise leads to vapor transfer to the bubble (i.e. increasing volume) for vapor equilibrium and hinders particle capture while providing more steam for particle growth by condensation.
6. Condensation of vapor on particles occurs when bubble vapor pressure is greater than wet particle vapor pressure (higher for wet insoluble particles than soluble particles).

Modeling of Aerosol Retention

- Aerosol capture:
    - Condensation of excess steam moves particles to surface (difference in vapor pressures)
    - High gas temperature leads to thermal gradient and thermophoresis
    - High gas velocity leads to impaction
    - Curved surface motion due to bubble formation (also by sedimentation, inertial deposition, diffusion – dependent on relative bubble velocity)
- Particle growth is very sensitive to temperature (Herranz, Escudero, Peyres, Polo, & Lopez-Jimenez, 1996).

Observations and Inferences

Based on an assessment of the models present in SPARC, the identified issues and assumptions are summarized below (Herranz, Escudero, Peyres, Polo, & Lopez-Jimenez, 1996).

Hydrodynamic modeling

1. Bubbles are assumed to be ellipsoidal only, while bubbles may be of various shapes. Consequently, bubble shape does not affect bubble rise velocity in SPARC.
2. Bubble diameter is calculated from experimental correlations. It only depends on inlet gas composition. Correlations for initial globule diameter are included, but do not cover high flows typical of accident sequences i.e. jet regimes. Characterization of globule to bubble transition happens linearly, which may be a poor approximation. However, lack of data on this is an issue.
3. Bubble rise velocity is captured based on experimental correlations. Uncertainties associated with rise velocities may be countered using Churn Turbulent Flow models. Effect of contaminants and walls on rise velocity and bubble formation needs to be modeled.
4. Bubble diameter has an upper bound of 0.561 cm due to dependence on steam mass fraction.
5. Accurate calculation of particle size distribution needs to be characterized.
6. Recommendation to improve the modeling of the following (Herranz, Escudero, Peyres, Polo, & Lopez-Jimenez, 1996):
   a. **Globule rupture models**: Globules rupture into bubbles, which play an important role in particle deposition. Phenomena related to globule rupture is poorly characterized due to lack of experimental data. Bubble size distribution is also not characterized.
   b. **Churn-turbulent flow:** This flow regime is the transition between bubbly and droplet flow. It requires void fraction as a variable in order to be characterized. Lack of modeling reduces the accuracy of aerosol deposition estimation.
   c. **Presence of a tensoactive compound:** This compound is one which contains both hydrophilic and hydrophobic groups within the same molecule. Their presence increases bubble surface tension, enabling them to rise like rigid spheres and consequently, a delay factor is introduced in this analysis. It is therefore important to model their effects.
   d. **Pool contaminant models**: This includes modeling of tensoactive compounds, as well as other contaminants which can affect pool decontamination efficiency by altering pool liquid viscosity and density. Experimental studies have shown that for smaller bubble diameters (0.5-2 mm), the bubble rise velocity reduces in the presence of contaminants.
   e. **Wall effect models:** The wall effect is the possible interaction between the gaseous flow carrying radioactive material entering the pool, and the pool liquid whose continuity has been altered by the presence of solid obstructions. This effect affects bubble rise velocity and bubble shape. Therefore, a model for it should be included in pool safety analysis codes.

Thermal-hydraulic modeling

1. SPARC assumes overall chemical equilibrium and thermodynamic equilibrium, including at the inlet where the aerosols enter. This assumption may not always be valid.
2. Condensation in SPARC is arbitrarily affected by a factor of 3. Condensation is assumed to occur immediately after injection.
3. Thermal-hydraulic modeling is very sensitive to bubble shape; however, SPARC models only an ellipsoidal bubble shape, which leads to questions over its ability to model the thermal-hydraulics of other bubble shapes.
4. Thermophoresis is not modeled. However, condensation, impaction (inertial, centrifugal), sedimentation and diffusion are modeled. In addition, diffusiophoresis is modeled during bubble rise.

Aerosol retention

- The phenomenological sequence for gaseous flow into the suppression pool for particle retention is not clearly defined. Bubble formation, injection, condensation following injection algorithms may not be applicable to all scenarios. Aerosol entrainment needs to be considered.
- Processes are assumed to be in series rather than in parallel. Therefore, use of an incorrect sequence of phenomena may impact calculations. SPARC assumes instant equilibrium, which prioritizes aerosol retention mechanisms. Experimental data needed to confirm this, following which it can be implemented into BUSCA and SUPRA.

SPARC B/98 – Improved SPARC model

The improved SPARC B/98 version of the SPARC-90 code was provided the ability to model immersed jets for high injection velocity for a quencher or single orifice injection process. This code also calculates rising bubble size by superposition of two lognormal size distributions, an improvement over the single rising bubble diameter which depends on steam fraction in the injected gas as calculated by SPARC. In addition, new correlations which consider the influence of the finite water pool size to calculate the bubble swarm rise velocity are incorporated into SPARC B/98. Aerosol removal is calculated in the jet regime by impaction, turbulent diffusion, steam condensation, thermophoresis, diffusiophoresis and Brownian diffusion. A sensitivity study between code predictions for SPARC B/98 and SPARC-90 showed improved modeling results by SPARC B/98 for aerosol removal due to the effects of steam condensation, pool temperature and the injected gas flow rate (Gao, et al., 2017). In addition, there is also a version of SPARC which has been modified to model agglomeration of particles (Hashimoto, Soda, Uno, & Nakatani, 1988).

SPARC 90 Jet – Improved SPARC model

SPARC 90-Jet is an upgrade of SPARC-90, which is the older SPARC version developed for low inlet gas velocities. SPARC 90-Jet can analyze jet hydrodynamics by means of a jet subroutine (Berna, Escriva, Munoz-Cobo, & Herranz, 2015). The jet subroutine remains active till the velocity of the gas entering the suppression pool goes above the threshold velocity. The code solves conservation equations related to mass, momentum and energy to calculate results. The following observations and insights are pertinent to SPARC 90-Jet (Escriche, 2017):

1. Characterization of hydrodynamic equations of submerged jets is recommended. The validity of the important equations (entrainment/deposition balance of droplets, the droplet-droplet interaction, the droplet characterization etc.), developed in the annular flow regime domain, should be established.
2. The modelling extension to phase change conditions is recommended. Processes of steam condensation/evaporation might play an important role by enhancing/hindering decontamination and by changing droplet dynamics.
3. Thermal exchanges between the gas jet and the surrounding water have not been considered, neither sensible nor latent heat transfer.
4. At the inlet, the only particle depletion mechanisms considered are inertial impaction, interception and Brownian diffusion. Thermophoresis and diffusiophoresis have been neglected. This may lead to underprediction for the DF, in particular for smaller particles with diameters lower than 1 μm.
5. Aerosol agglomeration/de-agglomeration processes have not been considered. It is assumed that interaction among aerosols cannot take place during the jetting region.
6. Droplets coalescence/break-up processes have not been considered. It is assumed that droplet does not occur within the jetting region.
7. Only one constant diameter for entrained droplets is considered in each computational cell. A particle size discrete distribution function such as the lognormal distribution needs to be considered.
8. Correlations for aerosol scrubbing by the entrained droplets have been chosen from those developed for wet scrubbers, due to the lack of information about submerged gaseous jets.

Overview of BUSCA

The BUSCA (Bubble Scrubbing Algorithm) safety analysis computer code was developed by the United Kingdom Atomic Energy Authority; the Paul Scherrer Institute converted it into a FORTRAN code. BUSCA models the decontamination of a bubble containing a mixture of non-condensable gases, steam and aerosol particles as it rises through a water pool. Thermal-hydraulics, removal of soluble vapor and aerosol contaminants are also modeled. Typical inputs include the suppression pool parameters (pressure, temperature, nozzle submergence depth etc.), various hydrodynamic parameters (initial bubble volume, flow rates etc.), and aerosol characteristics (mass, median radius, minimum particle size etc.). Typical outputs include the DF and bubble parameters at the time the bubble breaks the pool surface (EPRI, 2014). In this section, the working of BUSCA is briefly outlined, followed by the gaps present in the code.

BUSCA Characteristics

BUSCA provides a computational framework to model various aspects of phenomena associated with hydrodynamics, thermal-hydraulics, and aerosol retention.

Modeling of Hydrodynamics

1. DF has a low degree of variation on globule diameters (> 3 cm), since decontamination mostly takes place due to bubble rise. Also, DF decreases with increasing bubble size.

2. DF decreases with increasing bubble rise velocity (swarm velocity) since the rise velocity defines the time for which the bubble remains in the suppression pool, and the time for which decontamination mechanisms act on it.
3. Hydrodynamic models:
    a. Formation of an initial globule
    b. Primary bubble decay/rupture
    c. Bubble diameter and shape
    d. Rise velocity and bubble velocity
4. BUSCA can calculate different bubble shapes. Changes in bubble diameter cause major changes in the maximum to minimum bubble diameter ratio (Herranz, Escudero, Peyres, Polo, & Lopez-Jimenez, 1996).
5. Globule diameter evolves according to pool conditions (evaporation and condensation, pressure changes). BUSCA uses stability criteria to capture globule transition to bubbles, which is sudden (following a threshold globule diameter). The Weber criterion determines critical globule diameter. Bubble rise velocity is based on the type of venting. Methodology to calculate bubble diameter and shape are different for SPARC and BUSCA. A lognormal bubble size distribution is modeled in BUSCA.
6. Rise regime/swarm velocity is proportional to the residence time of the gas inside the pool. BUSCA models two possible bubble regimes, cluster and plume, and assumes a constant value of the void fraction as 0.5.
7. Aerosol size distribution at the gas inlet is assumed to be lognormal.

Modeling of Thermal-hydraulics

1. Chemical and thermal equilibrium is calculated based on environmental conditions.
2. Condensation and evaporation in the bubble throughout the entire gas rise period is estimated.
3. Model is based on non-condensable experiments, while bubble evolution is estimated through thermal-hydraulic processes.
4. The first mechanism to act is inertial impaction. No sensitivity is shown to the solubility of the aerosol injected.
5. Spherical bubbles while calculating particle growth due to condensation are assumed.

Modeling of Aerosol Retention

1. Phenomena modeled include condensation, thermophoresis, impaction (inertial, centrifugal), sedimentation and diffusion.
2. The moving grid technique is used to track particle evolution.
3. Aerosol retention shows inverse proportion to bubble diameter due to the volume fraction affecting all mechanisms.
4. Impaction velocity is estimated based on the assumption that bubbles are spherical.

Observations and Inferences

Hydrodynamics

1. Lack of experimental data for hydrodynamics (EPRI, 2014).

2. No models present to predict characteristic parameters in the region between injection and fully developed flow.
3. Steam fraction leads to uncertainties with respect to bubble diameter.
4. Extreme thermal-hydraulic cases like maximum evaporation (saturated pool with injection of non-condensable gases), and maximum condensation (cold pool with steam injection) may give bubble diameter in the stable zone greater than the rupture criterion.
5. Bubble rise velocity correlations limited to isolated bubble regime, so rise regime effects not considered. Bubble shape can change bubble velocity.
6. Globule to bubble transition is poorly characterized due to lack of experimental data. Decontamination may occur mainly in the rupture zone, so it needs to be characterized properly.
7. There is uncertainty associated with the characterization of bubble rise regimes.
8. BUSCA gives bad predictions with high pool heights due to hydrodynamics model in the code assuming a bubbly gas flow which is different from the actual regime, which is turbulent.
9. Recommendation to improve the modeling of the following (Herranz, Escudero, Peyres, Polo, & Lopez-Jimenez, 1996):
    a. **Globule rupture models**: Globules rupture into bubbles, which play an important role in particle deposition. Phenomena related to globule rupture is poorly characterized due to lack of experimental data. Bubble size distribution is also not characterized.
    b. **Churn-turbulent flow:** This flow regime is the transition between bubbly and droplet flow. It requires void fraction as a variable in order to be characterized. Lack of modeling reduces the accuracy of aerosol deposition estimation.
    c. **Presence of a tensoactive compound:** This compound is one which contains both hydrophilic and hydrophobic groups within the same molecule. Their presence increases bubble surface tension, enabling them to rise like rigid spheres and consequently, a delay factor is introduced in this analysis. It is therefore important to model their effects.
    d. **Pool contaminant models**: This includes modeling of tensoactive compounds, as well as other contaminants which can affect pool decontamination efficiency by altering pool liquid viscosity and density. Experimental studies have shown that for smaller bubble diameters (0.5-2 mm), the bubble rise velocity reduces in the presence of contaminants.
    e. **Wall effect models:** The wall effect is the possible interaction between the gaseous flow carrying radioactive material entering the pool, and the pool liquid whose continuity has been altered by the presence of solid obstructions. This effect affects bubble rise velocity and bubble shape. Therefore, a model for it should be included in pool safety analysis codes.

Thermal-hydraulic modeling

1. Shows greater decontamination by sedimentation and impaction due to differences of growth in particles due to steam condensation.

2. Shows significant efficiency in retention of submicron particles, which is a discrepancy with experimental results.
3. Diffusiophoresis is modeled independent of particle size.

Aerosol Retention

1. Aerosol retention is modeled in series and not parallel. Incorrect sequence means incorrect DF characterization.
2. Centrifugal deposition may be affected by spherical bubble approach. BUSCA, however, uses the spherical bubble approach for surface velocity, such that it would not be capable of suitably dealing with either ellipsoid bubbles or elliptical caps.
3. A phenomenon which acts against retention and which is not currently considered is aerosol entrainment.

Overview of SUPRA

SUPRA Characteristics

The SUPRA (Suppression Pool Retention Analysis) code was developed by the Electric Power Research Institute (EPRI) (Fynbo, Haggblom, & Jokiniemi, 1990). It models aerosol retention in the suppression pool by dividing it into three zones: (1) Injection zone (formation and release of gas bubbles or slugs, or with gas jets), Bubble rise zone (a uniform initial bubble size is assumed and no interaction between bubbles is allowed; the transfer processes are taken to be those for a single isolated rising bubble), and (3) Surface zone (Desorption of dissolved gases can occur in the surface zone, as can liquid entrainment by the gas stream). The code uses a spatial domain with a fourth order Runge-Kutta, Adams-Moulton predictor-corrector scheme to perform its calculations. Empirical relations are used for hydrodynamics of the gas flow, bubble departure size as a function of the flow rate, bubble rise velocity as a function of bubble size, and heat and mass transfer coefficients at the phase interfaces. A system of equations is integrated along the entire depth of the pool, after which conservation equations are integrated in time domain for time history. Key parameters are evaluated at spatial locations. Typical inputs include the suppression pool parameters (pressure, temperature, nozzle submergence depth, orifice diameter etc.), various hydrodynamic parameters (inlet gas temperature, flow rate, mass fraction of steam etc.), and aerosol characteristics (density, radius) (Wassel, Mills, Bugby, & Oehlberg, 1984). Studies have shown that the SUPRA model was more complete than SPARC, since it provides better results for high gas humidity, but underestimates pool scrubbing similar to SPARC. The MAAP-3 code computes pool scrubbing using SUPRA results (Fynbo, Haggblom, & Jokiniemi, 1990). SUPRA provides a computational framework to model various aspects of phenomena associated with aerosol retention and hydrodynamics, and also for phenomena associated with thermal-hydraulics.

Modeling of Aerosol Retention and Hydrodynamics

The following aspects of hydrodynamics and aerosol processes are modeled in SUPRA (Wassel, Mills, Bugby, & Oehlberg, 1984):

1. Bubble hydrodynamics including shape and volume

2. Aerosol transport due to convective flows resulting from the condensation or evaporation of steam
3. Particle growth caused by water vapor sorption by soluble aerosol material
4. Pool time history is used to calculate internal DFs, by solving appropriate conservation equations
5. Aerosol deposition/removal in the bubble rise zone is calculated due to:
    a. Aerosol removal due to sedimentation
    b. Aerosol removal due to flow impingement in the injection zone
    c. Aerosol removal due to internal circulation in the injection zone
    d. Inertial aerosol deposition in the rising bubble zone
    e. Aerosol removal due to Brownian diffusion
    f. Aerosol removal due to thermophoresis
    g. Aerosol removal due to diffusiophoresis
6. Desorption from the pool surface

Modeling of thermal-hydraulics

The following thermal-hydraulic models are present in SUPRA (Wassel, Mills, Bugby, & Oehlberg, 1984):

1. Conservation of mass, vapor species and energy for a binary gas phase
2. Transfer of gas species through a bubble surface
3. Pool temporal analysis
4. Evaporation from the pool surface
5. One-dimensional equations for the following:
    a. Conservation of mass
    b. Conservation of chemical species (water vapor)
    c. Conservation of energy
    d. Transfer perimeter (Characteristic of the interference area, in which changes in gas temperature and composition occur in the direction of the flow), heat and mass transfer coefficients are calculated
6. Solution of the gas phase equations, which are treated as a single stream heat exchanger, gives the differential DF (defined as the ratio of the rate of aerosol mass entering the pool to the rate of aerosol mass exiting the pool), while an overall balance on the pool gives the integral DF (defined as the ratio of total aerosol mass entering the pool to the total aerosol mass exiting the pool, integrated over a time period).
7. Mass transfer equations are formulated for mass transfer into or out of rising bubbles and the pool surface, as well as entrainment from pool surface.

Gaps in SUPRA

Gaps in Hydrodynamics

1. Deposition mechanisms are uncoupled and additive.
2. Particles are homogeneously distributed within a given bubble.

3. No agglomeration, particle growth; size bin contains particles identical to monodisperse aerosols. Residence time is lower than 15 s which is inadequate for agglomeration. Particle size only changes due to steam condensation if humidity ratio is > 85%.
4. SUPRA can produce non-conservative DF predictions for insoluble aerosols (Gao, et al., 2017).
5. Condensation on aerosol particles is not considered.
6. Swarm rise velocity is unavailable.
7. Immersed jet injection is not modeled.

Gaps in thermal-hydraulic modeling

1. Pool conditions do not change during gas residence time, which may not always be the case if the gas momentum and temperature contribute in raising the pool temperature during the gas residence time, albeit its short duration
2. Pool is assumed to be well-mixed and unstratified, which may not always be the case
3. Equilibrium is assumed at interface, which may not always be the case

Insights from the validation of SUPRA against experimental results

1. Satisfactory agreement seen during comparison against experimental results for steam-non-condensable gas bubble rise and phase change (Fynbo, Haggblom, & Jokiniemi, 1990).
2. Satisfactory agreement was also seen with methyl iodide removal experimental data.
3. Results from a parametric study (values selected close to BWR severely degraded core accident sequences):
    a. **Aerosol particle size and distribution** – A diameter lower than 0.1-0.2 μm results in diffusion, while a diameter greater than 0.1-0.2 μm means sedimentation and inertia are important.
    b. **Mass fraction of non-condensable gas** – The DF increases with decreasing non-condensable gas (increasing steam concentration) due to convective deposition associated with steam condensation. Increasing non-condensable gas concentration reduces the condensation rate and convective/diffusive mass transfer. However, the DF increases for steam/hydrogen mixtures as hydrogen increases, due to low gas density and resulting high gas velocity. Convective deposition is very important.
    c. **Gas mass flow rate** – This parameter governs initial bubble size. Laminar flow means bubble size increases with flow rate; transition regime and turbulent regimes mean smaller stable bubbles form at higher flow rates. Residence time is longer for smaller bubbles, resulting in more retention.
    d. **Quencher submergence depth** – The DF increases with increasing depth.
    e. **Pool water temperature** – The DF decreases with increasing pool temperature due to decreasing condensation rate and increasing rate of bubble size reduction, mass transfer, and increased evaporation. In addition, solubility decreases. However, a high DF for a saturated pool can be achieved with low concentration of non-condensable gases.

4. Models are based on and verified by experimental data; the entire code is not validated. Improvements will be made based on that.